

UNCLASSIFIED

AD NUMBER
ADB045499
NEW LIMITATION CHANGE
TO Approved for public release, distribution unlimited
FROM Distribution authorized to U.S. Gov't. agencies only; Test and Evaluation; Aug 1979. Other requests shall be referred to Air Force Materials Laboratory, Attn: AFML/MBC, Wright-Patterson AFB, OH 45433
AUTHORITY
AFWAL ltr, 3 Jul 1983

THIS PAGE IS UNCLASSIFIED

AFML-TR-79-4107

ADB045499

POLYMER/SOLVENT AND POLYMER/POLYMER INTERACTION STUDIES

J. C. HOLSTE

C. J. GLOVER

D. T. MAGNUSON

K. C. B. DANGAYACH

T. A. POWELL

D. W. CHING

D. R. PERSON

CHEMICAL ENGINEERING DEPARTMENT

TEXAS A&M UNIVERSITY

COLLEGE STATION, TEXAS 77843

AUGUST 1979

TECHNICAL REPORT AFML-TR-79-4107

Interim Report for period June 1978 — May 1979

Distribution limited to U. S. Government agencies only; (Test and Evaluation). Other requests for this document must be referred to AFML/MBP, Air Force Materials Laboratory, Wright-Patterson Air Force Base, Ohio 45433.

AIR FORCE MATERIALS LABORATORY
AIR FORCE WRIGHT AERONAUTICAL LABORATORIES
AIR FORCE SYSTEMS COMMAND
WRIGHT-PATTERSON AIR FORCE BASE, OHIO 45433


Best Available Copy

20040226226

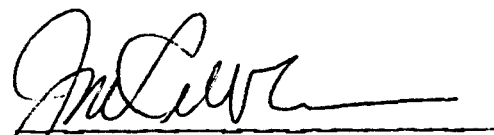
NOTICE

When Government drawings, specifications, or other data are used for any purpose other than in connection with a definitely related Government procurement operation, the United States Government thereby incurs no responsibility nor any obligation whatsoever; and the fact that the government may have formulated, furnished, or in any way supplied the said drawings, specifications, or other data, is not to be regarded by implication or otherwise as in any manner licensing the holder or any other person or corporation, or conveying any rights or permission to manufacture, use, or sell any patented invention that may in any way be related thereto.

This technical report has been reviewed and is approved for publication.


I. J. Goldfarb, Engr.
R. L. Van Deusen, Chief
Polymer Branch

FOR THE COMMANDER


J. M. Kelble, Chief
Nonmetallic Materials Division

"If your address has changed, if you wish to be removed from our mailing list, or if the addressee is no longer employed by your organization please notify AFML/MBP, W-PAFB, OH 45433 to help us maintain a current mailing list".

Copies of this report should not be returned unless return is required by security considerations, contractual obligations, or notice on a specific document.

REPORT DOCUMENTATION PAGE		READ INSTRUCTIONS BEFORE COMPLETING FORM
1. REPORT NUMBER AFML-TR-79-4107	2. GOVT ACCESSION NO.	3. RECIPIENT'S CATALOG NUMBER
4. TITLE (and Subtitle) POLYMER/SOLVENT AND POLYMER/POLYMER INTERACTION STUDIES		5. TYPE OF REPORT & PERIOD COVERED Interim Report 1 June 1978 - 31 May 1979
		6. PERFORMING ORG. REPORT NUMBER
7. AUTHOR(s) J. C. Holste, C. J. Glover, D. T. Magnuson, K. C. Dangayach, T. A. Powell, D. W. Ching, D. R. Person		8. CONTRACT OR GRANT NUMBER(s) F33615-78-C-5078
9. PERFORMING ORGANIZATION NAME AND ADDRESS Chemical Engineering Department Texas A&M University College Station, TX 77843		10. PROGRAM ELEMENT, PROJECT, TASK AREA & WORK UNIT NUMBERS 2303Q506
11. CONTROLLING OFFICE NAME AND ADDRESS Air Force Materials Laboratory		12. REPORT DATE August 1979
		13. NUMBER OF PAGES 116
14. MONITORING AGENCY NAME & ADDRESS (if different from Controlling Office)		15. SECURITY CLASS. (of this report)
		15a. DECLASSIFICATION/DOWNGRADING SCHEDULE
16. DISTRIBUTION STATEMENT (of this Report) Distribution limited to U.S. Government agencies only; (test and evaluation). Other requests for this document must be referred to AFML/MBP, Air Force Materials Laboratory, Wright-Patterson AFB, Ohio 45433.		
17. DISTRIBUTION STATEMENT (of the abstract entered in Block 20, if different from Report)		
18. SUPPLEMENTARY NOTES		
19. KEY WORDS (Continue on reverse side if necessary and identify by block number) Polymer Solutions, Heterocyclic Polymers, Polysulfones, Pl700, RADEL, Reactive Plasticizers, Gas Chromatography, Piezoelectric Sorption, Ternary Mixtures, Phase Equilibrium, Flory Solution Theory.		
20. ABSTRACT (Continue on reverse side if necessary and identify by block number) Polymer/polymer and polymer/solvent interaction information can be obtained from solution thermodynamic studies. In this work, gas chromatography and piezoelectric sorption techniques were used to obtain experimental solution data. A brief review of experimental theory and practice is presented for both techniques.		

A solvent search for PBT using gas chromatography indicated several promising solvents, however, careful beaker tests at room temperature, 120 and 190°C established the absence of solvents other than the known strong acids. From this and previous work, we conclude that there is little chance of finding a viable organic solvent either for the most promising rigid rod polymers (PBT and PBO) or the "doctored" polymers (swivels or phenylated PBO's or PBT's).

Saturation concentration measurements for "good" solvents for Radel polysulfone indicate that chloroform is a viable low-boiling process solvent. We find that chloroform is capable of dissolving at least 20% by weight of Radel. DMF dissolves even larger amounts, but it has a much higher boiling temperature. Efficient solvent removal after processing is accomplished much more conveniently with a low-boiling solvent.

Relative rankings of solvents according to the strength of specific interactions with the PATS plasticizer are presented for 40, 70, and 100°C. This report presents only preliminary data; the final results will be given in the final report.

Phase equilibrium data for the P1700 polysulfone/ATS plasticizer/methylene chloride (MeCl) system were obtained using a piezoelectric sorption apparatus. Data were obtained for the P1700/MeCl and ATS/MeCl binaries, and for ternary mixtures containing 30% ATS and 70% P1700 by weight on a dry polymer basis. Measurements were made at 40 and 60°C at solvent partial pressures ranging from essentially zero to near the saturated vapor pressure of MeCl at the experimental temperatures. Liquid phase MeCl concentrations ranged from 0 to 15% by weight. The ATS/MeCl system displays Henry's law behavior, but the P1700/MeCl and ATS/MeCl mixtures do not. More detailed data analysis and a theoretical analysis will be presented in the final report.

The Flory theory for non-interacting polymers has been extended to the case of a ternary solution containing one polymer and two solvents. This theory is used to describe ternary solution data at finite solvent concentrations obtained by gas chromatography. Preliminary chromatography results for a tri- ϕ PBO/m-cresol/formic acid mixture at 190°C are presented to illustrate the experimental technique and the use of the theory.

PREFACE

This report is an account of work performed by the Texas A&M Research Foundation, College Station, Texas 77843, on polymer/polymer and polymer/solvent interactions. The work was conducted under contract F33615-78-C-5078 for the Air Force Materials Laboratory. The performance period was 1 June 1978 through 31 May 1979.

The work was performed in the Chemical Engineering Department of Texas A&M University with Dr. James C. Holste and Dr. Charles J. Glover serving as the principal investigators. The Radel work and the PBT chromatography investigations were done by Dr. D. T. Magnuson. The PBT beaker tests were performed by Mr. David R. Person under the direction of Dr. Magnuson. The P1700 polysulfone work was performed by Mr. K. C. Dangayach, while Mr. Ted A. Powell made the PATS measurements. Mr. Dominic Ching was responsible for the theoretical work on the ternary mixtures. The project engineer was Dr. Ivan J. Goldfarb, AFML/MBP, Air Force Materials Laboratory, Wright-Patterson AFB, Ohio.

TABLE OF CONTENTS

SECTION	PAGE
I INTRODUCTION	1
II EXPERIMENTAL TECHNIQUES AND THEORY	4
1. THERMODYNAMIC CONCEPTS AND DEFINITIONS	4
2. EXPERIMENTAL THEORY	15
3. EXPERIMENTAL TECHNIQUES	21
III PBT RESULTS	29
IV RADEL POLYSULFONE RESULTS	36
V PRELIMINARY PATS RESULTS	38
VI P1700 POLYSULFONE/ATS PLASTICIZER/DICHLOROMETHANE RESULTS	42
VII TERNARY MIXTURES	47
1. THEORY	48
2. EXPERIMENTAL	58
REFERENCES	64
APPENDIX	66

LIST OF ILLUSTRATIONS

FIGURE		PAGE
1	Gas Chromatography Apparatus	102
2	Schematic diagram of piezoelectric apparatus	103
3	Polymer and Plasticizer Structures	104
4	Solubility Parameter Plot Showing Energy of Specific Interactions for Solvents with PBT 2122-23 at 190°C	105
5	Distillation Apparatus Used for Solvent Purification	108
6	Reflux Apparatus Used for PBT Solubility Tests	109
7	Solubility Parameter Plot Showing Energy of Specific Interaction for Solvents with PATS at 40°C and 70°C	110
8	Solubility Parameter Plot Showing Energy of Specific Interaction for Solvents with PATS at 100°C	111
9	Solubility of Dichloromethane in P1700 Polysulfone as a Function of Pressure at 40°C and 60°C	112
10	Activity of Dichloromethane in P1700 Polysulfone as a Function of Solvent Weight Fraction at 40°C	113
11	Activity of Dichloromethane in P1700 Polysulfone as a Function of Solvent Weight Fraction at 60°C	114
12	Activity of Formic Acid in Triphenylated PBO as a Function of Solvent Weight Fraction	115
13	Activity of <u>m</u> -Cresol in Triphenylated PBO as a Function of Solvent Weight Fraction	116

LIST OF TABLES

TABLE		PAGE
1	Solvent Group Designations	78
2	Code Designations for Solvents	79
3	Physical Properties of Solvents at 25°C	81
4	Gas Chromatography Results for PBT at 463 K (190°C)	84
5	Reference Line Parameters for PBT Analysis at 190°C	89
6	Specific Interaction Parameters for Solvents Inter-acting with PBT at 463 K (190°C)	90
7	Beaker Test Results for Solvents on PBT	91
8	Saturation Concentrations of Radel Polysulfone in Various Solvents	92
9	Gas Chromatography Results for PATS Plasticizer at 313 K (40°C)	93
10	Gas Chromatography Results for PATS Plasticizer at 343 K (70°C)	94
11	Gas Chromatography Results for PATS Plasticizer at 373 K (100°C)	95
12	Reference Line Parameters for PATS Analysis	97
13	Specific Interaction Parameters for Solvents Inter-acting with PATS Plasticizer	98
14	Activity Expressions for Binary and Ternary Systems	99
15	Illustrative Gas Chromatography Data for Formic Acid/ <u>m</u> -Cresol/Triphenylated PBO System	100
16	Illustrative Phase Equilibrium Results for Formic Acid/ <u>m</u> -Cresol/Triphenylated PBO System	101

SECTION I

INTRODUCTION

The principal objective of the research described in this report is the investigation of polymer/polymer and polymer/solvent interactions for polymers of both short-term and long-term practical interest for use as structural materials. The general areas of interest are thermally-stable aromatic heterocyclic polymers, matrix polymer/plasticizer systems, and polymer/polymer miscibilities. Results of previous investigations of these systems have been given in three previous reports.¹⁻³ In this report, we give the results of experimental investigations for several polymers: a polybenzothiazol, two polysulfones, two sulfone-based plasticizers, and a polysulfone/plasticizer mixture. In addition, we present theoretical expressions that have been developed during this contract that describe the solution thermodynamics of a ternary mixture containing two solvents and one rigid-rod polymer.

Two experimental techniques were used in the investigations of the solution properties for the polymers of interest: gas chromatography and piezoelectric sorption.

¹Bonner, D.C., Holste, J.C., Glover, C.J., Magnuson, D.T., Eversdyk, D.A., and Dangayach, K., "Polymer-Polymer Interactions," AFML-TR-78-163, U.S. Air Force Materials Laboratory (1978).

²Bonner, D.C., "Determination of Solvents for Thermally Stable Polymers," ARML-TR-77-73, U.S. Air Force Material Laboratory (1977).

³Bonner, D.C., "Determinations of Solvents for Thermally Stable Aromatic Heterocyclic Polymers," ARML-TR-76-51, U.S. Air Force Materials Laboratory (1976).

The gas chromatography measurements are most useful for determining the relative strengths of interaction between a polymer and a large number of solvents, while the piezoelectric sorption apparatus provides the most efficient method for gathering phase equilibrium data between a solvent and one or more polymers at finite solvent concentrations. Gas chromatography also shows great potential as a method for investigating ternary mixtures containing two solvents and a single polymer, and we show in the report some illustrative data for this case. Further experimental improvements must be made to obtain acceptable results, but the required improvements appear to be well within the realm of possibility. The experimental techniques are described in some detail in Section II which is designed to present a review of our current experimental theory and practice. A brief review of the thermodynamic concepts and relations used in our work also is included in Section II.

The results for a complete gas chromatographic solvent scan for a polybenzothiazol polymer (PBT-2122-23) have been completed and are presented in Section III. In addition, preliminary beaker tests have been completed and are also reported; only a final series of beaker tests are required to complete the PBT investigations.

A complete solvent scan (determination of relative strengths of interaction between the solvents and the polymer) already has been reported¹ for the Radel polysulfone polymer. In Section IV we present the results of some determinations of saturation concentrations of Radel in several potentially useful processing solvents.

Acetylene-terminated reactive plasticizers are of interest for use with other matrix polymers or as thermosetting materials in their own right. We presently are investigating the interactions of a PATS plasticizer with a variety of solvents, and in Section V we present preliminary results for this plasticizer at several temperatures.

Polymer/polymer miscibility predictions are of extreme interest for predicting the phase behavior of polymer blends. We presently are determining the phase equilibrium behavior of a ternary mixture containing a polysulfone polymer (PI700), a reactive plasticizer (ATS) and a solvent (dichloromethane). The experimental measurements will be used to test various techniques for predicting the phase behavior of both polymer/polymer/solvent and polymer/polymer systems. The experimental results obtained to date on this system using the piezoelectric sorption device are presented in Section VI of this report, while some gas chromatography results were presented previously.²

The increased solubility of triphenylated PBO in mixtures of formic acid and m-cresol reported previously³ generated an interest in the measurement and theoretical description of ternary mixtures containing one polymer and two solvents. We have developed an extension of the Flory theory that is applicable to this case and attempted experimental verification by finite dilution gas chromatography. Unfortunately, experimental difficulties introduced sufficient uncertainty into the data to prevent a stringent test for the theory. The experimental results are presented in Section VII along with the theoretical results as an illustration of the nature of the phase equilibrium data that could be obtained with the gas chromatography technique. Further measurements on the particular system reported here are not planned because of decreased interest in triphenylated PBO as a structural material.

SECTION II

EXPERIMENTAL TECHNIQUES AND THEORY

In this section we present a general introduction to the thermodynamic concepts and definitions used in our work. We also present a summary of both the theory and practice of the experimental techniques used in our investigations.

1. THERMODYNAMIC CONCEPTS AND DEFINITIONS

The thermodynamic concepts to be discussed here may be found in a variety of textbooks and reference materials.⁴ The notation used varies widely with various authors, and we here use our own notation to develop the concepts of interest to our work.

a. General Thermodynamic Definitions

We begin with the statement that the fugacity of a component in solution is the same in liquid and vapor phases that are in equilibrium:

$$\hat{f}_i^v = \hat{f}_i^l. \quad (\text{II-1})$$

Here \hat{f}_i^v and \hat{f}_i^l are the fugacities of component i in solution in the vapor and liquid phases respectively. (This statement is equivalent to the statement that the chemical potentials for component i are identical in the liquid and vapor phases at thermodynamic equilibrium.) We then define the activity of component i by

$$a_i = \hat{f}_i / f_i^r, \quad (\text{II-2})$$

⁴See, for example, Smith, J.M., and Van Ness, H.C., Introduction to Chemical Engineering Thermodynamics, 3rd edition, McGraw-Hill (1975).

where f_i^r is a reference state fugacity. The reference state for the activity is completely arbitrary, and three different reference states will be used in the course of this work: f_i^o = pure saturated liquid solvent at the temperature of interest

$$= Z_i P_i^s \exp \left(\int_V^\infty (Z_i - 1) \frac{dV}{V} \right)$$

f_i^* = pure solvent vapor at 1 atmosphere pressure and the temperature of interest

$$= P^* \exp \left(\int_0^{P^*} (Z_i - 1) \frac{dP}{P} \right) = P^* \phi_i^*$$

f_i^h = Henry's law value
 $= H_i^w$

Here: Z_i = compressibility factor of pure component i

$$= \frac{PV}{RT}$$

P_i^s = saturated vapor pressure for pure component i at the temperature of interest

P^* = 1 atmosphere pressure

V = molar volume

H_i^w = Henry's law constant based on weight fractions in the liquid phase

P = pressure

The thermodynamic quantity of greatest interest usually is the activity of the solvent in the liquid phase. Combining Equations II-1 and II-2, and using the first reference state defined above produces:

$$a_{i0}^l = \hat{f}_i^l / f_i^o = \hat{f}_i^v / f_i^o. \quad (\text{II-3})$$

The fugacity of component i in solution in the vapor phase is most conveniently related to experimentally observable quantities:

$$\hat{f}_i^v = y_i \hat{\phi}_i^v P \quad (\text{II-4})$$

where: y_i = mole fraction of component i in the vapor phase

P = total system pressure

$\hat{\phi}_i^v$ = fugacity coefficient for component i in solution in the vapor phase.

Then, from Equations II-3 and II-4 we obtain:

$$a_{io}^\ell = y_i \hat{\phi}_i^v P / f_i^o. \quad (\text{II-5})$$

Polymer-solvent phase equilibrium information most often is described using activity coefficients based either on the weight fraction or the segment fraction of solvent in the liquid phase. The weight fraction activity coefficient Ω_i is defined by

$$\Omega_i = a_{io}^\ell / w_i = \hat{\phi}_i^v y_i P / w_i f_i^o = (\hat{\phi}_i^v P / f_i^o) K_i^w, \quad (\text{II-6})$$

where $K_i^w = y_i / w_i$ is the partition coefficient based on weight fraction. (It is the quantity K_i^w that is determined directly in gas chromatography measurements, and the quantity $K_i^w P$ that is obtained from the piezoelectric sorption apparatus.) The segment fraction activity coefficient Γ_i is defined by

$$\Gamma_i = a_{io}^\ell / \psi_i = y_i \hat{\phi}_i^v P / \psi_i f_i^o, \quad (\text{II-7})$$

where ψ_i , the segment fraction, is given by

$$\psi_i = w_i v_{isp}^* / (w_1 v_{1sp}^* + w_2 v_{2sp}^*). \quad (\text{II-8})$$

Here the quantity v_{isp}^* represents a specific characteristic volume reduction parameter for component i . Finally, phase equilibrium information also can be expressed using a Henry's law constant, where

$$H_i^w = y_i \hat{\phi}_i^v P / w_i = \hat{\phi}_i^v P / w_i = \hat{\phi}_i^v K_i^w P. \quad (\text{II-9})$$

For all the above expressions, w_i is the weight fraction of component i in the liquid phase, and P_i is the partial pressure of solvent in in the vapor phase.

The fugacity coefficient for component i in solution in the vapor phase is related to the vapor phase equation of state by

$$\hat{\phi}_i^v = Z_m \exp \left\{ \int_V^\infty \left[\left(\frac{\partial (nZ_m)}{\partial n_i} \right)_{T,nV,n_{j \neq i}} - 1 \right] \frac{dV}{V} \right\} \quad (\text{II-10})$$

where: $Z_m = \frac{PV}{RT}$ compressibility factor for the mixture,

n = total number of moles of substance present

n_i = number of moles of component i .

The compressibility factor for the mixture is best expressed in terms of the density version of the virial equation of state. For the pressure ranges involved in our work (less than 1 MPa), the density version of the virial equation provides an adequate description of the fluid behavior over a much wider range of temperatures than the pressure version if the series is truncated after two terms.

In general,

$$Z_m = 1 + B_m/V + C_m/V^2 + \dots \quad (\text{II-11})$$

where B_m and C_m are the second and third virial coefficients for the mixture.

Statistical mechanics provides exact mixing rules for these coefficients:

$$B_m = \sum_{i,j}^N y_i y_j B_{ij}, \quad (\text{II-12})$$

and

$$C_m = \sum_{i,j,k}^N y_i y_j y_k C_{ijk}, \quad (\text{II-13})$$

where N is the total number of components in the system. Expressions for $\hat{\phi}_1^V$ valid for the gas chromatography case and for the piezoelectric sorption case will be presented along with the theory for each individual apparatus.

b. Polymer Solution Theory

The description of a polymer solution is based on the assumption of a concentration-independent binary interaction parameter. Even though the interaction actually is not necessarily independent of concentration, the result is useful for describing actual experimental data. The expression that is most useful for our purposes was developed by Flory^{5,6} and is given by

$$\ln \left(\frac{a_{10}^{\ell}}{\phi_1} \right) = \left(\frac{y}{x_{12}} - \frac{1}{x_{12}} \right) \phi_2 + \frac{2}{y} + \chi_{12} \phi_2^2, \quad (\text{II-14})$$

where ϕ_1 is the volume fraction of component 1 in the liquid phase, y is an orientation parameter describing the degree of rigidity of the rod-like polymer, x_{12} is the ratio of the polymer molar volume to that of the solvent, and χ is the binary interaction parameter. In this and ensuing discussions, component 1 denotes the solvent and component 2 the polymer. The limits as $y \rightarrow 1$ and $y \rightarrow x_{12}$ yield the rigid-rod and the random-coil polymer cases respectively. For the respective extreme cases, the above expression reduces to:

Case I: (rigid rod)

$$\ln \left(\frac{a_{10}^{\ell}}{\phi_1} \right) = 2 + \chi_{12} \phi_2^2; \quad (\text{II-15})$$

⁵Flory, P.J., Proc. Roy. Soc., A234, 60 (1956).

⁶Flory, P.J., Proc. Roy. Soc., A234, 73 (1956).

Case II: (random-coil)

$$\ln \left(\frac{a_{10}^{\ell}}{\Phi_1} \right) = (1 - \frac{1}{x_{12}}) \Phi_2 + \frac{2}{x_{12}} + \chi_{12} \Phi_2^2. \quad (\text{II-16})$$

The weight fraction activity coefficient is related to the activity used here by

$$\left(\frac{a_{10}^{\ell}}{\Phi_1} \right) = \left(\frac{a_{10}^{\ell}}{w_1} \right) \left(\frac{w_1}{\Phi_1} \right) = \Omega_1 \left(\frac{w_1}{\Phi_1} \right), \quad (\text{II-17})$$

where (assuming ideal solution behavior in the liquid phase)

$$\frac{w_1}{\Phi_1} = \frac{w_1 + \frac{\rho_1}{\rho_2} w_2}{w_1 + w_2}. \quad (\text{II-18})$$

The case of the solvent at infinite dilution (the case most often encountered in gas chromatography) occurs at the limit as $w_1 \rightarrow 0$ and $w_2 \rightarrow 1$. We then obtain

$$\left(\frac{a_{10}^{\ell}}{\Phi} \right)^{\infty} = \Omega_1^{\infty} \rho_1 / \rho_2 \quad (\text{II-19})$$

$$\ln \left(\frac{a_{10}^{\ell}}{\Phi_1} \right)^{\infty} = 2 + \chi_{13}^{\infty} \quad (\text{rigid-rod}) \quad (\text{II-20})$$

$$\ln \left(\frac{a_{10}^{\ell}}{\Phi_1} \right)^{\infty} = 1 + \chi_{13}^{\infty} + \frac{1}{x_{12}} \quad (\text{random-coil}) \quad (\text{II-21})$$

or,

$$\chi_{13}^{\infty} = \ln \left(\frac{\rho_1}{\rho_2} \Omega_1^{\infty} \right) - 2 \quad (\text{rigid-rod}) \quad (\text{II-22})$$

$$\chi_{13}^{\infty} = \ln \left(\frac{\rho_1}{\rho_2} \Omega_1^{\infty} \right) - \left(1 + \frac{1}{x_{12}} \right). \quad (\text{random-coil}) \quad (\text{II-23})$$

Here the last two equations show explicitly how the interaction parameter at infinite dilution of solvent can be obtained from gas chromatography if the density of the solvent and the polymer are known. Note that different forms must be applied to the rigid-rod and random-coil cases. Furthermore, for polymers of appreciable molecular weight, $1/x_{12} \approx 0$. The explicit relations relating the parameters of interest to the variables actually observed in the experiment are given in the section describing each of the experimental techniques.

c. Solvent Scan Theory

The solvent scan procedure has two principal objectives: the determination of solvents in which the polymer undergoes dissolution, and the measurement of the relative strengths of interaction between the polymer and the individual solvents. In general, a strong interaction is required to overcome the combinatorial effects on the entropy of mixing and permit dissolution. The procedure is based loosely on the approach first described by Hildebrand and Scott⁷ where the concept of a solubility parameter is used. This solubility parameter δ represents the cohesive energy density of the condensed phase (in this case the liquid), and it is related to the internal energy change upon vaporization ΔU_v by

$$\delta = \left(\frac{\Delta U_v}{V} \right)^{1/2}, \quad (\text{II-24})$$

where V is the molar volume. The cohesive energy contains contributions from hydrogen bonding (or other specific interactions), interactions between

⁷Hildebrand, J.H. and Scott, R.L., The Solubility of Non-Electrolytes, p. 136, Reinhold (1950).

permanent dipole moments in the molecules, and interactions between induced dipole moments in the molecules (dispersion or van der Waal's forces). Hansen⁸ extended the method of Hildebrand and Scott by defining the solubility parameter in terms of components for each of the forces:

$$\delta^2 = \delta_p^2 + \delta_h^2 + \delta_d^2 \quad (\text{II-25})$$

where δ_d , δ_p and δ_h represent the dispersion, permanent dipole and hydrogen-bonding components of the solubility parameter. The general approach used by Hansen to predict solubilities was to require that each of these individual components of the solubility parameters for each component be equal, i.e., $\delta_p(1) = \delta_p(2)$, $\delta_h(1) = \delta_h(2)$ and $\delta_d(1) = \delta_d(2)$. The dispersion component is ignored in the present procedure, since the energies of induced dipole interactions will be much smaller than those associated with hydrogen-bonding or other specific interactions. Bonner³ has pointed out that the hydrogen bonding parameter may not be a reliable test for mixtures since the polymer/solvent specific interactions may differ appreciably from the solvent/solvent interactions represented by the δ_h value for the solvent. Instead, he proposes that an experimentally-determined interaction energy be used in place of the hydrogen bonding parameter of Hansen. Thus one criterion for solubility would be for both the solvent and the polymer to have identical values for δ_p and to have $\Lambda^{1/2}(\text{solvent}) = \delta_h(\text{polymer})$, where Λ represents the energy density associated with the specific interaction. The value of the polar solubility parameter can be estimated using the method of Beerbower⁸

$$\delta_p = 18.3\mu/V^{0.5}, \quad (\text{II-26})$$

⁸Hansen, C.N. and Beerbower, A., Encyclopedia of Chemical Technology, Supplement Volume 1971, p. 889, Wiley (1971).

and the specific interaction parameters are determined using a method to be described below. It is possible that even the criterion associated with the polar solubility parameter becomes unimportant if the specific interactions are sufficiently strong. Such a result may occur in the case of the Radel polysulfone¹, where the relative efficacy of the solvent appears to follow exactly the order of the relative specific interaction parameter, with no apparent dependence on the polar solubility parameter.

Bonner³ and his co-workers⁹ have defined a Gibbs energy of sorption by

$$\Delta G_{\text{ads}} = RT \ln \frac{a_1^{\ell}}{a_1^{\text{v}}} \quad (\text{II-27})$$

where $a_1^{\ell} = \hat{f}_1^{\ell}/f_1^{\text{h}}$ and $a_1^{\text{v}} = \hat{f}_1^{\text{v}}/f_1^*$. Note that different reference states are used for the liquid and vapor phases and that neither are the same as that used for the previous discussions of activity coefficients. Then, remembering that the fugacity of the component in solution is identical in the vapor and liquid phases, we obtain

$$\Delta G_{\text{ads}} = RT \ln \frac{f_i^*}{f_i^{\text{h}}} \quad (\text{II-28})$$

We note here that this definition of the energy of sorption compares the fugacity of the solvent as a vapor at one atmosphere pressure to the Henry's law fugacity for the component in the liquid solution. Then, recalling that $f_i^{\text{h}} = H_i^{\text{w}}$ and invoking Equation II-9, we obtain an expression for the Gibbs energy of sorption in terms of the experimental value $K_i^{\text{w}}P$:

$$\Delta G_{\text{ads}} = RT \ln \left(\frac{P^* \phi_1^*}{H_i^{\text{w}}} \right) = RT \ln \left(\frac{P^* \phi_1^*}{K_i^{\text{w}}P \hat{\phi}_i^{\text{v}}} \right) \quad (\text{II-29})$$

⁹Dangayach, K.C.B., "Solvent Determination for Thermally Stable Polymers -- PDIAB," M. S. Thesis, Texas Tech University (1976), unpublished.

The Gibbs energy of sorption defined above then is written as the linear combination of a term directly proportional to the polarizability, a term directly proportional to the permanent dipole moment, and a specific interaction contribution:

$$\Delta G_{\text{ads}} = G + a\alpha_1 + b\mu_1 + \Lambda_1, \quad (\text{II-30})$$

where G is a constant arising from the choice of reference state, α_1 is the polarizability, μ_1 is the permanent dipole moment, Λ_1 is the specific interaction parameter, and a , b are proportionality constants. The experimental procedure uses a number of non-polar solvents with no specific interactions to establish a dispersion contribution base line, i.e. the proportionality constant a . This contribution then is subtracted to yield the dipole and, specific interaction sum

$$\Delta G_{\text{add}} = b\mu_1 + \Lambda_1 = \Delta G_{\text{ads}} - a\alpha_1 - G. \quad (\text{II-31})$$

Then, a group of polar but not specifically interacting solvents is used to evaluate the proportionality constant b in the ΔG_{add} quantity. Considerable uncertainty may arise in this step because of the difficulty in determining whether or not specific interactions are present for a given solvent. In many cases, ethers appear to behave as non-specifically interacting polar compounds, but this probably is not generally true. Then, specific interaction parameters are calculated for the remaining solvents from

$$\Lambda_1 = \Delta G_{\text{add}} - b\mu_1. \quad (\text{II-32})$$

The solubility criteria following the method of Hansen then can be summarized as follows:

$$1). \quad \delta_d(\text{solvent}) \approx \delta_d(\text{polymer})$$

$$2). \quad \delta_p(\text{solvent}) \approx \delta_p(\text{polymer})$$

$$3). \quad \sqrt{\Lambda} \approx \delta_h(\text{polymer}).$$

(Values of δ_p and δ_h for the polymer may be estimated using the group contribution methods of Fedors.^{10,11}) In general, a substantial contribution must be obtained from the specific interactions to accomplish dissolution of the polymer. The solubility criterion only serve to identify potential solvents; beaker tests must be performed as a final step.

¹⁰Fedors, R.F., Polym. Eng. Sci., 14, 147 (1974).

¹¹Fedors, R.F., Polym. Eng. Sci., 14, 472 (1974)

2. EXPERIMENTAL THEORY

In this section we present brief discussions of the basic theory for each of the experimental techniques used in this work. The expressions relating the thermodynamic properties of interest to the observable variables encountered in gas chromatography or piezoelectric sorption measurements are presented in this section; the experimental apparatus and procedure will be discussed in a subsequent section.

a. Gas Chromatography

Many excellent references of gas chromatography are available,^{12,13} therefore our discussion here will be brief. Chromatography uses the response of a moving fluid phase in equilibrium with a stationary phase to a perturbation of the flowing phase to obtain thermodynamic properties of interest. In the case of gas chromatography, the flowing phase is a gas and the stationary phase may be either a liquid or a solid, and the perturbation of the flowing phase is accomplished by injecting a minute quantity of sample into the gas phase. The time required for the perturbation to traverse the column is related directly to the amount of interaction between the solvent and the stationary phase. (In our experiments the stationary phase is a polymer or plasticizer sample.) The additional time spent in the column by the perturbation (beyond the residence time of the inert carrier gas) due to solvent/stationary phase interactions is known as the retention time, and it is related directly to the slope of the equilibrium sorption isotherm.

¹²Purnell, H., Gas Chromatography, Wiley (1962).

¹³Littlewood, A.B., Gas Chromatography, 2nd ed., Academic Press (1970).

At infinite dilution (or for the case of finite solvent concentrations along a linear isotherm) the retention time is a direct measure of the equilibrium distribution (partition coefficient) between the phases in the column. For the experimental work reported here, we are interested only in the infinite dilution or linear isotherm cases. The partition coefficient then is related to the retention time by:

$$K_i^w = \frac{y_i}{w_i} = \frac{m_2}{M_1 F(t_g - t_a)}, \quad (\text{II-33})$$

where: K_i^w , y_i , and w_i have been defined previously,

m_2 = total mass of polymer in the chromatograph column,

M_1 = molecular weight of the injected solvent,

F = molar gas phase flow rate at column conditions,

t_g = elution time for the injected solvent sample,

t_a = elution time for injected inert sample, and

$t_g - t_a$ = retention time for the injected solvent.

The retention time sometimes is expressed as an equivalent gas-phase volume corrected to a reference temperature per mass of polymer. This specific retention volume is given by:

$$V_g^\circ = \frac{(t_g - t_a) F T_o R Z f_p}{m_2 T P_o} \quad (\text{II-34})$$

where:

T = column temperature

T_o = reference temperature (usually $0^\circ\text{C} = 273.2 \text{ K}$)

Z = compressibility factor of carrier gas at ambient conditions.

The volumetric flow rate at column conditions is related to the flow rate measured at ambient conditions by

$$F = \frac{QP_a}{RT_a} \quad (\text{II-35})$$

where:

- Q = volumetric flow rate measured at ambient conditions
- T_a = ambient temperature
- P_a = ambient pressure
- P_o = column outlet pressure,
- f_p = correction factor to obtain flow rate corresponding to the appropriate average column pressure.

For the measurements reported here, the column outlet always was exhausted to the atmosphere so that P_a = P_o, but we shall retain the last factor in Equation II-35 for the sake of completeness. The pressure correction factor is given by

$$f_p = \frac{3}{2} \frac{(P_i/P_o)^2 - 1}{(P_i/P_o)^3 - 1} \quad (\text{II-36})$$

where P_i is the inlet pressure to the chromatograph column. We then combine Equations II-33 through II-36 to obtain working relations for the partition coefficient:

$$K_i^w = \frac{m_2 T_a R}{M_1 P_a (t_g - t_a) Q}, \quad (\text{II-37})$$

and the specific retention volume:

$$V_g^o = \frac{(t_g - t_a) Q}{m_2} f_p \left(\frac{T_o}{T_a} \right) \left(\frac{P_a}{P_o} \right). \quad (\text{II-38})$$

With the partition coefficient now known, all that is necessary for the completion of Equations II-6 or II-9 is an appropriate expression for the fugacity of component in the vapor phase. For the case where the density virial expansion is truncated after the second term Equations II-10 through 12 lead to

$$\begin{aligned}\phi_i^v &= Z_m \exp \left(\int_v^\infty \left(2 \sum_j^N y_j B_{ij} \right) \frac{dV}{V^2} + \dots \right) \\ &= Z_m \exp \left(\frac{2 \sum_j^N y_j B_{ij}}{V} \right) = Z_m \exp \left(\frac{P}{Z_m RT} \left(2 \sum_j^N y_j B_{ij} \right) \right).\end{aligned}\quad (\text{II-39})$$

For the infinite dilution case, where the gas phase is essentially pure carrier gas, this result reduces to

$$\phi_i^v = Z_j \exp \left(\frac{2 P B_{ij}}{Z_j RT} \right) \quad (\text{II-40})$$

where component i is the injected solvent and component j is the inert carrier gas. Equation II-39 also reduces easily to the expression for the fugacity coefficient of a pure solvent vapor:

$$\phi_i^v = Z_i \exp \left(\frac{P B_{ii}}{Z_i RT} \right). \quad (\text{II-41})$$

Working relations for the various reference state fugacities now can be written down by inspection:

$$f_i^o = Z_i P_i^s \exp \left(\frac{B_{ii} P_i^s}{Z_i RT} \right) \quad (\text{II-42})$$

$$f_i^* = Z_i P^* \exp \left(\frac{B_{ii} P^*}{Z_i RT} \right) \quad (\text{II-43})$$

$$f_i^h = H_i^W = K_i^W P Z_j \exp\left(\frac{PB}{Z_j RT}\right). \quad (\text{II-44})$$

We have now provided the working relations required to calculate from infinite dilution gas chromatography data the activity coefficients, Gibbs energy of sorption, or Flory-Huggins interaction parameters as defined in the previous section. It should be noted that one must be careful not to confuse the carrier gas properties with those of the injected solvent sample, hence the need for detailed attention to the subscripts in the above relations.

b. Piezoelectric Sorption Apparatus

A single crystal of quartz exhibits a mechanical resonance when an electric field causes a shear stress in the crystal due to the piezoelectric effect. The resonant frequency of such a crystal depends not only on the mechanical properties of the quartz crystal, but also on the mass loading applied to the surface of the crystal. Sauerbrey¹⁴ has shown that the change in frequency is directly proportional to the mass loading, and therefore the weight fraction of solvent sorbed by the polymer may be given by

$$w_i = \frac{m_s}{m_s + m_p} = \frac{\Delta F_2}{\Delta F_1 + \Delta F_2}, \quad (\text{II-45})$$

where:

m_s = mass of solvent sorbed by polymer

m_p = mass of dry polymer applied to crystal

ΔF_1 = frequency change due to dry polymer coating

ΔF_2 = frequency change due to the solvent sorbed by the polymer.

¹⁴Sauerbrey, H.Z., Z. Phys., 155 206 (1959).

In this case, the vapor phase generally is pure solvent, therefore

$$\hat{\phi}_i^V = \phi_i^V = Z_i \exp\left(\frac{B_{ii}P_i}{Z_iRT}\right), \quad (\text{II-46})$$

and Equation II-9 becomes:

$$H_i^W = \frac{P_i Z_i}{w_i} \exp\left(\frac{B_{ii}P_i}{Z_iRT}\right). \quad (\text{II-47})$$

Here P_i is the partial pressure of solvent i in the vapor phase. The partial pressure generally is established by controlling the temperature of a liquid reservoir and using the Antoine equation to calculate the vapor pressure:

$$\ln P_i = A - B/(T_s + C) \quad (\text{II-48})$$

where T_s is the temperature of the saturated solvent reservoir, and A, B , and C are constants characteristic of the solvents. P_i and w_i therefore are determined easily with this apparatus, so that Equation II-47 can be used to calculate Henry's law constants directly. Weight fraction activity coefficients also can be obtained easily by noting that

$$\Omega_i = \frac{H_i^W}{f_i^O} \quad (\text{II-49})$$

where f_i^O is given by Equation II-42. Other desired forms for phase equilibrium data representation also can be obtained using the thermodynamic relations discussed above.

3. EXPERIMENTAL TECHNIQUES

In this section we describe the experimental techniques used in our investigations. The general thermodynamic concepts employed and the mathematical expressions relating the observed variables to the thermodynamic properties of interest are presented in an earlier section.

a. Gas Chromatography

Much information pertaining to gas chromatography is available in the literature, so we have cited only a few representative references.^{12,13} There also are many possible arrangements for gas chromatography measurements; we have used two such arrangements in our work.

The arrangement used for the PBT measurements is shown schematically in Figure 1a. In this case, the chromatograph oven contains two columns: the test column contains the polymer or plasticizer sample to be investigated, and the reference column contains an inert packing material. The sample material usually is coated on an inert substrate material, but on occasion solid polymer packings have been used.¹⁵ A constant carrier gas (helium) flow rate to the system is maintained by a flow controller (not shown) on the inlet line. The flow rate through the test column is measured using a soap bubble film flowmeter at the column outlet. Note that here one must be careful to attach the meter to the appropriate column to obtain meaningful results. The inlet flow rate also is monitored using a rotameter; this provides an indication of gross instabilities in flow rate that might occur

¹⁵Eversdyk, D. A., "Solvent Interactions with a Triphenylated Benzoxazole Polymer," M.S. Thesis, Texas A&M University (1977), unpublished.

during the actual experiment. The solvent trap prevents noxious, toxic, corrosive and carcinogenic solvents from escaping to the atmosphere. The sample is injected into the test column at the injection port (labeled I on Figure 1a), and its exit from the column is detected by the detector (D) at the outlet. The thermal conductivity type detector (TCD) compares the thermal conductivities of the test and reference outlet streams to detect the presence of the injected solvent. The TCD output is displayed continuously on a chart recorder and retention times are determined from the recordings. The flow rates through the test and reference columns must be approximately equal to provide balanced detector output. The flow rates in the respective arms are adjusted using the valves at the column inlets, but the procedure is cumbersome and time-consuming. The column inlet pressure is measured with a Bourdon-tube pressure gauge located outside the oven in the inlet line. The pressure drop across the valve at the head of the test column therefore must be minimized to obtain correct values for the column inlet pressure. In other words, the test column valve should remain wide open and adjustment should be made on the reference column arm. The column is exhausted to the atmosphere through low impedance lines, therefore the column outlet is at atmospheric pressure, which is measured using a barometer.

The PATS plasticizer measurements were made using the arrangement shown in Figure 1b. The reference column has been eliminated (along with the need for balancing flow rates), by routing the carrier gas first through the TCD, then through the column, and finally out through the TCD, solvent trap and soap bubble flow meter. With this arrangement the TCD detects the presence of solvent vapor by comparing the thermal conductivities of the intake and exhaust gases from the column, and the flow rates in both arms of the TCD are balanced

automatically. The flow rate through the system now is adjusted using the upstream flow controller (not shown); this is much easier than using a metering valve. In addition, ambiguity concerning the use of the soap bubble flow meter is removed, reducing the probability of operator error. The inlet and outlet temperatures are measured as before. The addition of a capillary by-pass (labeled C on Figure 1b) is a second significant modification to the apparatus. This by-pass allows a small fraction (ideally 5 to 10%) of the injected sample to by-pass the column and pass directly to the detector. The elution time for the portion by-passing the column is proportional to the dead volume outside the column, while the elution time for an inert sample passing through the column is proportional to the sum of the void volume in the column and the dead volume outside the column. The difference in elution times therefore provides a measure of the void volume actually in the column. In addition, manual marking of the injection time on the chart recording no longer is required, thereby eliminating another potential source of significant experimental error. The solvent injections for the PATS measurements were made between the TCD and the capillary by-pass, but these injections also could be made ahead of the TCD inlet. The latter arrangement could be used to detect problems associated with injection technique (these can cause significant errors in GC work).

The solvent injection pumps shown on Figure 1 were not used for either the PBT or PATS measurements, but they were used with the ternary system studies discussed in Section VII. A continuous injection of solvent into the heated inlet line provides a finite concentration of one or more solvents in the vapor phase. The steady-state condition in the column then consists of a

stationary phase in equilibrium with a vapor phase, where both phases contain a finite concentration of solvent. The response of the system to a perturbation of this steady state (a solvent injection) provides phase equilibrium information at finite solvent concentrations. Further discussion of the finite concentration experiment for a ternary system is presented in Section VII.

Several comments on experimental procedures and techniques are in order. First, the equations relating the chromatography results to phase equilibrium information are derived assuming zero pressure gradient along the column. The pressure drop across the column therefore must be kept as small as possible to obtain true thermodynamic information. Second, the derivations also depend upon the assumption that thermodynamic equilibrium is attained between the vapor and stationary phases. This requires that both the carrier gas flow rate and the solvent sample size be kept as low as possible. We have assumed that we are truly observing the equilibrium properties when we can detect no dependence of the results upon either the carrier gas flow rate or the sample size. In the case where the sample size dependence cannot be eliminated completely the results are extrapolated to zero sample size. Sample-size dependence occurs more frequently in glassy polymers, particularly for poor solvents, because the mass transfer process required to achieve thermodynamic equilibrium are hindered in the glassy state.

The most convenient injection procedure is to dip the tip of a one microliter syringe in the solvent of interest, extract the syringe from the solvent, dry the outside of the needle and then draw the needle full of air. The sample/air combination then is injected into the column. After the peak has eluted from the column, the syringe is drawn full of air and

another injection made. The procedure is repeated until there is no solvent in the injected air sample. Each of the successive peaks then represents a smaller sample size and several points for extrapolation to zero sample size can be obtained quite easily and rapidly.

In general, great care must be exercised to assure that equilibrium conditions actually are present in the column when making thermodynamic measurements using gas chromatography. This requires careful experimental procedure and frequent consistency checks. Gas chromatography can be a very powerful tool when used by the cautious experimenter, but it is worse than useless when used carelessly.

b. Piezoelectric Sorption Apparatus

The piezoelectric sorption apparatus is quite simple in principle. The dependence of the electromechanical resonance frequency of a quartz crystal on mass loading at the crystal surface is used to determine directly the weight fraction of solvent sorbed by a polymer exposed to a solvent vapor. (The relation between the weight fraction of sorbed solvent and the frequency decreases are given in Section II.2.b.) All that is required for this apparatus is a chamber for the crystal and source of solvent vapor.

The general measurement procedure is as follows:

- 1.) Measure the resonant frequency of the uncoated crystal, f_r^0 .
- 2.) Coat the crystal with polymer using a coating solution containing approximately 0.05% polymer by weight. A drop of coating solution is allowed to spread uniformly over the electrode surface.
- 3.) Dry the crystal in a vacuum oven until a constant resonant frequency (f_r^1) is obtained, indicating that all free solvent has been removed.
- 4.) Expose the crystal to a solvent vapor, allow the system to come to equilibrium, and measure the resonant frequency, f_r^2 . (Generally Step 4 is repeated several times to ensure the equilibrium value is obtained.)

The frequency changes appropriate to the analysis of the data (see II.2.b) are given by

$$\Delta F_1 = f_r^1 - f_r^0 \quad (\text{II-46})$$

and

$$\Delta F_2 = f_r^2 - f_r^1. \quad (\text{II-47})$$

The apparatus is shown schematically in Figure 2. The glass flask containing the sample is suspended in a temperature-controlled water bath and connected to a vacuum pump and to a liquid solvent reservoir through lines containing vacuum valves. The flask has an O-ring seal at the upper end to facilitate removal of the crystal mount for crystal replacement. The electrical leads to the crystal are tungsten wire to allow the fabrication of wire-glass bonds at the feedthroughs. The solvent reservoir is located in a separate temperature bath (a Dewar flask), and contains liquid solvent. The solvent partial pressure is controlled using the temperature dependence of the pure solvent saturated vapor pressure by adjusting the reservoir temperature. The only measurements required for use of this apparatus are two temperature measurements and one resonant frequency measurement. We generally use crystals with resonant frequencies of approximately 10 MHz, but the actual magnitude of the frequency is not important.

The polymer-coated crystal is placed in the sample chamber, and the sample chamber then is evacuated. The valve to the vacuum pump (#2) is closed and the solvent vapor is admitted by opening valve #1. The system is allowed to come to a stable frequency reading (usually in about three to ten minutes), the reading is recorded, and the procedure is reversed. Valve #1 is closed and valve #2 is opened, evacuating the sample chamber. Again, the system is allowed to stand until a stable frequency reading is obtained (this reading should correspond to that of the dry polymer coating on the crystal). The entire procedure is repeated several times until reproducible readings are obtained. The result is recorded, and the temperature of the liquid solvent reservoir is changed to provide a different solvent partial pressure.

This apparatus provides an economical and rapid means of obtaining phase equilibrium data for a single solvent at finite concentration in a polymer solution. It is similar in principle to the devices that use a quartz spring balance to measure the equilibrium sorption, but the piezoelectric sorption device achieves equilibrium in a matter of minutes compared to as long as days for the quartz spring devices. However, the piezoelectric sorption apparatus cannot be used to obtain phase equilibrium information for ternary mixtures where two solvents are present; gas chromatography appears to be the only viable technique for such investigations. In summary, the straightforward data analysis, the ease of operation, and the rapid data acquisition capability make this an extremely attractive apparatus for polymer/solvent phase equilibrium studies at finite solvent concentrations.

SECTION III

PBT RESULTS

The attractive mechanical properties of the polybenzothiazole polymer referred to as PBT make it a promising structural material. In addition, preliminary beaker tests indicating the possibility that organic solvents might be available for this polymer aroused considerable interest in this particular polymer. As result, more than 80 solvents have been investigated using gas chromatography and more than 50 relative specific interaction parameters have been measured. In this section we present the results for the gas chromatograph solvent scans and for a preliminary series of beaker tests. A second set of beaker tests must be completed to finish the PBT investigations.

The structure of the PBT polymer is shown in Figure 3. The sulfur atoms attached to the central benzene ring tend to skew the structure slightly, therefore making the nitrogen atoms slightly more accessible to potential solvents than in the polybenzoxazol polymers investigated in previous work.¹⁻³ The particular PBT sample investigated in this work was sample number 2122-23.

1. GAS CHROMATOGRAPHY RESULTS

The single solvent scan procedure described in Section II was used to investigate the interactions of a large number of solvents with the PBT polymer. Three separate columns were packed in the course of the work. The first exhibited an irreversible change in properties during a series of benzyl chloride injections. Measurements made before the change were reproducible, and measurements made after the change were reproducible, but the former did not agree with the latter. This effect has not been observed in any previous solvent scan, and we speculate that it probably was caused by the release of a small

amount of methanesulfonic acid (MSA) that had remained sorbed in the PBT polymer when the column was packed. Benzyl chloride exhibits a relatively strong interaction with the polymer, and this interaction may have stimulated the release of the residual MSA. A second column was packed but never used. Preliminary measurement indicated an abnormally large pressure drop across the column so it was repacked before the problem was traced to a plugged line near the detector block of our chromatograph. After several unsuccessful attempts at repair, the detector block and connecting lines were replaced, and a third column packed and mounted in the chromatograph. The remainder of the solvent scan work was done using this column.

The column packing material was prepared by dissolving PBT in MSA and then adding Chromo P packing with constant stirring. The mixture was heated to 136°C for 24 hours with occasional stirring, and the solvent was evaporated with continued stirring until the packing material was free-flowing. The material then was placed in an oven at 125°C and dried for 24 hours. The loading fraction for the column packing material was 9.6% by weight.

The first and second columns were nearly identical, each containing approximately 0.12 g of PBT in a two foot length of 1/8 inch O.D. stainless steel tubing. The third column contained considerably less PBT (0.02 g) in a 20 inch length of tubing, but the column behavior appeared to be satisfactory and many of the measurements were made using this column.

We have organized the list of potential solvents into groups and assigned an alphanumeric code designation to each of the individual solvents in an attempt to facilitate the graphical representation of the solvent scan results. The alphabetic symbol indicates the general class to which the solvent belongs, while the numeral identifies the specific solvent. The general classes of

solvents are identified along with their alphabetic designation in Table 1. The solvents are organized according to alphanumeric code in Table 2, and Table 3 contains a list of all solvents in alphabetic order along with the appropriate code designation. Hence, Table 2 is used to identify a solvent for which the code is known, while Table 3 is used to determine the code for a particular individual solvent.

The experimentally-determined retention volumes and Gibbs energies of sorption are given in Table 4 along with values for the weight fraction activity coefficient Ω_1 and the binary interaction parameter χ_1^∞ . The solvent physical properties required for the subsequent analysis are listed in Table 3. The nonpolar, nonspecifically interacting normal alkanes (heptane through decane) are used to determine G and a in Equation II-30. These values then are used in Equation II-31 to calculate values of ΔG_{add} for aliphatic compounds. For aromatic compounds, the ΔG_{ads} for benzene is used along with the slope obtained from the normal alkanes to establish a different value of G , then ΔG_{add} values are calculated as before. For this polymer, Equation II-31 becomes:

$$\Delta G_{\text{add}} = \Delta G_{\text{ads}} + 31.90 - 0.95 \times 10^{-18} \alpha_1 \quad (\text{aliphatic compounds}) \quad (\text{III-1})$$

$$\Delta G_{\text{add}} = \Delta G_{\text{ads}} + 28.51 - 0.95 \times 10^{-18} \alpha_1 \quad (\text{aromatic compounds}). \quad (\text{III-2})$$

The choice of solvents used to establish the value of the dipole moment proportionality constant (b in Equation II-32) is somewhat difficult and a bit arbitrary. Appropriate solvents should have permanent dipole moments but not exhibit specific interactions, however the absence of specific interactions is somewhat hard to ascertain. In this case we have used the solvents 1-octene, methyl ethyl ketone, and methyl isobutyl ketone to determine that $b = 0.306 \times 10^{30}$ kJ/mole-C-m, so that Equation II-32 becomes

$$\Lambda = \Delta G_{\text{add}} - 0.306 \times 10^{30} \mu_1. \quad (\text{III-3})$$

Equation III-3 then is used to calculate specific interaction parameters for each of the solvents not used as a reference solvent in the determination of the proportionality constants. These values also are listed in Table 4 along with the calculated ΔG_{add} results.

The proportionality and additive constants are summarized in Table 5. The intercept for the dispersion line is G , while the slope yields a . The slope of the permanent dipole reference line yields b , while the intercept should be zero. The departure of the dipole intercept from zero provides some information about the residual uncertainty in the determination of G . We note that for the PBT case, the residual uncertainty is less than one per cent of the intercept for the dispersion reference line.

The experimentally-determined values for the specific interaction parameter for each solvent are listed in Table 6 in order of decreasing interaction strength. The solvents marked with the asterisks were included in the first series of beaker tests (to be described later) along with some solvents that were not included in the chromatographic tests because of various undesirable physical properties. The values of $\sqrt{\Lambda}$ are plotted as a function of the solvent δ_p in Figure 4. Values of δ_p and δ_h for the polymer (estimated by the method of Fedor^{10,11}) are indicated on Figure 4 as well. The solvents whose interaction parameters lie in the rectangle described by the extremum estimates for $\delta_p(\text{polymer})$ and $\delta_h(\text{polymer})$ are the most likely candidates as potential solvents for the polymer, but particularly in the case of the rod-like polymers any solvent with a large specific interaction parameter must be checked in beaker tests. We have completed one series of beaker tests on potential

solvents, but another series of beaker tests will be required to complete the PBT solvent scan.

2. BEAKER TESTS

The first series of gas chromatographic results on the PBT polymer indicated strong interactions for benzyl chloride, o-chlorophenol, methanol, ethanol and brombenzene. One dozen solvents, including the above and several additional solvents whose physical or chemical properties made them undesirable for chromatographic testing were sealed in glass tubes along with one or two flakes of the PBT polymer. The solvent/polymer mixtures were observed for one week at ambient temperature, followed by six hours at 120°C and three hours at 190°C.

The results of these beaker tests are summarized in Table 7. The substantial color changes observed in the liquid phase in the benzyl chloride and o-chlorophenol cases originally were interpreted as dissolution of the polymer. This apparently positive result suggested a number of additional solvents for the chromatography solvent scan, which then were investigated.

A second series of beaker tests with o-chlorophenol and benzyl chloride was made to verify the first set. For this series we attempted to develop a reusable seal for sealed beaker tests using vial caps and Teflon film or silicon rubber septa, but after repeated unsuccessful attempts, the reusable seal concept was abandoned and we returned to sealed glass tubes. Blank tests were also made to determine whether the discoloration in the liquid phase might be due to solvent oxidation or decomposition at the relatively high temperatures encountered in the previous test.

When it was found from these blank tests that both benzyl chloride and

o-chlorophenol exhibited substantial color changes when sealed in the tubes with no polymer present, extensive measures were developed to remove dissolved oxygen from the solvent samples used in the beaker tests. Both solvents were distilled under an inert atmosphere (nitrogen gas) using the apparatus shown in Figure 5. The steady flow of nitrogen gas prevents oxygen from contacting the solvent, and after the second distillation we sealed these solvents (still under nitrogen) in glass tubes. During the first distillation a dark residue remained in the boiler, but no such residue was observed after a second distillation. The doubly-distilled solvents sealed into a nitrogen-filled tube then did not discolor noticeably even when exposed to the high temperature for much longer periods of time than in the previous beaker tests.

The de-oxygenated solvents then were used in beaker tests with the polymer. Benzyl chloride and PBT were sealed successfully in a tube without including oxygen. After the benzyl chloride/PBT sample had been maintained at 190°C for several days, the PBT surface had discolored slightly, but no noticeable discoloration of the liquid phase occurred. The surface discoloration indicated a reasonably strong interaction, but no dissolution was observed.

Two similar attempts with o-chlorophenol/PBT samples failed because the more viscous solvent was not able to displace oxygen trapped among the PBT flakes as the tube was filled. Consequently, a new apparatus was constructed to reflux the o-chlorophenol containing the PBT flakes without exposure to oxygen after the distillation. The reflux apparatus is shown in Figure 6. The reflux condensers prevent the evaporating o-chlorophenol from entering the atmosphere, and the dry nitrogen stream prevents oxygen and water from contacting the solvent. Here the second distillation of solvent is condensed directly into a vial containing the PBT sample. The system then is arranged

as shown, and the polymer is exposed to boiling solvent under an inert atmosphere. After eight hours at the boiling point of o-chlorophenol (175°C) no color change was observed in the liquid phase although the polymer surface again had discolored.

The careful series of beaker tests described here show that the preliminary conclusion that dissolution had occurred in the benzyl chloride and o-chlorophenol solvents was erroneous. These solvents do exhibit strong interactions with the polymer, but they do not effect dissolution. We have begun a series of beaker tests (including solvent blanks) to investigate the solvents showing stronger specific interactions with the PBT than o-chlorophenol. These tests should be completed soon, and they will complete the solvent scan work on the PBT polymer.

SECTION IV

RADEL POLYSULFONE RESULTS

Radel is a commercially-available (Union Carbide) polysulfone polymer which has attractive mechanical and thermal properties in addition to a high glass transition temperature and excellent resistance to water degradation. The structure of this polymer is shown in Figure 3. We previously have reported¹ complete solvent scan results for this polymer which identified several potential solvents, including some with low boiling points.

Since viable solvents for actual processing operations must be capable of dissolving substantial amounts of polymer, we have investigated the saturation concentrations at ambient temperature of Radel in the solvents identified in the previous solvent scan. The solution behavior was investigated by first weighing a small amount of Radel (0.01 to 0.99 g) in a weighing vial. After adding solvent to the vial and closing the cap, the mixture was weighed again to determine the mass of solvent added. The vial was shaken vigorously to facilitate dissolution, and a determination as to whether or not dissolution occurred was made visually. In some cases (which will be noted), unambiguous determinations of complete dissolution were not always possible. The procedure then was repeated for increasing concentrations until dissolution no longer could be effected.

The results of the saturation concentration tests are summarized in Table 8. The boiling points of the solvents also are listed in this table, along with the various concentrations tested for each solvent. In each case, the presence of polymer in the liquid solution was verified by placing a drop

of solution on a microscope slide or between two microscope slides. The solvent was allowed to evaporate, leaving behind a polymer film. The solubilities in the three non-viable solvents (1,2-dichloroethane, tetrahydrofuran and furan) are so small that the colored diffraction patterns associated with very thin films could be observed in the residual polymer film. As a result, these solvents are not considered promising for processing operations. The dichloromethane (methylene chloride) results are somewhat ambiguous because in this case it was difficult to determine whether or not dissolution has occurred. In all cases a cloudy white precipitate appeared after the mixture had set in the vial for a few minutes. The 15.5% mixture was very viscous and may not have been completely dissolved; further investigations under a microscope would provide useful information in this case. As a result, dichloromethane is a borderline processing solvent: the solubilities are not particularly high, but its low boiling point (40°C) is a considerable advantage in solvent removal procedures. The solvent recommended by the manufacturer (N,N-dimethyl formamide) has very high solubilities, but the high boiling point of this solvent makes solvent removal difficult at best. The most attractive solvent appears to be chloroform. It is capable of dissolving 20% by weight of polymer, yet its boiling point is relatively low (61°C).

We conclude from these studies that trichloromethane (chloroform) is a viable process solvent for the Radel polysulfone. It is particularly attractive for operations where solvent removal is important because its boiling point is much lower than that of N,N-dimethyl formamide. DMF, however, appears to be the most attractive solvent when considered strictly on the basis of total solubilities.

SECTION V

PRELIMINARY PATS RESULTS

The attractive thermal and mechanical properties of polysulfones and their relatively high glass transition temperatures make them somewhat difficult to form into desired shapes. An alternative to the solvent dissolution considered in the previous section is to use a reactive plasticizer to lower the glass transition temperature until forming is completed. The plasticizer then is reacted by raising the temperature, this results in a composite material with a high transition temperature. Since the plasticizer and polymer must be miscible to avoid phase separation during the curing process, plasticizers with structures similar to that of the polymers provide a reasonable beginning point.

Solvent specific interaction parameters for plasticizers are of interest both for the identification of potential solvents and for potential future use in predicting miscibility behavior of plasticizers with various polymers. In this report we present measurements on two sulfone-based plasticizers with acetylene end-groups providing the reactive nature of the material. In this section we present the results of a partially-complete solvent scan for a PATS plasticizer, while the following section contains phase equilibrium data for the ATS plasticizer. The structures for both of these compounds are given in Figure 3.

Because of the reactive nature of the plasticizer, one must work at the lowest possible temperature. Unfortunately, solvents with relatively high boiling points are not measured easily in a chromatograph at temperatures significantly below their boiling points. Our approach is to first investi-

gate all solvents useable at 40°C, then increase the column temperature to 70°C and inject all solvents which can be tested at that temperature. Measurements at 40°C are then repeated, followed by injections made at 100°C, 40°C, 130°C, 40°C, and 160°C. The repeated measurements at 40°C provide an indication of curing in the plasticizer if it occurs. Kinetic data for this system lead us to expect little polymerization of plasticizer below 160°C, but the approach described above eliminates the possibility of ambiguous data due to undetected reactions in the plasticizer. We have completed runs at 40, 70, and 100°C for two columns packed with the PATS plasticizer. The agreement between results from the two columns is quite satisfactory and as yet no appreciable alteration of the solvent interaction due to plasticizer curing has been observed.

The experimentally-determined specific retention volumes and Gibbs energies of adsorption at 40, 70, and 100°C are listed in Tables 9, 10, and 11 respectively. The values of Ω_1^∞ and χ_1^∞ listed have been calculated assuming $\hat{\phi}_1^v$ and ϕ_1^v to be unity; this assumption introduces only about 5% uncertainty and provides a substantial savings in computational time and complexity. The nonpolar, nonspecifically interacting normal alkanes (pentane through heptane in this case) were used to determine values of G and a in Equation II-30 for each temperature. Then Equation II-31 in the following form is used to calculate ΔG_{add} :

$$\Delta G_{\text{add}}(40^\circ\text{C}) = \Delta G_{\text{ads}} - \begin{Bmatrix} 25.22 \\ 23.8 \end{Bmatrix} - 1.62 \times 10^{18} \alpha_1 \begin{Bmatrix} \text{aliphatics} \\ \text{aromatics} \end{Bmatrix} \quad (\text{V-1})$$

$$\Delta G_{\text{add}}(70^{\circ}\text{C}) = \Delta G_{\text{ads}} - \begin{Bmatrix} 29.64 \\ 26.8 \\ 27.7 \end{Bmatrix} - 1.54 \times 10^{18} \alpha_1 \begin{Bmatrix} \text{aliphatics} \\ \text{aromatics} \\ \text{cyclics} \end{Bmatrix} \quad (\text{V-2})$$

$$\Delta G_{\text{add}}(100^{\circ}\text{C}) = \Delta G_{\text{ads}} - \begin{Bmatrix} 28.49 \\ 26.0 \\ 26.4 \end{Bmatrix} - 1.14 \times 10^{18} \alpha_1 \begin{Bmatrix} \text{aliphatics} \\ \text{aromatics} \\ \text{cyclics} \end{Bmatrix} \quad (\text{V-3})$$

ΔG_{add} values obtained using Equations V-1 through V-3 also are listed in Tables 9 through 11. A few polar materials which were assumed to have no specific interactions (generally ethers) were used along with the nonpolar reference solvents to determine values of the dipole moment proportionality constant b for each temperature. These values of b then were used to generate the following forms of Equation II-32 for calculating PATS specific interaction parameters:

$$\Lambda = \Delta G_{\text{add}} - \begin{Bmatrix} 0.530 \\ 0.572 \\ 0.048 \end{Bmatrix} \times 10^{30} \mu_1, \text{ for } \begin{Bmatrix} 40^{\circ}\text{C} \\ 70^{\circ}\text{C} \\ 100^{\circ}\text{C} \end{Bmatrix}. \quad (\text{V-4})$$

The resulting specific interaction parameters are shown for each solvent in Table 9 through 11.

The proportionality and additive constants are summarized for all temperatures in Table 12, along with compounds used to determine them. The values are listed as slopes and intercepts since they were determined from plots of ΔG_{ads} vs α_1 and ΔG_{add} vs μ_1 . The intercept for the dispersion reference line is G , while the slope is a . The slope of the dipole line gives b and the intercept should be zero. Residual values in the dipole intercept provide some information about the uncertainties in the determinations of the G values. The dispersion lines for the aromatic and cyclic compounds were

assumed to have the same slope as the aliphatic compounds, and an experimental datum was used to determine G.

The specific interaction parameters for solvents interacting with the PATS plasticizer are presented in order of decreasing interaction strength for all temperatures in Table 13. Plots of \sqrt{A} vs δ_p are shown in Figure 7 and 8. Group contribution parameters for the sulfone group are not available, so we cannot estimate δ_p and δ_h for the plasticizer. We do note however, that in the case of the Radel polysulfone¹, the solvent rankings followed essentially the same ranking as the specific interaction parameter. As in previous investigations, alcohols, chlorinated hydrocarbons, and amines are the group exhibiting the largest specific interactions.

Future efforts on the PATS material will include attempts to investigate the uncured material at 130°C and 160°C, although in the latter case we may not be able to complete the measurements before appreciable polymerization occurs. The interactions of the solvents with the cured plasticizer also will be measured at one temperature for comparison with the results for the uncured material. Finally, beaker tests must be performed on the solvents with the largest specific interactions to complete the PATS solvent scan. These measurements currently are in progress.

SECTION VI

Pl700 POLYSULFONE/ATS PLASTICIZER/DICHLOROMETHANE RESULTS

Polysulfone polymers have attractive mechanical and thermal properties, therefore they are of considerable interest as structural materials, particularly as matrix resins for composite materials. These polymers are difficult to form into desired shapes because of their high glass transition temperatures (T_g), so the use of a plasticizing additive to reduce T_g during processing is advantageous. After the forming is completed, an appropriate plasticizer can be reacted to form longer chains and increase T_g substantially. During the reaction process, which is usually activated by increased temperature, the polymer and the plasticizer must remain in a single phase. The study of miscibility behavior in polymer/plasticizer systems therefore is of considerable current interest. The physical properties of Radel are more suitable for a working polymer than those of Pl700, but we have chosen to begin our ternary solution studies with the Pl700/ATS system since it is thought to remain in a single phase region over the entire range of polymer concentrations. We shall establish a base of knowledge and a theoretical approach using this totally miscible system, before extending our studies to more difficult systems (such as Radel/ATS) which are not necessarily miscible over the entire concentration range.

The structures of the Pl700 polysulfone polymer and the ATS (acetylene-terminated sulfone) plasticizer are shown in Figure 3. (The reactive nature of the plasticizer is due to the acetylene end-groups.) Detailed GC solvent scan results were presented for polysulfone in the 1978 final report¹, and

some GC results for P1700, ATS and one mixture of the two were reported in 1977². In this section we report results obtained for P1700 and ATS at finite concentrations of dichloromethane using a piezoelectric sorption apparatus. We have measured P1700/dichloromethane solutions, ATS/dichloromethane solutions, and a ternary solution containing ATS and P1700 in the ratio of 3 to 7 by weight (30 wt % ATS on a dry-polymer basis). Our latest results indicate that the infinite dilution GC results are not the most appropriate information for miscibility predictions, for reasons that soon will become apparent.

The P1700/dichloromethane results at both 40 and 60°C are shown in Figure 9. Here we have plotted the solubility of the vapor in the polymer as a function of the solvent partial pressure. The solubility is presented as a volume of vapor (at standard temperature and pressure) per volume of polymer. The nonlinear behavior below 5 kPa (40 mm Hg) is typical of sorption processes that involve adsorption phenomena as well as absorption.^{16,17} The adsorption here involves solvent molecules that are immobile in the polymer phase (but not necessarily located at the surface as is the case in most adsorption processes). In fact, we have shown by repeating the measurements on crystals with various polymer-coating thicknesses that this is not a surface effect, and it does in fact represent immobile molecules in the bulk phase. These effects occur primarily below T_g , where relaxation times at the molecular level are very long. The linear variation with partial pressure observed

¹⁶Barrer, R.M., Barrie, J.A., and Slater, J., J. Poly. Sci., 27, 177 (1958).

¹⁷Michaels, A.S., Vieth, W.R., and Barrie, J.A., J. Appl. Phys., 34, 1 (1963).

at the higher pressures is typical of solutions obeying Henry's law. Here we are looking principally at the contributions of solvent molecules that are mobile in the polymer phase. The usual solution description theories are applicable only to the latter, and the effects due to the immobile molecules first must be subtracted. It is obvious that since infinite dilution gas chromatography samples the behavior at infinite dilution, GC results will be most sensitive to the adsorption process and they cannot be used with confidence in the solution theory. Instead, measurements at finite solvent concentrations are required to obtain information about the true solution properties of this system.

The solvent activities at 40°C and 60°C for the P1700/dichloromethane, ATS/dichloromethane and P1700/ATS/dichloromethane systems are shown in Figures 10 and 11 respectively as a function of the weight fraction of solvent in the condensed phase. Again, the adsorption-like behavior is shown by a nonlinear behavior at low solvent concentrations for the case of P1700/dichloromethane. At higher concentrations, the linear dependence again indicates Henry's Law behavior. The ATS/dichloromethane system obeys Henry's law over the entire range, indicating that adsorption-type effects are not important here. This is not surprising since the plasticizer is above its glass transition temperature. The results for the ternary mixture lie between those of the pure materials, and they resemble the polysulfone most closely at low concentrations, while at high concentrations they tend to approach the plasticizer values. The mixture is in its glassy state also, so the adsorption contribution is not unexpected.

To fully utilize the information described above, we must develop an analysis procedure that will allow us to subtract the adsorption contribution from the

data before applying the standard solution theories. Then, binary interaction parameters can be determined for Pl700/dichloromethane and ATS/dichloromethane using the binary solution data. The binary values obtained in this fashion then can be used with the ternary solution data to determine a binary parameter for the Pl700/ATS interaction. The Pl700/ATS binary interaction parameter (χ_{23}) is most useful information for developing polymer miscibility predictions. The relative magnitudes of the Pl700/ATS and the Radel/ATS interaction parameters should yield important information about the range of χ_{23} values that correspond to complete miscibility in polymer/plasticizer mixtures. We currently are completing the analytical technique and soon will begin measurements of Radel systems.

The results presented in this section indicate that phase equilibrium data at finite solvent concentrations are required to eliminate adsorption-like effects in order to derive appropriate binary interaction parameters from the conventional solution theories. Such finite concentration data can be obtained efficiently and accurately from a piezoelectric sorption device for both binary and ternary mixtures. (The device is applicable only if there is only one volatile component in the ternary mixture.) As a result, it is particularly straightforward to obtain information pertaining to polymer/plasticizer miscibilities with this apparatus. The finite concentration data presented here also indicate that gas chromatograph data obtained at infinite dilution for polymers or polymer/plasticizer mixtures in the glassy state would be of little use in determining binary interaction parameters for use in miscibility predictions. (At infinite dilution, the GC principally samples the adsorption effects rather than the actual solution effects.)

In summary, the gas chromatograph then is most useful for determining relative strengths of solvent/polymer interactions (solvent scans), for investigating the infinite dilution solution properties of polymers above the glass transition, and for phase equilibrium measurements in ternary systems containing two volatile components. On the other hand, the piezoelectric sorption apparatus provides the most efficient method for studying the solution properties pertaining to polymer/plasticizer miscibilities and for phase equilibrium measurements at finite concentrations of a single volatile solvent.

SECTION VII

TERNARY MIXTURES

The observation in earlier phases of this work^{1,15} that mixtures of m-cresol and formic acid effected dissolution of a triphenylated-PBO sample when neither of the individual solvents succeeded has prompted further interest in the thermodynamic behavior of ternary solutions. As a result, we have investigated both the theory of mixtures containing a rod-like polymer and two solvents, and an experimental technique for the study of the thermodynamic properties of such mixtures. The theoretical treatment has been completed, and it complements the recent series of papers by Flory¹⁸⁻²² on the solution thermodynamics of various solutions containing rod-like polymers. The experimental technique is still under development, but we present here preliminary results which indicate the nature of the data that can be obtained with such a technique.

¹⁸Flory, P.J., and Abe, A., Macromolecules, 11, 1119 (1978).

¹⁹Abe, A., and Flory, P.J., Macromolecules, 11, 1122 (1978).

²⁰Flory, P.J., and Frost, R.S., Macromolecules, 11, 1126 (1978).

²¹Frost, R.S., and Flory, P.J., Macromolecules, 11, 1134 (1978).

²²Flory, P.J., Macromolecules, 11, 1138 (1978).

1. THEORY

Many polymer solutions show pronounced deviation from ideality even at polymer concentrations of one percent or less. These deviations are due to enthalpy and entropy effects which arise from the large differences in size between solvent and solute molecules. Flory^{6,23} proposed a theory of equilibrium properties for polymer solutions based on a lattice model which accounts for the chain-like nature of polymer molecules. The development of the Flory thermodynamic equations for rod-like polymer solutions containing two solvents is as follows. A partition function Q_M for a system of rigid rod-like particles with partial orientation about an axis was derived assuming: (1) equal probability of occupancy of lattice sites by polymer segments and thus no gathering of polymer; and (2) random occurrence of '1' and '2' molecules and holes in the remainder of the lattice. The lattice model is limited in that it does not allow for variations in volume due to mixing effects and changes in external pressure.

The basic approach consists of computing the microcanonical ensemble partition function Q_M for a lattice model containing n_0 sites of which n_3 are of polymer, n_1 are of solvent 1, and n_2 are of solvent 2. Each of the solvent molecules is taken to occupy a single lattice site while the polymer chains will occupy a series of adjacent sites. The number of segments in a chain, x , is defined by the ratio of the molar volumes of the polymer and the solvent. A rod-like molecule inclined at an angle ψ to the orientation

²³Flory, P.J., Principles of Polymer Chemistry, Cornell University Press, 1953.

axis will be divided into $y = x \sin \psi$ submolecules, each containing x/y segments and requiring therefore x/y vacant lattice cells.

Flory shows that the number of distinguishable ways that the $(j+1)$ th polymer molecule can be arranged on the lattice is given by

$$v_{j+1} = (n_o - xj) \left[\frac{n_o - xj}{n_o - xj + \sum_{i=1}^j y_i} \right]^{(x-y_{j+1})} \left(\frac{n_o - xj}{n_o} \right)^{y_{j+1}-1}$$

$$= (n_o - xj)^x / [(n_o - xj + yj)^{x-y_{j+1}} (n_o)^{y_{j+1}-1}]. \quad (\text{VII-1})$$

Let the distribution of orientations of the solute molecules be represented by the number n_k . Then:

$$Q'_M = q_1^{n_1} q_2^{n_2} q_3^{n_3} \prod_{j=1}^{\infty} v_j / \prod_k n_k!.$$

Then,

$$Q'_M = Q_M / q_1^{n_1} q_2^{n_2} q_3^{n_3}$$

leads to:

$$Q_M = \left[\frac{(n_o - xn_3 + yn_3)!}{(n_o - xn_3)! n_o^{(y-1)n_3}} \right] \frac{(n_o - xn_3)! n_3!}{n_1! n_2! n_3! \prod_k n_k!} \quad (\text{VII-2})$$

Flory⁶ shows that

$$\frac{n_3!}{\prod_k n_k!} = y^{2n_3},$$

hence,

$$Q_M = \left[\frac{(n_o - xn_3 + yn_3)!}{n_o^{(y-1)n_3} n_1! n_2! n_3!} \right]^y n_3^{2n_3}. \quad (\text{VII-3})$$

The Gibbs energy of mixing, ΔG^M , is given by:

$$\Delta G^M = \Delta H^M - T\Delta S^M \quad (\text{VII-4})$$

where ΔH^M is the enthalpy of mixing and ΔS^M is the entropy of mixing. For a material to dissolve in a solvent, the Gibbs energy of mixing must be negative for the process. The entropy of mixing in rod-like polymer solutions generally is strongly negative, so that the heat of mixing determines whether dissolution occurs or not. If ΔH^M is zero or negative, dissolution may take place. A general expression for the Gibbs energy of mixing can be given as a function of the mole numbers, the axis ratio of the solute particles, and a disorientation parameter. The noncombinatorial contribution to the Gibbs energy of mixing, ΔH^M , may be taken to be proportional to the product of the number of molecules of one type and the volume fraction (ϕ_1) of the other. $RT\chi$ is that part of the change in Gibbs energy attributable to segment-solvent contacts which occur upon transferring a mole of solvent from pure solvent to a large amount of polymer ($\phi_3=1$), i.e.

$$\Delta H^M = RT\chi n_3 \phi_1. \quad (\text{VII-5})$$

The entropy is related to the number of distinguishable microscopic states

accessible to a system,

$$\Delta S^M = k \ln Q_M. \quad (\text{VII-6})$$

In 1956, Flory⁶ published a lattice theory for solutions of semi-flexible and rod-like polymers in a single solvent. We extend the Flory treatment to solutions containing two solvents and one rod-like polymer. Further derivations are divided into sections dealing first with binary and then with ternary mixtures. The general derivation is presented here; the mathematical detail is contained in the Appendix.

a. Binary System

When the Flory theory for binary system containing rod-like polymers is applied the Gibbs energy of mixing can be represented by Equation A-5, Appendix:

$$\begin{aligned} \frac{\Delta G^M}{RT} = & \left\{ n_1 \ln \phi_1 + n_3 \ln \phi_3 - (n_1 + y n_3) \ln \left[1 - \phi_3 \left(1 - \frac{y}{x_{13}} \right) \right] \right. \\ & \left. - n_3 \left[\ln(x_{13} y^2) - y + 1 \right] \right\} + \left(n_1 x_1 \phi_3 \chi \right). \end{aligned} \quad (\text{VII-7})$$

Here χ is an interaction parameter, ϕ_1 and ϕ_3 are volume fractions given by

$$\phi_1 = \frac{x_1 v_1}{x_1 v_1 + x_3 v_3},$$

$$\phi_3 = 1 - \phi_1,$$

where n_1 and n_3 refer to the number of moles of solvent and polymer, respectively, and v_1 and v_3 are the specific volumes of the solvent and the polymer, respectively. The term x_{13} is the ratio between the polymer molar volume and the solvent molar volume, given by the equation

$$x_{13} = \frac{M_3 \rho_1}{M_1 \rho_3}, \quad (\text{VII-8})$$

where M_3 is the number average molecular weight at the polymer, M_1 is the solvent molecular weight and ρ_i is the mass density of component i .

The equilibrium characteristics of a polymer solution may be determined from its Gibbs energy through the calculation of the partial molar Gibbs energy (chemical potentials). Differentiation of ΔG^M with respect to the number of moles of the various components yields expressions for their chemical potentials: (See Appendix),

$$\begin{aligned} \frac{(\mu_1 - \mu_1^\circ)}{RT} &= \left(\frac{\partial \Delta G^M / RT}{\partial n_1} \right)_{n_2, n_3, T, P} \\ &= \frac{\partial}{\partial n_1} \left[\frac{\Delta H^M}{RT} - \frac{\Delta S^M}{R} \right]_{n_2, n_3, T, P} \\ &= \ln \phi_1 + \left(1 - \frac{1}{x_{13}}\right) \phi_3 + \frac{2}{y} + \left(n_3 - \frac{2n_1}{y^2} - \frac{2n_3}{y}\right) \frac{\partial y}{\partial n_1} + x \phi_3^2. \end{aligned}$$

Here μ_1 is the chemical potential of the solvent in solution, and μ_1° is the chemical potential of the pure, saturated solvent at the same temperature. From the Appendix, equation A-8:

$$\frac{\partial y}{\partial n_1} \left[n_3 - \frac{2n_3}{y} - \frac{2n_1}{y^2} \right] = -\phi_3 \left(1 - \frac{y}{x_{13}} \right).$$

Therefore,

$$\ln a_1 = \ln \phi_1 + \left(\frac{y}{x_{13}} - \frac{1}{x_{13}} \right) \phi_3 + \frac{2}{y} + x_{13} \phi_3^2. \quad (\text{VII-9})$$

$$\begin{aligned} \ln a_3 = \ln \left(\frac{\phi_3}{x_{13}} \right) + (y-1) \phi_3 + 2 - \ln y^2 \\ + x_{31} (1-\phi_3)^2 x_{13}. \end{aligned} \quad (\text{VII-10})$$

The polymer solution thermodynamic equations directly relate experimental GC data to the interaction parameter.

As an example, we consider two limiting cases of the Flory theory:

(I) $y = 1$, and (II) $y = x_{13}$. Case I gives the result for an anisotropic solution of rod-like molecules in a binary system, while Case II describes an isotropic solution of random coil polymer molecules in a binary system.

For these two limiting cases, Equation VII-9 becomes:

$$\ln \left(\frac{a_1}{\phi_1} \right) = \frac{2}{y} + x_{13} \phi_3^2 = 2 + x_{13} \phi_3^2 \quad (\text{Case I}),$$

$$\ln \left(\frac{a_1}{\phi_1} \right) = \left(1 - \frac{1}{x_{13}} \right) \phi_3 + x_{13} \phi_3^2 \approx \phi_3 + x_{13} \phi_3^2 \quad (\text{Case II}).$$

At infinite dilution, $\phi_3 \rightarrow 1$ and these expressions further reduce to:

$$\ln \left(\frac{a_1}{\phi_1} \right)^\infty = 2 + x_{13}^\infty \quad (\text{Case I})$$

$$\ln \left(\frac{a_1}{\phi_1} \right)^\infty = 1 + x_{13}^\infty \quad (\text{Case II}).$$

Furthermore, for $\Omega_1 = a_1/w_1$ = weight fraction activity coefficient, we obtain the following results relating the interaction parameter to Ω_1^∞ (which is obtained experimentally from GC data):

$$x_{13}^\infty = \ln \left(\frac{\rho_2}{\rho_1} \Omega_1^\infty \right) - 2 \quad (\text{Case I}) \quad (\text{VII-11})$$

$$x_{13} = \ln \left(\frac{\rho_2}{\rho_1} \Omega_1^\infty \right) - 1 \quad (\text{Case II}). \quad (\text{VII-12})$$

b. Ternary System

The derivation of the equations for the case of rod-like polymers in a ternary system is fully explained in the Appendix. The Gibbs energy of mixing for a ternary system is given by Equations A-13 and A-17,

$$\begin{aligned} \frac{\Delta G^M}{RT} = & \{n_1 \ln \phi_1 + n_2 \ln \phi_2 + n_3 \ln \phi_3 - (n_1 + n_2 + n_3) y\} \frac{2}{y} \\ & - n_3 [\ln(x_{13} y^2) - y + 1] + n_1 \phi_2 \chi_{12} + n_2 \phi_3 \chi_{23} \\ & + n_3 \phi_1 \chi_{31}, \end{aligned} \quad (\text{VII-13})$$

where

$$\phi_1 = \frac{n_1 x_1 v_1}{n_1 x_1 v_1 + n_2 x_2 v_2 + n_3 x_3 v_3},$$

and

$$\phi_3 = 1 - \phi_1 - \phi_2.$$

The solvent-polymer interaction parameters χ_{13} and χ_{23} in Equation VII-13 can be obtained individually from data for the binary system. The term x_{13} is the ratio between the polymer molar volume and the molar volume of solvent 1.

The chemical potential of component i is found by differentiating Equation VII-13 with respect to n_i :

$$\begin{aligned} \frac{\mu_1 - \mu_1^\circ}{RT} &= \left(\frac{\partial \Delta G^M / RT}{\partial n_1} \right)_{n_2, n_3, T, P} \\ &= \ln \phi_1 + \left(1 - \frac{1}{x_{13}}\right) \phi_3 + \phi_2 \left(1 - \frac{1}{x_{13}}\right) + \frac{2}{y} + (n_3 \\ &\quad - \frac{2n_1}{y^2} - \frac{2n_2}{y^2} - \frac{2n_3}{y}) \frac{\partial y}{\partial n_1} + (\phi_2 \chi_{12} + \phi_3 \chi_{13}) (\phi_2 \\ &\quad + \phi_3) - \chi_{23} \left(\frac{1}{x_{12}}\right) \phi_2 \phi_3. \end{aligned} \quad (\text{VII-14})$$

From the Appendix, Equation A-16

$$\frac{\partial y}{\partial n_1} \left[n_3 - \frac{2n_1}{y^2} - \frac{2n_2}{y^2} - \frac{2n_3}{y} \right] = -\phi_3 \left(1 - \frac{y}{x}\right).$$

Therefore, substituting the above equation into Equation VII-14 we obtain the chemical potential,

$$\begin{aligned} \frac{\mu_1 - \mu_1^\circ}{RT} &= \ln a_1 = \ln \phi_1 + \frac{\phi_3}{x_{13}} (y-1) + \phi_2 \left(1 - \frac{1}{x_{12}}\right) + \frac{2}{y} \\ &\quad + (\phi_2 \chi_{12} + \phi_3 \chi_{13}) (\phi_2 + \phi_3) \\ &\quad - \chi_{23} \left(\frac{1}{x_{12}}\right) \phi_2 \phi_3. \end{aligned} \quad (\text{VII-15})$$

The expression can be reduced to the random coil case by taking $y = x$. The result is shown in Table 14.

Similarly,

$$\begin{aligned} \ln a_2 = \ln \phi_2 + \frac{\phi_3}{x_{23}}(y-1) + \phi_1 \left(1 - \frac{x_2}{x_1}\right) + \frac{2}{y} + (\phi_1 \chi_{21} \\ + \phi_3 \chi_{23})(\phi_1 + \phi_3) - \chi_{13} \left(\frac{x_2}{x_1}\right) \phi_1 \phi_3, \end{aligned} \quad (\text{VII-16})$$

and,

$$\begin{aligned} \ln a_3 = \ln \phi_3 + \frac{\phi_2}{x_{32}}(y-1) + \phi_1 \left(1 - \frac{x_3}{x_1}\right) + \frac{2}{y} + (\phi_1 \chi_{31} \\ + \phi_2 \chi_{32})(\phi_1 + \phi_2) - \chi_{12} \left(\frac{x_3}{x_1}\right) \phi_1 \phi_2. \end{aligned} \quad (\text{VII-17})$$

The activity expressions for binary and ternary systems with random-coil polymer and the rod-like polymer are summarized in Table 14.

The parameter χ provides a measure of the interactions for the system. Large values of χ correspond to poor solvent media, and low values of χ to good solvent media because $(\mu_1 - \mu_1^0)$ increases with increasing χ .

Huggins calculated values of the solvent-solvent interaction parameter χ_{12} shown in Equation VII-13 using Hildebrand-Scatchard Regular Solution theory²⁴

$$\chi_{ij} = \chi_s + v_i (\delta_i - \delta_j)^2 / RT. \quad (\text{VII-18})$$

The solubility parameter, δ , is defined as the square root of the cohesive-energy density. If a polymer and a series of solvents have similar polarity, the polymer is soluble only in those solvents whose cohesive-energy density

²⁴Gardon, J.L., Encyclopedia of Polymer Science and Technology, 3, Wiley (1971).

is not too different from its own. The solubility parameter is defined as

$$\delta^2 = (\Delta H_v - RT)/V. \quad (\text{VII-19})$$

The term ΔH_v is the molar enthalpy of vaporization, V is the molar volume.

The parameter χ_s in Equation VII-18 is an entropy term and is about equal to the inverse of the number of nearest neighbors of a dissolved molecule or segment. The experimental values of χ_s range from about 0.2 to 0.5²⁴. Prausnitz²⁵ found the mean value of χ_s for non-polar polymers in a large number of non-polar solvents to be 0.34. The χ values are found to be concentration dependent if the experiments are run over a wide range of polymer concentrations. Discrepancies in χ_s values indicate some of the hazards of predicting χ values. In the present study the mean value, $\chi_s = 0.34$, has been adopted for all cases. The combined Flory-Huggins and Hildebrand-Scatchard approach is an adequate approximation for the interpretation of many polymer solution data.

²⁵ Prausnitz, J.M., Molecular Thermodynamics of Fluid-Phase Equilibrium, Prentice-Hall New Jersey, (1969).

2. EXPERIMENTAL

In addition to the theoretical study described in the previous section, we have studied the formic acid/m-cresol/triphenylated PBO system experimentally using gas chromatography. Major experimental problems introduced unacceptably large errors into the experimental results, but we choose to present these results here as an illustration of the nature of data which this technique provides. The experimental problems encountered in this work can be overcome by careful experimental design, and we feel that the technique described here will prove to be extremely useful in the future. The particular polymer/solvent system involved appears to be of little further practical interest, so we plan no further measurements on this system.

Ternary systems containing two solvents and a polymer may be investigated at finite solvent concentrations by using the syringe pumps shown in Figure 1 to inject solvent into the carrier gas stream on a continuous basis. The steady-state system attained in the chromatograph column then consists of a stationary liquid phase containing the polymer and both solvents in equilibrium with a vapor phase containing the polymer and both solvents in equilibrium with a vapor phase containing finite partial pressures of one or both solvents. The steady-state system then is perturbed by injection of a minute quantity of one solvent into the carrier gas stream, and the time required for the perturbation to pass through the column is measured. A completely general description of the relation between the retention time and the phase behavior in the column is not available,

but two recent descriptions ^{26,27} appear to represent adequately the case where the activity coefficient is approximately independent of solvent concentration. The experimental data presented here have been analyzed using these descriptions, and we plan further efforts to obtain a comprehensive description of the general case of ternary mixtures at finite solvent concentrations.

The measured retention times are used to calculate specific retention volumes according to Equation II-34 in the usual fashion. The retention volumes in turn are used to calculate the weight fraction activity coefficients Ω_i and the weight fractions in the liquid phase for the injected solvent using the following relations (as given by Ching)²⁶:

$$\Omega_i = \frac{RT \cdot Z_m}{V_{gi}^s M_i} \frac{\hat{\phi}_i}{P_i^s \exp(B_{ii} P_i^s / RT)} \quad (\text{VII-20})$$

and

$$W_i = \frac{y_i \hat{\phi}_i P}{\Omega_i P_i^s \exp [B_{ii} (P_i^s - y_i P) / RT]} \quad (\text{VII-21})$$

where:

$$\begin{aligned} \hat{\phi}_i &= \frac{1}{Z_m} \exp \left[\frac{2}{V} \left(\sum_{j=1}^m y_j B_{ij} \right) \right] \\ &= \frac{1}{Z_m} \exp \left[\frac{2}{V} (y_1 B_{i1} + y_2 B_{i2} + y_4 B_{i4}) \right] \end{aligned}$$

²⁶Ching, D.W., "Experimental Solution Thermodynamics of a Ternary Solvent/Polymer/Solvent System by Inverse Gas Chromatography," M.S. thesis, Texas A&M University (1978), unpublished.

²⁷Dincer, S., Bonner, D.C., and Elefritz, R.A., Industrial and Engineering Chemistry, Fundamentals, 18 54 (1979).

- $T_0 = 273.2 \text{ K}$
- $R = \text{gas constant}$
- $P = \text{column pressure}$
- $Z_m = \text{compressibility factor for vapor phase mixture}$
- $T = \text{column temperature}$
- $V_{gi}^\circ = \text{specific retention volume for solvent } i$
- $M_i = \text{molecular weight of solvent } i$
- $V = \text{molar volume of vapor mixture}$
- $y_i = \text{mole fraction of component } i \text{ in the vapor phase}$
- $B_{ij} = \text{interaction second virial coefficient for components } i \text{ and } j$
- $P_i^s = \text{vapor pressure of pure, saturated component } i \text{ at the column temperature}$
- $B_{ii} = \text{second virial coefficient for pure component } i \text{ (vapor phase).}$

The results of a series of experimental runs on the formic acid/
m-cresol/triphenylated PBO system at approximately 250°C are listed in Table
 15 along with the calculated specific retention times. Equations VII-30
 and VII-31 then were used to calculate the values for Ω_i and w_i which are
 listed in Table 16. The values of the total solvent partial pressure and
 the vapor phase compositions given in the same table are obtained from mass
 balances on the materials introduced into the carrier gas stream. The
 activities listed in Table 16 are calculated using the theory developed in
 the earlier portion of this section.

The triphenylated polymer is assumed to behave in the extreme limiting
 case of the rigid rod. Therefore, Equation VII-11 is used to determine

values for χ_{13}^{∞} and χ_{23}^{∞} based on the experimental values of Ω_1^{∞} and Ω_2^{∞} . Values for χ_{12} and χ_{21} are estimated using Equation VII-18. These values for the interaction parameter then are used to obtain predicted values for the activities at various liquid phase compositions for comparison with the values obtained experimentally. In addition, one can also calculate values for ΔG^M based on the experimental retention volumes and then solve Equation VII-13 for an experimental value of y . In certain systems this would provide valuable information concerning the degree of rigidity of the polymer. For the particular case at hand, this calculation was not deemed useful due to the considerable experimental uncertainties. The activities for the experimental liquid phase compositions were calculated, and they are shown in Table 16 along with the other phase equilibrium results.

The activities of formic acid and m-cresol (both experimental and theoretical) are plotted as a function of weight fraction in Figures 12 and 13. They seem to be in general qualitative agreement, but problems with errors in experimental work prevent a strong test for the theory. The experimentally determined activities shown in Figures 12 and 13 contain at least $\pm 25\%$ estimated error, propagated from several sources. The carrier gas flow rate could not be measured during the experiment. Consequently, long-term fluctuations may have resulted in an actual flow rate that was slightly different from that measured before sample injection. The small amount of polymer sample available necessitated the use of a very short column. This caused low precision in the retention time determination for formic acid. For m-cresol, retention times were longer and more precise. However, for the finite concentration experiments, with this solvent an

unstable base line was observed that contributed additional uncertainty. This instability is felt to be due to condensation of the m-cresol and formic acid in the column outlet and inlet tubing resulting from uneven heating of this line. The relatively high boiling points of these compounds are poorly suited for the experimental geometry.

In spite of these difficulties, several observations can be made. The vapor-liquid equilibrium measurements that have been made for the formic acid/m-cresol/triphenylated PBO system indicate that both solvents interact strongly with the polymer and that m-cresol interacts more strongly with the polymer than does formic acid. The solvent-polymer interaction parameters for both solvents are small and negative, indicating strong interactions with the polymer. However, the m-cresol/polymer interaction parameter is more negative, implying a stronger interaction for it than for the formic acid. The weight fraction activity coefficient values (Table 16) for m-cresol are significantly smaller than those for the formic acid, also indicating that n-cresol has a stronger interaction with the polymer than does the formic acid, and therefore preferentially solvates the polymer.

The limiting assumptions of the theory should be kept in mind as more precise data are obtained to test it. First, the original Flory theory was derived for nonpolar systems and provides only a rough approximation for systems containing polar molecules. Second, the extended Flory theory, the various interaction parameters are important parameters in predicting the relationship between activity and concentration. The solvent/polymer parameters used were those obtained experimentally at infinite dilution.

The solvent/solvent parameter was obtained using an average entropy contribution of 0.34 for non-polar solvents, since polar solvent data are not available. Dependence of these parameters on concentration and deviations due to the polar nature of the m-cresol and formic acid molecules would contribute to deviation from the theory.

To fully understand this system, further investigation should be made: (1) to obtain more precise data on a wider polymer concentration range, (2) to compare the behavior of vapor-liquid equilibrium in good solvent systems and poor solvent systems and (3) to investigate the concentration and temperature dependence of the various χ 's. In addition, further work on the experimental theory is required to adequately describe the case where the (VII-18) Ω values are strongly concentration dependent.

REFERENCES

1. Bonner, D.C., Holste, J.C., Glover, C.J., Magnuson, D.T., Eversdyk, D.A., and Dangayach, K., "Polymer-Polymer Interactions," AFML-TR-78-163, U.S. Air Force Materials Laboratory (1978).
2. Bonner, D.C., "Determination of Solvents for Thermally Stable Polymers," AFML-TR-77-73, U.S. Air Force Materials Laboratory (1977).
3. Bonner, D.C., "Determinations of Solvents for Thermally Stable Aromatic Heterocyclic Polymers," AFML-TR-76-51, U.S. Air Force Materials Laboratory (1976).
4. See, for example, Smith, J.M., and Van Ness, H.C., Introduction to Chemical Engineering Thermodynamics, 3rd edition, McGraw-Hill (1975).
5. Flory, P.J., Proc. Roy. Soc., A234, 60 (1956).
6. Flory, P.J., Proc. Roy. Soc., A234, 73 (1956).
7. Hildebrand, J.H., and Scott, R.L., The Solubility of Non-Electrolytes, p. 136, Reinhold (1950).
8. Hanson, C.N., and Beerbower, A., Encyclopedia of Chemical Technology, Supplement Volume 1971, p. 889, Wiley (1971).
9. Dangayach, K.C.B., "Solvent Determination for Thermally Stable Polymers--PDIAB," M.S. Thesis, Texas Tech University (1976), unpublished.
10. Fedors, R.F., Polym. Eng. Sci., 14, 147 (1974).
11. Fedors, R.R., Polym. Eng. Sci., 14, 472 (1974).
12. Purnell, H., Gas Chromatography, Wiley (1962).
13. Littlewood, A.B., Gas Chromatography, 2nd ed., Academic Press (1970).
14. Sauerbrey, H.Z., Z. Phys., 155, 206 (1959).
15. Eversdyk, D.A., "Solvent Interactions with a Triphenylated Benzoxazole Polymer," M. S. Thesis, Texas A&M University (1977), unpublished.
16. Barrer, R.M., Barrie, J.A., and Slater, J., J. Poly. Sci., 27, 177 (1958).
17. Michaels, A.S., Vieth, W.R., and Barrie, J.A., J. Appl. Phys., 34, 1 (1963).
18. Flory, P.J., and Abe, A., Macromolecules, 11, 1119 (1978).
19. Abe, A., and Flory, P.J., Macromolecules, 11, 1122 (1978).

20. Flory, P.J., and Frost, R.S., Macromolecules, 11, 1126 (1978).
21. Frost, R.S., and Flory, P.J., Macromolecules, 11, 1134 (1978).
22. Flory, P.J., Macromolecules, 11, 1138 (1978).
23. Flory, P.J., Principles of Polymer Chemistry, Cornell University Press (1953).
24. Gardon, J.L., Encyclopedia of Polymer Science and Technology, "3, Wiley (1971).
25. Prausnitz, J.M., Molecular Thermodynamics of Fluid-Phase Equilibrium, Prentice-Hall, (1969).
26. Ching, D.W., "Experimental Solution Thermodynamics of a Ternary Solvent/Polymer/Solvent System by Inverse Gas Chromatography," M. S. Thesis, Texas A&M University (1978), unpublished.
27. Dincer, S., Bonner, D.C., and Elefritz, R.A., Industrial and Engineering Chemistry, Fundamentals, 18, 54 (1979).

APPENDIX

MATHEMATICAL DETAIL FOR DEVELOPMENT OF FLORY THERMODYNAMIC EQUATIONS FOR SOLUTIONS OF A ROD-LIKE POLYMER

1. BINARY SYSTEM

(1=solvent, 3=polymer, and $n_o = n_1 + xn_3$)

The entropy of mixing term is given by Equations VII-3 and VII-6:

$$\begin{aligned} \Delta S^M &= k \ln \left[\frac{(n_o - xn_3 + n_3 y)!}{(n_o - xn_3)! n_o} \frac{(n_o - xn_3)! n_3!}{n_1! n_3!} \right] \\ &= k \ln \left[\frac{(n_1 + yn_3)!}{(n_1! n_3!) (n_1 + xn_3)^{(y-1)n_3}} \frac{n_3!}{\prod_k n_k!} \right] \end{aligned} \quad (A-1)$$

Applying $n_3! / \prod_k n_k! \approx y^{2n_3}$ and Stirling's approximation for the factorials,

$\ln(n!) = (n \ln n - n)$, we obtain

$$\begin{aligned} \frac{\Delta S^M}{k} &= \ln \left[\frac{(n_1 + yn_3)^{n_1 + yn_3} e^{-(n_1 + yn_3)}}{n_1^{n_1} e^{-n_1} n_3^{n_3} e^{-n_3} (n_1 + xn_3)^{(y-1)n_3}} y^{2n_3} \right] \\ &= (n_1 + yn_3) \ln(n_1 + yn_3) - (n_1 + yn_3) - n_1 \ln n_1 + n_1 \\ &\quad - n_3 \ln n_3 + n_3 - (y-1)n_3 \ln(n_1 + xn_3) + 2n_3 \ln y \\ &= (n_1 + yn_3) \ln(1 + y \frac{n_3}{n_1}) - (n_1 + yn_3) - n_3 \ln n_3 + n_1 \\ &\quad + n_3 - (y-1)n_3 \ln(1 + x \frac{n_3}{n_1}) + n_3 \ln n_1 + 2n_3 \ln y. \end{aligned}$$

Also,

$$\frac{\phi_1}{\phi_3} = \frac{x_1 n_1}{x_3 n_3} = \frac{n_1}{x_{13} n_3},$$

(A-2)

$$\phi_1 + \phi_3 = 1, \text{ and } x_{13} = \frac{x_3}{x_1}.$$

Upon introducing the volume fractions, ϕ_1 and ϕ_3 , we have

$$\begin{aligned} \frac{\Delta S^M}{k} &= (n_1 + y n_3) \ln(1 + \frac{y \phi_3}{x \phi_1}) - y n_3 \ln(1 + \frac{\phi_3}{\phi_1}) + n_3 \ln(1 \\ &\quad + \frac{\phi_3}{\phi_1}) - y n_3 + n_3 + n_3 \ln y^2 \frac{\phi_1}{\phi_3} x \\ &= n_1 \ln(1 + \frac{y \phi_3}{x \phi_1}) + y n_3 \ln(1 + \frac{y \phi_3}{x \phi_1}) - y n_3 \ln(\frac{1}{\phi_1}) \\ &\quad + n_3 \ln(\frac{1}{\phi_1}) - y n_3 + n_3 + n_3 \ln(x y^2) + n_3 \ln \frac{\phi_1}{\phi_3} \\ &= y n_3 \ln(\phi_1 + \frac{y}{x} \phi_3) + n_1 \ln(\phi_1 + \frac{y}{x} \phi_3) - y n_3 + n_3 \\ &\quad + n_3 \ln(x y^2) - n_3 \ln \phi_3 - n_1 \ln \phi_1 \\ &= (n_1 + y n_3) \ln[1 - \phi_3(1 - \frac{y}{x})] + n_3 [\ln(x y^2) - y + 1] \\ &\quad - n_1 \ln \phi_1 - n_3 \ln \phi_3. \end{aligned}$$

(A-3)

The enthalpy of mixing is given by Equation VII-5

$$\frac{\Delta H^M}{kT} = n_1 \phi_3 \chi_{13}.$$

(A-4)

The Gibbs energy of mixing is given by

$$\begin{aligned} \frac{\Delta G^M}{kT} = & n_1 \ln \phi_1 + n_3 \ln \phi_3 - (n_1 + y n_3) \ln [1 - \phi_3 (1 - \frac{y}{x})] \\ & - n_3 [\ln x y^2 - y + 1] + n_3 \phi_1 \chi_{13}. \end{aligned} \quad (A-5)$$

Differentiating ΔG^M with respect to y , equating to zero, which minimizes ΔG^M , and solving the resulting expression for ϕ_3 , one obtains

$$-\frac{2}{y} = \ln [1 - (1 - \frac{y}{x}) \phi_3],$$

or

$$\phi_3 = \frac{x}{x-y} [1 - \exp(-\frac{2}{y})].$$

Then

$$\begin{aligned} \left(\frac{\partial \phi_3}{\partial n_1} \right)_{n_2, n_3, T, P} &= \frac{(x-y) \frac{\partial x}{\partial n_1} - x \left(\frac{\partial x}{\partial n_1} - \frac{\partial y}{\partial n_1} \right)}{(x-y)^2} [1 - \exp(-\frac{2}{y})] \\ &\quad - \frac{x}{x-y} \exp(-\frac{2}{y}) \left(\frac{2}{y^2} \right) \frac{\partial y}{\partial n_1} \\ &= \frac{x \frac{\partial y}{\partial n_1}}{x-y} \frac{1}{x-y} [1 - \exp(-\frac{2}{y})] \\ &\quad - \frac{x}{x-y} \exp(-\frac{2}{y}) \left(\frac{2}{y^2} \right) \frac{\partial y}{\partial n_1} \\ &= \frac{\partial y}{\partial n_1} \left[\frac{\phi_3}{x-y} + \phi_3 \frac{2}{y} - \frac{x}{x-y} \frac{2}{y} \right]. \end{aligned} \quad (A-6)$$

$$\text{Since } 1 = \frac{n_1 x_1 v_1}{x_1 n_1 v_1 + n_3 v_3 x_3},$$

$$\frac{\partial \phi_1}{\partial n_1} = \frac{\phi_1 \phi_3}{n_1}.$$

Similarly,

$$\frac{\partial \phi_3}{\partial n_1} = \frac{\phi_1 \phi_3}{n_1}. \quad (\text{A-7})$$

So, substituting for $\frac{\partial \phi_3}{\partial n_1}$, equation A-6 becomes,

$$-\frac{\phi_1 \phi_3}{n_1} = \frac{\partial y}{\partial n_1} \left[\frac{\phi_3}{x-y} + \phi_3 \frac{2}{y} - \frac{x}{x-y} \frac{2}{y} \right],$$

or,

$$\begin{aligned} -\phi_3 &= \frac{n_1}{\phi_1} \left[\frac{\phi_3}{x-y} + \frac{2 \phi_3 (x-y) - 2x}{(x-y)y^2} \right] \frac{\partial y}{\partial n_1} \\ &= \left[\frac{xn_3}{x-y} + \left(\frac{-2\phi_3}{(x-y)y} - \frac{2x(1-\phi_3)}{(x-y)y^2} \right) \frac{n_1}{\phi_1} \frac{\partial y}{\partial n_1} \right] \\ &= \left[\frac{xn_3}{x-y} - \frac{2xn_3}{(x-y)y} - \frac{2xn_1}{(x-y)y^2} \right] \frac{\partial y}{\partial n_1} \\ &= \frac{x}{x-y} \left[n_3 - \frac{2n_3}{y} - \frac{2n_1}{y^2} \right] \frac{\partial y}{\partial n_1}. \end{aligned}$$

Hence,

$$\frac{\partial y}{\partial n_1} \left[n_3 - \frac{2n_3}{y} - \frac{2n_1}{y^2} \right] = -\phi_3 \left(1 - \frac{y}{x} \right). \quad (\text{A-8})$$

The chemical potential of component 1 is found by taking the derivative of ΔG^M (Equation A-5) with respect to n_1 ,

$$\begin{aligned} \frac{\mu_1 - \mu_1^0}{RT} &= \left[\frac{\partial (\Delta G^M/RT)}{\partial n_1} \right]_{n_2, n_3, T, P} \\ &= \frac{\partial}{\partial n_1} \left[\frac{\Delta H^M}{RT} - \frac{\Delta S^M}{R} \right]_{n_2, n_3, T, P} \end{aligned} \quad (A-9)$$

From Equation A-4, the derivative of the enthalpy term is

$$\left[\frac{\partial \frac{\Delta H^M}{RT}}{\partial n_1} \right]_{n_2, n_3, T, P} = \phi_3 \chi_{13} + n_1 \chi_{13} \left[\frac{\partial \phi_3}{\partial n_1} \right]_{n_2, n_3, T, P}.$$

Substituting Equation A-7, leads to

$$\begin{aligned} \left[\frac{\partial \frac{\Delta H^M}{RT}}{\partial n_1} \right]_{n_2, n_3, T, P} &= \phi_3 \chi_{13} - n_1 \chi_{13} \frac{\phi_1 \phi_3}{n_1} \\ &= \phi_3 \chi_{13} - \chi_{13} (1 - \phi_3) \phi_3 \\ &= \chi_{13} \phi_3^2 \end{aligned}$$

From Equation A-2,

$$\begin{aligned} -\frac{\partial}{\partial n_1} \frac{\Delta S^M}{R} \bigg|_{n_2, n_3, T, P} &= \ln \phi_1 + \frac{\phi_1 \phi_3 n_1}{n_1 \phi_1} - \frac{n_3}{n_1} \phi_3 \frac{\phi_1}{\phi_3} + \frac{2}{y} \\ &\quad + \frac{2n_1}{y} \left(-\frac{1}{y} \frac{\partial y}{\partial n_1} \right) - n_3 \left[\frac{2}{y} \frac{\partial y}{\partial n_1} - \frac{\partial y}{\partial n_1} \right] \\ &= \ln \phi_1 + \phi_3 - \frac{n_3}{n_1} \phi_1 + \frac{2}{y} + \frac{\partial y}{\partial n_1} \left[-\frac{2n_1}{y^2} \right. \\ &\quad \left. - \frac{2n_3}{y} + n_3 \right]. \end{aligned}$$

Substituting Equation A-8 gives,

$$\left(- \frac{\partial \Delta S^M / R}{\partial n_1} \right)_{n_2, n_3, T, P} = \ln \phi_1 + \phi_3 - \frac{n_3}{n_1} \phi_1 + \frac{2}{y} - \phi_3 \left(1 - \frac{y}{x_{13}} \right).$$

Therefore, Equation A-9 becomes,

$$\begin{aligned} \ln a_1 &= \frac{\mu_1 - \mu_1^0}{RT} = \ln \phi_1 + \phi_3 \left(1 - \frac{\phi_1}{x_{13}} \right) + \frac{2}{y} + \phi_3 \left(\frac{y}{x_{13}} - 1 \right) + x_{13} \phi_3^2 \\ &= \ln \phi_1 + \left(\frac{y}{x_{13}} - \frac{1}{x_{13}} \right) \phi_3 + \frac{2}{y} + x_{13} \phi_3^2. \end{aligned} \quad (A-10)$$

Similarly, differentiating ΔG^M with respect to n_3 , we obtain:

$$\ln a_3 = \ln \left(\frac{\phi_3}{x_{13}} \right) + (y - 1) \phi_3 + 2 - \ln y^2 + x_{13} x_{13} (1 - \phi_3)^2. \quad (A-11)$$

2. TERNARY SYSTEM

$$(n_o = n_1 + x n_3 + n_2, \quad 1, 2 = \text{solvents}, \quad 3 = \text{polymer})$$

We extend the Flory theory for rod-like polymer to ternary system based on the same lattice model for partition function. Again, we start with Equation:

$$Q_M = \left[\frac{(n_o - x n_3 + y n_3)!}{(y-1)^{n_3} n_1! n_2! n_3!} \right] \frac{n_3!}{\prod_k n_k!}.$$

The entropy of mixing term is $\Delta S^M = k \ln Q_M$.

$$\text{Assuming } \frac{n_3!}{\prod_k n_k!} \approx y^{2n_3},$$

we obtain

$$\Delta S^M = k \ln \left[\frac{(n_o - xn_3 + yn_3)!}{n_1! n_2! n_3! n_o^{(y-1)n_3}} y^{2n_3} \right]$$

$$= k \ln \left[\frac{(n_1 + n_2 + n_3 y)! y^{2n_3}}{n_1! n_2! n_3! (n_1 + xn_3 + n_2)^{(y-1)n_3}} \right] .$$

Applying Stirling's approximation, the above equation becomes,

$$\begin{aligned} \frac{\Delta S^M}{k} &= (n_1 + n_2 + n_3 y) \ln(n_1 + n_2 + n_3 y) - (n_1 + n_2 + n_3 y) \\ &\quad - n_1 \ln n_1 + n_1 - n_3 \ln n_3 + n_3 - n_2 \ln n_2 + n_2 \\ &\quad - yn_3 \ln(n_1 + xn_3 + n_2) + n_3 \ln(n_1 + xn_3 + n_2) \\ &\quad + 2n_3 \ln y . \end{aligned} \quad (A-12)$$

From Equation A-3, the enthalpy term for a ternary system is given by

$$\Delta H^M = n_1 \phi_2 \chi_{12} + n_2 \phi_3 \chi_{23} + n_3 \phi_1 \chi_{31} . \quad (A-13)$$

Differentiating the Gibbs energy of mixing ($\Delta G^M = \Delta H^M - T\Delta S^M$) with respect to y and equating to zero,

$$\begin{aligned} \left(\frac{\partial (\frac{\Delta G^M}{kT})}{\partial y} \right)_{n_1, n_2, T, P} &= -T \left(\frac{\partial (\frac{\Delta S^M}{kT})}{\partial y} \right)_{n_1, n_2, T, P} \\ &= - \left[\ln \left(\frac{n_1 + n_2 + n_3 y}{n_1 + n_2 + n_3 x} \right) + \frac{2}{y} \right] = 0 . \end{aligned} \quad (A-14)$$

$$\text{Since } \phi_1 = \frac{n_1 v_1 x_1}{x_1 n_1 v_1 + n_2 v_2 x_2 + n_3 v_3 x_3} ,$$

$$\frac{\phi_2}{\phi_1} = \frac{n_2 x_2}{n_1 x_1}, \quad \phi_1 + \phi_2 + \phi_3 = 1,$$

and

$$x_{12} = \frac{x_2}{x_1}.$$

Also,

$$\left(\frac{\partial \phi_1}{\partial n_1} \right)_{n_2, n_3, T, P} = \frac{\phi_1 \phi_2}{n_1} + \frac{\phi_1 \phi_3}{n_1}$$

$$\left(\frac{\partial \phi_2}{\partial n_1} \right)_{n_2, n_3, T, P} = - \frac{\phi_1 \phi_2}{n_1}$$

$$\text{and} \quad \left(\frac{\partial \phi_3}{\partial n_1} \right)_{n_2, n_3, T, P} = - \frac{\phi_1 \phi_3}{n_1}.$$

Rearranging Equation A-14,

$$\begin{aligned} \frac{2}{y} &= \ln \frac{1 + \frac{n_3}{n_1} x_{13} + \frac{n_2}{n_1}}{1 + \frac{n_3}{n_1} y + \frac{n_2}{n_1}} \\ &= \ln \frac{1 + \frac{\phi_3}{\phi_1} + \frac{\phi_2}{\phi_1} \frac{1}{x_{12}}}{1 + \frac{\phi_3}{\phi_1} \frac{y}{x_{13}} + \frac{\phi_2}{\phi_1} \frac{1}{x_{12}}} \\ &= \ln \frac{\phi_1 + \phi_2 \frac{1}{x_{12}} + \phi_3}{\phi_1 + \phi_3 \frac{y}{x_{13}} + \phi_2 \frac{1}{x_{12}}} \\ &= \ln \phi_1 + \phi_2 \frac{1}{x_{12}} + \phi_3 - \ln \phi_1 + \phi_3 \frac{y}{x_{13}} + \phi_2 \frac{1}{x_{12}}. \end{aligned} \quad (\text{A-15})$$

When $x_{12} = 1$, we obtain:

$$\frac{2}{y} = \ln \left[\phi_1 - \phi_3 \left(1 - \frac{y}{x_{13}} \right) \right] .$$

Solving the resulting expression for ϕ_3 gives

$$\phi_3 = \frac{x_{13}}{x_{13} - y} \left[1 - \exp\left(-\frac{2}{y}\right) \right] .$$

Then,

$$\begin{aligned} \left(\frac{\partial \phi_3}{\partial n_1} \right)_{n_2, n_3, T, P} &= - \frac{\phi_1 \phi_3}{n_1} \\ &= \frac{\partial y}{\partial n_1} \left[\frac{\phi_3}{x_{13} - y} + \phi_3 \frac{2}{y^2} - \frac{x_{13}}{x_{13} - y} \frac{2}{y^2} \right] , \end{aligned}$$

or

$$- \phi_3 = \frac{\partial y}{\partial n_1} \left(\frac{x_{13}}{x_{13} - y} \right) \left[n_3 - \frac{2n_1}{y^2} - \frac{2n_2}{y^2} - \frac{2n_3}{y} \right] . \quad (A-16)$$

Continuing the derivation from Equation A-12 for the entropy of mixing by introducing the volume fractions, we have

$$\begin{aligned} \frac{\Delta S^M}{k} &= (n_1 + n_2 + n_3 y) \left[\ln \left(\phi_1 + \frac{\phi_2}{x_{12}} + \phi_3 \frac{y}{x_{13}} \right) - \ln(\phi_1 + \phi_3 \right. \\ &\quad \left. + \frac{\phi_2}{x_{12}}) \right] + n_3 \left[\ln x_{13} y^2 - y + 1 \right] - n_3 \ln \left[\frac{n_1}{n_3} \frac{\phi_3}{\phi_1} \right] - (n_1 + n_2 \\ &\quad + n_3) \ln \phi_1 + n_2 \ln n_1 + n_3 \ln n_1 - n_3 \ln n_3 - n_2 \ln n_2 . \end{aligned}$$

Substituting Equation A-15, we obtain

$$\frac{\Delta S^M}{k^*} = (n_1 + n_2 + n_3 y) \left(\frac{2}{y} \right) + n_3 [\ln x_{13} y^2 - y + 1] - n_3 \ln \phi_3 - n_2 \ln \phi_2 - n_1 \ln \phi_1 . \quad (A-17)$$

Differentiating the entropy term with respect to n_1 , we obtain

$$\begin{aligned} \left[\frac{\partial \left(\frac{-\Delta S^M}{R} \right)}{\partial n_1} \right]_{n_2, n_3, T, P} &= \ln \phi_1 + \frac{n_1}{\phi_1} \frac{\partial \phi_1}{\partial n_1} + \frac{n_3}{\phi_3} \frac{\partial \phi_3}{\partial n_1} + \frac{n_2}{\phi_2} \frac{\partial \phi_2}{\partial n_1} \\ &\quad + \frac{2}{y} - \frac{2n_1}{y^2} \frac{\partial y}{\partial n_1} - \frac{2n_2}{y^2} \frac{\partial y}{\partial n_1} - n_3 \left[\frac{2}{y} \frac{\partial y}{\partial n_1} \right. \\ &\quad \left. - \frac{\partial y}{\partial n_1} \right] . \end{aligned} \quad (A-18)$$

The derivative of the ternary system enthalpy term (Equation A-13) with respect to n_1 is

$$\begin{aligned} \left[\frac{\partial (\Delta H^M / kT)}{\partial n_1} \right]_{n_2, n_3, T, P} &= \frac{\partial}{\partial n_1} [n_1 \phi_2 \chi_{12} + n_2 \phi_3 \chi_{23} + n_3 \phi_1 \chi_{31}] \\ &= \phi_2 \chi_{12} + n_1 \chi_{12} \frac{\partial \phi_2}{\partial n_1} + n_2 \chi_{23} \frac{\partial \phi_3}{\partial n_1} + n_3 \chi_{31} \frac{\partial \phi_1}{\partial n_1} \\ &= \phi_2 \chi_{12} + n_1 \chi_{12} \left(-\frac{\phi_1 \phi_2}{n_1} \right) + n_2 \chi_{23} \left(-\frac{\phi_1 \phi_3}{n_1} \right) \\ &\quad + n_3 \chi_{31} \left(\frac{\phi_1 \phi_2}{n_1} + \frac{\phi_1 \phi_3}{n_1} \right) \\ &= \phi_2 \chi_{12} (1 - \phi_1) - \chi_{23} \left(\frac{1}{x_{12}} \right) \phi_2 \phi_3 + \chi_{31} \frac{n_3}{n_1} \phi_1 (\phi_2 + \phi_3) \\ &= \phi_2 \chi_{12} (\phi_2 + \phi_3) - \chi_{23} \left(\frac{1}{x_{12}} \right) \phi_2 \phi_3 + \chi_{31} \frac{\phi_3}{x_{13}} (\phi_2 + \phi_3) . \end{aligned}$$

Since the χ_{ij} 's are pair interaction parameters,

$$\chi_{ij} = \chi_{ji} \left(\frac{x_i}{x_j} \right) \cong \chi_{ji} \left(\frac{v_i}{v_j} \right),$$

therefore,

$$\begin{aligned} \left(\frac{\partial \Delta H^M / kT}{\partial n_1} \right)_{n_2, n_3, T, P} &= (\phi_2 \chi_{12} + \phi_3 \chi_{13}) (\phi_2 + \phi_3) \\ &\quad - \chi_{23} \left(\frac{1}{x_{12}} \right) \phi_2 \phi_3. \end{aligned} \quad (A-19)$$

Hence, combining equations A-18 and A-19, we obtain the chemical potential,

$$\begin{aligned} \frac{\mu_1 - \mu_1^\circ}{RT} &= \left(\frac{\partial (\Delta G^M / RT)}{\partial n_1} \right)_{n_2, n_3, T, P} \\ \frac{\mu_1 - \mu_1^\circ}{RT} &= \ln \phi_1 + \phi_3 + \phi_2 - \frac{n_3}{n_1} \phi_1 - \frac{n_2}{n_1} \phi_1 + \frac{2}{y} + \frac{\partial y}{\partial n_1} \left[n_3 \right. \\ &\quad \left. - \frac{2n_1}{y} - \frac{2n_2}{y} - \frac{2}{y} n_3 \right] + (\phi_2 \chi_{12} + \phi_3 \chi_{13}) (\phi_2 + \phi_3) \\ &\quad - \chi_{23} \left(\frac{1}{x_{12}} \right) \phi_2 \phi_3. \end{aligned}$$

Substituting Equation A-16 into the above equation gives,

$$\begin{aligned} \frac{\mu_1 - \mu_1^\circ}{RT} &= \ln \phi_1 + \phi_3 \left(\frac{y}{x_{13}} - \frac{1}{x_{13}} \right) + \phi_2 \left(1 - \frac{x_1}{x_2} \right) + \frac{2}{y} \\ &\quad + (\phi_2 \chi_{12} + \phi_3 \chi_{13}) (\phi_2 + \phi_3) - \chi_{23} \left(\frac{1}{x_{12}} \right) \phi_2 \phi_3. \end{aligned} \quad (A-20)$$

Similarly,

$$\begin{aligned} \frac{\mu_2 - \mu_2^0}{RT} = & \ln \phi_2 + \phi_3 \left(\frac{y}{x_{23}} - \frac{1}{x_{23}} \right) + \phi_1 \left(1 - \frac{x_2}{x_1} \right) + \frac{2}{y} \\ & + (\phi_1 \chi_{21} + \phi_3 \chi_{23}) (\phi_1 + \phi_3) - \chi_{13} \left(\frac{x_2}{x_1} \right) \phi_1 \phi_3, \end{aligned} \quad (\text{A-21})$$

and

$$\begin{aligned} \frac{\mu_3 - \mu_3^0}{RT} = & \ln \phi_3 + \phi_2 \left(\frac{y}{x_{32}} - \frac{1}{x_{32}} \right) + \phi_1 \left(1 - \frac{x_3}{x_1} \right) + \frac{2}{y} \\ & + (\phi_1 \chi_{31} + \phi_2 \chi_{32}) (\phi_1 + \phi_2) - \chi_{12} \left(\frac{x_3}{x_1} \right) \phi_1 \phi_2. \end{aligned} \quad (\text{A-22})$$

TABLE 1
SOLVENT GROUP DESIGNATIONS

Code:	Solvent Group:
A	Acyclic saturated unbranched hydrocarbons
B	Acyclic saturated branched hydrocarbons
C	Acyclic unsaturated hydrocarbons (branched and unbranched)
D	Monocyclic hydrocarbons (saturated and unsaturated, with or without side chains)
E	Aromatic hydrocarbons (with or without side chains)
F	Cyclic compound with one or more hetero atoms
G	Carboxylic acids and anhydrides; Acids containing S or N
H	Monohydric alcohols
I	Polyhydric alcohols and phenols
J	Halogenated solvents
K	Ketones
L	Aldehydes and esters
M	Ethers
N	Amines
O	Nitro compounds and nitriles
P	Miscellaneous solvents

TABLE 2
CODE DESIGNATIONS FOR SOLVENTS

Code:	Solvent:	Code:	Solvent:
A1	Methane	G1	Formic acid
A2	Ethane	G2	Acetic acid
A3	<u>n</u> -Propane	G3	<u>n</u> -Propionic acid
A4	<u>n</u> -Butane	G4	<u>n</u> -Butyric acid
A5	<u>n</u> -Pentane	G5	Oxalic acid
A6	<u>n</u> -Hexane	G6	Pthalic acid
A7	<u>n</u> -Heptane	G7	Acetic anhydride
A8	<u>n</u> -Octane	G8	Propionic anhydride
A9	<u>n</u> -Nonane	G9	Pthalic anhydride
A10	<u>n</u> -Decane	G10	Methane sulfonic acid
A11	<u>n</u> -Undecane	G11	Nitric acid
A12	<u>n</u> -Dodecane	G12	Sulfuric acid
		G13	Benzene sulfonic acid
B1	2,2-Dimethyl-butane	H1	Methanol
B2	2-Methyl pentane	H2	Ethanol
B3	2-Methyl hexane	H3	1-Propanol
B4	<u>i</u> -Octane	H4	2-Propanol
C1	Ethylene	H5	1-Butanol
C2	Allene	H6	2-Butanol
C3	2-Hexene	H7	<u>i</u> -Butanol
C4	2-Heptene	H8	<u>l</u> -Pentanol
C5	1-Octene	H9	1-Hexanol
C6	2-Octene	H10	Cyclohexanol
C7	2,6-Dimethyl-3-heptene	H11	Allyl alcohol
		H12	Benzyl alcohol
D1	Cyclopentane	I1	Phenol
D2	Cyclohexane	I2	<u>o</u> -Cresol
D3	Methyl cyclohexane	I3	<u>m</u> -Cresol
D4	Ethyl cyclohexane	I4	<u>p</u> -Cresol
E1	Benzene	I5	Resorcinol
E2	Toluene	I6	<u>m</u> -Methoxy phenol
E3	<u>m</u> -Xylene	I7	Propylene glycol
E4	Ethyl benzene	I8	Resorcinol monoacetate
		I9	Ethylene glycol
F1	Furan	I10	1,5-Pentanediol
F2	Tetrahydrofuran		
F3	Pyrrole		
F4	Pyrrolidine		
F5	1,3-Dioxolane		
F6	<u>p</u> -Dioxane		
F7	Pyridine		
F8	Quinoline		
F9	Quinoxaline		

TABLE 2 (Continued)

Code:	Solvent:	Code:	Solvent:
J1	Dichloromethane	M1	Diethyl ether
J2	1,2-Dichloroethane	M2	Phenyl ether
J3	1-Chloropropane	M3	Di(<i>i</i> -propyl) ether
J4	Chloroform	M4	Di(<i>n</i> -propyl) ether
J5	Carbon tetrachloride	M5	2-Methoxy pentane (Methyl <i>i</i> -Butyl ether)
J6	1-Chlorobutane		
J7	2-Chlorobutane		
J8	1-Bromobutane	N1	<i>N</i> -acetyl ethanolamine
J9	2-Bromobutane	N2	Aniline
J10	Chlorobenzene	N3	<i>n</i> -Butyl amine
J11	Bromobenzene	N4	Diethyl amine
J12	Fluorobenzene	N5	Diethylene triamine
J13	Iodobenzene	N6	Dimethyl acetamide
J14	Benzyl chloride	N7	<i>N,N</i> -Dimethyl formamide
J15	<i>o</i> -Chlorophenol	N8	<i>N</i> -Ethyl acetamide
J16	Hexafluoro-iso-propanol	N9	Ethylene diamine
J17	Trifluoromethanol	N10	Formamide
J18	2,2,2-Trifluoroethanol	N11	1,2-Propane diamine
J19	Chlorosulfonic acid	N12	Tetramethyl urea
J20	Hydrochloric acid	N13	<i>N</i> -Methyl formamide
J21	Hydrofluoric acid	N14	<i>i</i> -Butyl amine
J22	Perfluorotributylamine		
J23	Dio-iodomethane	O1	Acetonitrile
J24	Pentachloroethane	O2	Acrylonitrile
J25	Tetrachloroethylene	O3	Propionitrile
J26	α,α -Dichlorotoluene	O4	Butyronitrile
J27	Benzoyl chloride	O5	Hydracrylonitrile
J28	<i>p</i> -Chlorophenol	O6	Nitrobenzene
		O7	Nitromethane
K1	Acetone	O8	Nitroethane
K2	2,4-Dimethyl-3-pentanone	O9	1-Nitropropane
K3	3-Methyl-2-butanone	O10	2-Nitropropane
K4	Methyl ethyl ketone		
K5	Methyl isobutyl ketone	P1	2-Dimethyl amino ethanol
K6	Diethyl ketone	P2	Dimethyl sulfoxide
K7	Cyclohexanone	P3	2-Ethoxy ethanol
K8	1-Methyl-2-pyrrolidone	P4	Ethylene carbonate
		P5	Hexamethyl phosphate triamide
L1	Acetaldehyde	P6	Monoethanolamine
L2	Propionaldehyde	P7	Sulfanilimide
L3	Butyraldehyde	P8	Triethyl phosphate
L4	Benzaldehyde	P9	Water
L5	Methyl acetate		
L6	Ethyl acetate		
L7	<i>n</i> -Propyl acetate		
L8	Methyl formate		
L9	Ethyl formate		
L10	Propyl formate		
L11	Diethyl phthalate		
L12	<i>m</i> -Dimethoxy benzene		
L13	<i>n</i> -Butyl acetate		

TABLE 3

PHYSICAL PROPERTIES OF SOLVENTS AT 25°C

Solvent	Code	MW	T _b (K)	$\alpha \times 10^{18}$ (m ⁻³)	$\mu \times 10^{30}$ (C·m)	δ (kJ/mol) ^{1/2}	δ_p (kJ/mol) ^{1/2}
Acetaldehyde	L1	44.05	294.00	4.60	9.07	---	---
Acetic acid	G2	60.05	391.15	5.11	5.80	---	---
Acetic Anhydride	G7	102.09	412.15	8.88	10.71	---	---
Acetone	K1	58.08	329.70	6.42	9.61	5.08	2.79
Acetonitrile	O1	41.05	354.75	4.40	13.14	5.38	4.01
N-acetyl ethanalamine	N1	103.12	428.15	10.22	14.18	---	---
Acrylonitrile	O2	53.06	350.15	6.19	12.78	---	---
Allyl alcohol	H11	58.08	369.00	6.74	5.17	---	---
Aniline	N2	93.13	457.15	12.13	5.04	---	---
Benzene	E1	73.11	353.30	10.38	0.0	5.57	0.30
Benzene sulfonic acid	G13	158.18	---	---	---	---	---
Benzoyl chloride	J27	140.57	470.35	14.60	10.54	7.46	3.46
Benzyl alcohol	H12	108.15	478.50	12.25	5.77	8.16	1.89
Benzyl chloride	J14	126.59	452.45	14.34	4.47	6.74	2.38
Bromobenzene	J11	157.06	429.20	13.48	5.67	6.46	1.77
1-Bromobutane	J8	137.03	374.75	11.22	6.94	6.29	---
2-Bromobutane	J9	137.03	364.15	11.26	7.44	---	---
1-Butanol	H5	74.12	390.80	8.76	5.54	7.13	1.33
2-Butanol	H6	74.12	372.7	8.66	5.47	6.74	1.32
1-Butanol	H7	74.12	381.0	8.60	9.24	---	---
n-Butyl acetate	L13	116.16	399.2	12.51	6.24	---	---
1-Butyl amine	N14	73.14	340.6	9.55	4.80	---	---
n-Butyl amine	N3	73.14	350.6	9.71	3.34	5.88	1.44
Butyraldehyde	L3	72.10	348.0	8.17	9.01	---	---
n-Butyric acid	G4	88.10	436.4	8.81	5.50	6.90	1.76
Butyronitrile	O4	69.10	391.0	8.02	13.58	---	---
Carbon tetrachloride	J5	153.82	349.7	10.24	0.00	5.48	0.00
Chlorobenzene	J10	112.56	404.9	12.33	5.40	6.19	1.36
1-Chlorobutane	J6	42.57	351.6	10.07	6.84	5.52	1.77

TABLE 3 (Continued)

Solvent	Code	MW	T _b (K)	$\alpha \times 10^{18}$ (m ⁻³)	$\mu \times 10^{30}$ (C.m)	δ (kJ/mol) ^{1/2}	δ_p (kJ/mol) ^{1/2}
Chloroform	J4	119.38	334.3	8.48	3.37	---	---
o-Chlorophenol	J15	128.56	448.05	12.96	4.54	8.50	1.47
p-Chlorophenol	J28	128.56	492.90	12.97	7.47	8.55	---
1-Chloropropane	J3	78.54	319.6	8.17	6.84	---	---
m-Cresol	I3	108.14	475.4	13.11	4.94	7.94	1.96
o-Cresol	I2	108.14	464.2	13.11	4.70	---	---
p-Cresol	I4	108.14	475.1	13.11	5.21	---	---
Cyclohexane	D2	84.16	353.9	10.71	0.00	5.47	0.00
n-Decane	A10	142.28	447.30	19.30	0.00	6.84	0.00
1,2-Dichloroethane	J2	98.96	356.6	8.34	5.01	5.36	1.54
α , α -Dichlorotoluene	J26	161.03	478.35	16.18	6.90	7.43	2.26
Diethyl amine	N4	73.14	328.6	9.63	3.97	5.37	0.74
Diethyl ether	M1	74.12	307.7	8.92	3.84	---	---
Diethyl ketone	K6	86.13	375.1	9.91	9.10	6.15	2.56
Di-iodomethane	J23	267.84	455.15	12.89	3.64	4.72	1.20
m-Dimethoxy benzene	L12	138.17	490.25	14.85	5.34	6.69	---
N,N-Dimethyl formamide	N7	73.10	426.15	7.84	11.34	6.62	3.65
p-Dioxane	F6	88.11	374.15	8.58	1.44	5.73	0.42
1,3-Dioxolane	F5	74.08	351.15	8.56	4.74	5.95	1.45
Ethanol	H2	46.07	351.40	5.02	5.64	6.15	1.36
Ethyl acetate	L6	88.10	350.30	8.33	5.94	5.64	---
Ethyl formate	L9	74.08	327.50	7.06	6.44	5.37	2.34
Ethylene glycol	I9	62.06	470.40	5.72	7.34	8.18	2.36
Fluorobenzene	J12	96.10	358.25	10.40	5.24	5.47	---
Formic acid	G1	46.03	373.95	3.28	5.07	---	---
Furan	F1	68.08	304.52	7.60	2.30	5.32	0.56
n-Heptane	A7	100.20	371.60	13.71	0.00	5.87	0.00
n-Hexane	A6	86.18	342.15	11.85	0.00	5.31	0.00
Methane sulfonic acid	G10	96.11	440.15	---	---	---	---
Methanol	H1	32.04	337.80	3.23	5.71	5.68	1.37
m-Methoxy phenol	I6	124.15	517.45	13.77	6.17	8.43	2.03
Methyl acetate	L5	74.08	330.15	6.94	5.60	5.46	1.67
Methyl ethyl ketone	K4	72.10	352.80	8.24	9.24	5.71	---
N-Methyl formamide	N13	59.07	453.65	5.99	12.78	8.77	4.17

TABLE 3 (Continued)

Solvent	Code	MW	T _b (K)	$\alpha \times 10^{18}$ (m ⁻³)	$\mu \times 10^{30}$ ^a (C·m)	δ (kJ/mol) ^{1/2}	δ_p (kJ/mol) ^{1/2}
Methyl formate	L8	60.05	304.70	5.10	5.91	4.95	1.63
i-Octane	B4	114.23	390.8	15.44	0.00	6.03	0.00
2-Methyl hexane	B3	100.20	363.2	13.67	0.00	5.73	0.00
Methyl isobutyl ketone	K5	100.16	389.60	11.83	9.34	5.91	---
1-Methyl-2-pyrrolidone	K8	99.13	475.15	10.64	13.64	6.63	3.96
Dichloromethane	J1	84.93	313.05	6.58	5.21	4.97	1.26
Nitrobenzene	O6	123.11	483.65	12.96	14.14	7.43	4.65
Nitroethane	O8	75.07	387.15	6.74	11.81	6.07	3.71
Nitromethane	O7	61.04	374.00	4.95	11.91	5.96	3.74
1-Nitropropane	O9	89.09	403.65	8.43	11.98	8.75	3.95
n-Nonane	A9	128.25	424.00	17.42	0.00	6.56	0.00
n-Octane	A8	114.23	398.90	15.54	0.00	6.20	0.00
i-Octane	C5	112.21	394.4	15.36	1.13	6.07	0.00
Oxalic acid	G5	90.04	430.15	---	8.77	---	---
Pentachloroethane	J24	202.30	435.15	14.08	3.07	6.54	0.99
1,5-Pentanediol	I10	104.15	533.15	11.16	12.14	6.76	4.08
1,2-Propane diamine	N11	74.13	393.65	9.46	6.54	6.21	---
1-Propanol	H3	60.09	370.40	6.90	5.60	6.69	1.35
Propionaldehyde	L2	58.08	321.00	6.35	9.17	4.38	---
Propionitrile	O3	55.08	370.50	6.26	13.44	5.62	4.15
n-Propyl acetate	L7	102.13	374.80	10.67	6.00	5.98	---
Pyridine	F7	79.10	388.50	9.51	7.67	6.35	2.57
Quinoline	F8	129.16	513.20	15.35	7.31	7.36	---
Quinoxaline	F9	130.15	502.65	14.74	1.70	8.92	0.56
Tetrachloroethylene	J25	165.83	394.3	12.02	0.00	6.10	1.97
Tetrahydrofuran	F2	72.12	340.15	7.97	5.84	5.11	1.41
Tetramethyl urea	N12	116.16	450.15	13.04	11.67	7.17	3.13
Toluene	E2	92.13	383.80	12.33	1.20	5.89	0.29
Triethyl phosphate	P8	182.16	488.15	16.50	10.01	6.44	3.32
m-Xylene	E3	106.17	412.25	13.91	1.17	6.31	0.28

^a 1 Debye = 3.3356x10⁻³⁰ C·m.

TABLE 4

GAS CHROMATOGRAPHY RESULTS FOR PBT AT 463 K (190°C)

Solvent	Code	$V_g^o \times 10^3$ (m^3/kg)	ΔG_{ads} (kJ/mol)	ΔG_{add} (kJ/mol)	Λ (kJ/mol)	δ_p (T) (kJ/mol)	Ω_1^∞	X_1^∞
Acetaldehyde	L1	—	temp.	exceeds	critical			
Acetone	K1	1.66	-20.98	+4.6	1.8	3.40	13.80 ^a	0.82 ^b
Acetonitrile	O1	4.19	-18.76	6.3	2.4	4.66	13.21	0.88
Benzene	E1	2.14	-18.65	—	—	—	13.55	0.95
Benzene sulfonic acid	G13	—	—	—	—	—	—	—
Benzoyl chloride	J27	10.50	-10.48	6.2	3.0	3.74	18.82	1.72
Benzyl alcohol	H12	40.01	-4.95	12.75	11.0	2.04	8.36	0.68
Benzyl chloride	J14	4.53	-10.93	+6.3	5.0	1.58	7.18	0.68
Bromobenzene	J11	15.37	-8.58	+8.6	6.9	2.09	4.47	0.49
1-Bromobutane	J8	0.44	-22.79	-1.6	—	—	54.15	2.58
2-Bromobutane	J9	0.56	-21.87	-0.8	—	—	26.32	1.20
1-Butanol	H5	6.10	-15.04	8.3	6.8	2.17	7.84	0.33
2-Butanol	H6	3.05	-17.71	5.8	4.2	2.17	10.58	0.60
n-Butylamine	N3	3.19	-17.59	4.9	4.0	1.23	7.68	0.11
n-Butyric acid	G4	50.53	-6.22	17.1	15.5	1.95	2.32	-0.76
Carbon tetrachloride	J5	4.16	-13.69	8.3	8.3	0.0	3.49	0.19

TABLE 4 (Continued)

Solvent	Code	$V_g^o \times 10^3$ (m^3/kg)	ΔG_{ads} (kJ/mol)	ΔG_{add} (kJ/mol)	Λ (kJ/mol)	$\delta_p(T)$ (kJ/mol)	Ω_1^∞	χ_1^∞
Chlorobenzene	J10	42.32	-5.96	11.7	10.2	2.01	1.34 ^a	-1.03 ^b
1-Chlorobutane	J6	0.32	-25.52	-3.5	—	—	80.30	2.71
o-Chlorophenol	J15	18.91	-8.55	+8.9	7.6	1.61	6.46	0.84
p-Chlorophenol	J28	2.86	-15.83	1.6	—	—	121.20	3.59
m-Cresol	I3	51.31	-5.38	12.0	10.6	2.13	5.69	0.49
Cyclohexane	D2	2.83	-20.40	1.20	1.3	0.0	10.31	0.56
n-Decane	A10	11.38	-13.37	—	—	—	10.14	0.58
1,2-Dichloroethane	J2	0.91	-21.22	2.55	1.0	1.77	23.68	1.95
α , α -Dichlorotoluene	J26	15.38	-8.48	7.50	5.4	2.45	13.95	1.47
Diethylamine	N4	1.64	-20.15	2.4	1.2	1.43	11.52	0.37
Diethyl ketone	K6	7.02	-18.71	3.6	0.96	3.18	19.36	1.15
Di-iodomethane	J23	6.86	-9.63	9.9	9.0	1.29	10.51	2.10
m-Dimethoxybenzene	L12	14.18	-9.39	7.2	5.6	1.89	23.72	1.90
N,N-Dimethyl formamide	N7	17.74	-10.98	13.2	12.6	4.02	7.50	0.53
p-Dioxane	F6	2.06	-19.87	3.6	3.2	0.47	17.26	1.49
1,3-Dioxolane	F5	1.14	-21.48	2.0	0.6	1.74	31.53	1.41
Ethanol	H2	4.99	-19.49	7.4	5.8	2.83	5.28	-0.14
Ethyl acetate	L6	1.78	-19.10	4.7	2.9	2.27	12.69	0.86

TABLE 4 (Continued)

Solvent	Code	$V_g^O \times 10^3$ (m ³ /kg)	ΔG_{ads} (kJ/mol)	ΔG_{add} (kJ/mol)	Δ (kJ/mol)	δ_p (T) (kJ/mol)	n_1^∞	χ_1^∞
Ethyl formate	L9	1.78	-21.08	4.0	2.0	2.72	9.89 ^a	0.59 ^b
Ethylene glycol	I9	0.95	-22.87	3.30	1.2	2.60	505.2	4.80
Fluorobenzene	J12	0.79	-21.87	-3.3	—	—	—	—
Formic Acid	G1	—	—	—	—	—	—	—
Furan	F1	2.06	-19.54	5.0	4.3	0.94	6.49	-0.03
n-Heptane	A7	3.05	-18.78	—	—	—	11.26	0.48
n-Hexane	A6	1.89	-22.36	—	—	—	12.55	0.49
Methane sulfonic acid	G10	—	—	—	—	—	—	—
Methanol	H1	4.72	-19.25	9.4	7.8	3.51	5.83	-0.01
m-Methoxyphenol	I6	116.19	-1.69	15.4	13.6	2.19	7.46	0.81
Methyl acetate	L5	1.78	-19.77	5.2	3.3	2.03	9.91	0.60
Methyl ethyl ketone	K4	1.00	-21.11	2.75	0.0	—	17.78	1.10
N-Methyl formamide	N13	144.42	-3.72	27.2	21.6	4.53	2.35	-0.74
Methyl formate	L8	1.31	-21.77	5.0	3.3	2.04	10.32	0.60
2-Methyl heptane	B4	0.59	-22.34	-5.2	—	—	74.03	2.42
2-Methyl hexane	B3	0.35	-24.81	-5.9	—	—	66.34	2.13
Methyl isobutyl ketone	K5	2.14	-17.91	2.6	—	—	21.26	1.35
1-Methyl-2-pyrrolidone	K8	126.92	-2.22	19.4	15.30	4.84	2.43	-0.56

TABLE 4 (Continued)

Solvent	Code	$V_g^0 \times 10^3$ (m ³ /kg)	ΔG_{ads} (kJ/mol)	ΔG_{add} (kJ/mol)	Λ (kJ/mol)	δ_p (T) (kJ/mol)	Ω_1^∞	χ_1^∞
Methylene chloride	J1	1.07	-21.22	+4.2	2.7	2.33	11.00 ^a	0.96 ^b
Nitrobenzene	06	13.94	-8.72	8.6	4.2	5.05	17.06	1.43
Nitroethane	08	1.27	-20.33	5.0	1.4	4.19	41.15	2.29
Nitromethane	07	1.75	-20.59	4.45	0.8	4.22	27.68	1.99
1-Nitropropane	09	1.51	-19.70	5.35	1.8	4.25	34.96	1.59
n-Nonane	A9	7.26	-15.45	—	—	—	10.50	0.55
n-Octene	A8	4.70	-17.03	—	—	—	10.87	0.52
1-Octene	C5	2.38	-17.06	0.20	—	—	19.80	1.16
Oxalic acid	G5	13.84	-11.78	—	—	—	18.71	1.43
Pentachloroethane	J24	2.86	-14.08	4.4	3.6	1.08	21.64	2.19
1,5-Pentanediol	I10	3.34	-16.05	5.05	2.6	4.30	381.08	5.22
1,2-Propane diamine	N11	1.06	-21.75	0.9	—	—	49.13	2.23
1-Propanol	H3	3.38	-19.54	5.5	4.0	2.46	10.03	0.54
Propionaldehyde	L2	1.42	-21.57	4.0	1.2	3.19	13.92	0.65
Propionitrile	O3	2.61	-19.45	6.2	3.0	4.77	21.81	1.37
n-Propyl acetate	L7	2.26	-17.62	3.95	2.0	2.11	14.31	1.01
Pyridine	F7	29.19	-8.75	13.95	11.7	2.73	1.88	-0.91

TABLE 4 (Continued)

Solvent	Code	$V_g^o \times 10^3$ (m^3/kg)	ΔG_{ads} (kJ/mol)	ΔG_{add} (kJ/mol)	Λ (kJ/mole)	δ_p (T) (kJ/mol)	Ω_1^∞	χ_1^∞
Quinoline	F8	0.35	-23.83	-7.4	—	—	1783.4	6.24
Quinoxaline	F9	6.44	-12.66	4.0	3.5	0.60	71.38	2.97
Tetrachloroethylene	J25	5.83	-12.10	8.2	8.2	0	5.39	0.82
Tetrahydrofuran	F2	3.23	-17.59	6.8	5.0	2.51	7.28	0.37
Tetramethyl urea	N12	14.85	-7.88	11.5	8.0	3.60	8.13	0.34
Toluene	E2	2.51	-17.89	—	—	—	17.93	1.27
Tri-ethyl phosphate	P8	36.34	-4.69	11.49	8.50	3.55	7.24	0.81
m-Xylene	E3	2.41	-16.91	—	—	—	8.64	0.56

TABLE 5
REFERENCE LINE PARAMETERS FOR PBT ANALYSIS
AT 190°C

Reference Line	Solvents Used	Slope (See note a)	Intercept (kJ/mol)
Dispersion:			
Aliphatic	<u>n</u> -heptane	0.95	-31.90
	<u>n</u> -octane		
	<u>n</u> -nonane		
	<u>n</u> -decane		
Aromatic	benzene	0.48	-23.78
	toluene		
	<u>m</u> -xylene		
Dipole:	1-octene	0.306	- 0.10
	methyl ethyl ketone		
	methyl isobutyl		
	ketone		

^a The values of the slopes are reported in $10^{18} \text{ kJ} \cdot \text{m}^3 / \text{mol}$ for the dispersion contribution and $10^{30} \text{ kJ} / (\text{mol} \cdot \text{C} \cdot \text{m})$ for the permanent dipole contribution.

TABLE 6
SPECIFIC INTERACTION PARAMETERS FOR SOLVENTS INTERACTING WITH
PBT AT 463 K (190°C)

Solvent	Λ (kJ/mol)	Solvent	Λ (kJ/mol)
N-Methyl formamide	21.6	Pentachloroethane	3.6
<u>m</u> -Butyric acid	15.5	Quinoxaline	3.5
<u>l</u> -Methyl-2-pyrrolidone	15.3	Methyl formate	3.3
<u>m</u> -Methoxy phenol	13.6	Methyl acetate	3.3
N,N-Dimethyl formamide	12.6	<u>p</u> -Dioxane	3.2
Pyridine	11.7	Propionitrile	3.0
Benzyl alcohol	11.0	Benzoyl chloride	3.0
<u>m</u> -Cresol	10.6	Ethyl acetate	2.9
*Chlorobenzene	10.2	Methylene chloride	2.7
Di-iodomethane	9.0	1,5-Pentanediol	2.6
Tri-ethyl phosphate	8.5	Acetonitrile	2.4
Carbon tetrachloride	8.3	<u>n</u> -Propyl acetate	2.0
Tetrachloroethylene	8.2	Ethyl formate	2.0
Tetramethyl urea	8.0	Acetone	1.8
*Methanol	7.8	1-Nitropropane	1.8
* <u>o</u> -Chlorophenol	7.6	Nitroethane	1.4
*Bromobenzene	6.9	Cyclohexane	1.3
1-Butanol	6.8	Ethylene glycol	1.2
*Ethanol	5.8	Diethylamine	1.2
<u>m</u> -Dimethoxy benzene	5.6	Propionaldehyde	1.2
α,α -Dichlorotoluene	5.4	1,2-Dichloroethane	1.0
Tetrahydrofuran	5.0	Diethyl ketone	0.96
*Benzyl chloride	5.0	Nitro methane	0.8
Furan	4.3	1,3-Dioxolane	0.6
Nitrobenzene	4.2		
2-Butanol	4.2		
1-Propanol	4.0		
<u>n</u> -Butylamine	4.0		

* Included in first series of breaker tests.

TABLE 7

BEAKER TEST RESULTS FOR SOLVENTS ON PBT

Solvent	Ambient Temp. (1 wk)	120°C (6 hr)	190°C (3 hr)
Methanol	No change	No change	No change
Ethanol	No change	No change	No change
Formic acid	Color change on PBT flakes	No further change	No further change
1-Dodecanethiol	No change	No change	No change
α -Chlorotoluene	Color change on PBT flakes	+Color change in solution	+Increased color change in solution
Chlorobenzene	No change	Slight color change on PBT	No further change
<i>m</i> -Dichlorobenzene	No change	Slight color change on PBT	No further change
<i>o</i> -Dichlorobenzene	No change	Slight color change on PBT	No further change
2,5-Dichloro- benzenethiol	Slight color change on PBT	Intense (dark red) color on PBT	
<i>o</i> -Chlorophenol	Slight color change on PBT	+Color change in solution	+Considerable color change in solution
Methane sulfonic acid	Dissolves PBT immediately		
Bromobenzene*	No change		

*open beaker

†caused by solvent oxidation, not dissolution

TABLE 8

SATURATION CONCENTRATIONS OF RADEL POLYSULFONE IN VARIOUS SOLVENTS

Solvent	T _b	Wt% Radel	Comments
N,N-Dimethyl formamide (DMF)	426.2 K (153°C)	<div>4.1</div> <div>12.3</div> <div>17.5</div> <div>19.0</div> <div>39.0</div>	Polymer dissolves in all cases. Films made from these solutions appeared like "cakes" of white plastic
Trichloromethane (Chloroform)	334.3 K (61.1°C)	<div>4.2</div> <div>4.4</div> <div>10.4</div> <div>12.1</div> <div>18.3</div> <div>20.0</div> <div>23.5</div>	<div>Dissolves very well</div> <div>Mixture is very viscous; the CHCl₃ does not wet all the polymer</div>
Dichloromethane	313.1 K (39.8°C)	<div>7.4</div> <div>9.6</div> <div>12.2</div> <div>15.5</div>	<div>Cloudy white haze on the side of the vial</div> <div>Cloudy white precipitate after setting in a closed vial for a few minutes</div>
1,2-Dichloroethane Tetrahydrofuran Furan	Sat. conc. < 1%		Not viable processing solvents

Note: These measurements were made at ambient temperature.

TABLE 9

GAS CHROMATOGRAPHY RESULTS FOR PATS PLASTICIZER AT 313 K (40°C)

Solvent	Code	$V^{\circ} \times 10^3$ (m ³ /kg)	ΔG_{ads} (kJ/mole)	ΔG_{add} (kJ/mole)	Λ (kJ/mole)	δ_p (mJ/m ^{3/2})	Ω_1^{∞}	χ_1^{∞}
Acetaldehyde	L1	9.78	10.36	7.39	2.56	27.7 ^a	22 ^b	2.87
Benzene*	E1	20.43	6.93	0.0	0.0	0.0	52	3.82
Ethyl ether †	M1	7.7	9.62	2.12	0.1	8.64	28	3.05
Furan	F1	6.25	10.39	1.05	-0.16	6.19	34	3.47
n-Heptane *†	A7	75.32	2.85	0.12	0.14	0.0	22	2.76
n-Hexane *†	A6	24.47	6.20	-0.21	-0.19	0.0	26	2.89
Methylene chloride	J1	6.91	9.53	5.25	2.48	14.87	34	3.77
n-Pentane *†	A5	8.4	9.50	0.09	0.12	0.0	29	2.9

^a Value at 25°C.^b Virial coefficient effects not included here (the resulting error is less than 10%).

* Polarizability reference solvent.

† Dipole reference solvent

TABLE 10

GAS CHROMATOGRAPHIC RESULTS FOR PATS PLASTICIZER AT 343 K (70°C)

Solvent	Code	$V_g \times 10^3$ (m ³ /kg)	ΔG_{ads} (kJ/mole)	ΔG_{add} (kJ/mole)	Λ (kJ/mole)	δ (T=25°C) P (mJ/m ³)	Ω_1^∞	Ω_1^∞
Acetaldehyde	L1	6.6	12.45	9.1	4.2	27.68 ^a	15 ^b	2.5
Acetone	K1	2.57	14.31	4.44	- 0.7	25.72	91	4.3
Benzene *	E1	6.4	10.85	0.0	0.0	0.0	58.5	4.0
Chloroform	J4	4.32	10.76	5.09	3.51	8.64	32	3.9
Cyclohexane *	D2	5.17	11.25	0.0	0.0	0.0	70	4.0
Diethyl. amine	N4	22.	7.59	6.3	4.3	8.96	8.5	1.8
Diethyl ether †	M1	1.9	14.6	1.3	- 0.5	8.64	52	3.6
Ethyl formate	I9	2.75	13.4	4.35	1.0	16.53	63	4.1
Furan †	F1	2.2	14.3	1.0	- 0.16	6.19	42	3.6
n-Hexane *†	A6	6.65	10.45	- 0.03	0.32	0.0	36	3.2
n-Heptane *†	A7	15.8	7.55	0.02	0.4	0.0	34	3.2
f-butylamine	N14	25.	7.	7.	4.5	11.02	11	2.1
Methanol	H1	49.	7.57	16.07	13.17	20.45	11	2.1
Methyl acetate	L5	2.7	13.4	4.3	1.4	14.79	69	4.2
Methylcyclohexane †	D3	9.42	9.09	- 1.18	- 0.81	0.0	62	3.9
Methylene chloride	J1	4.0	11.97	6.80	4.2	14.87	24	3.4
n-Pentane *†	A5	15.86	7.55	0.01	0.4	0.0	42	3.3
Tetrahydrofuran †	F2	4.6	12.05	3.41	0.42	14.88	57	3.9

^a Value at 25°C.^b Virial coefficient effects not included here (the resulting error is less than 10%).

* Polarizability reference solvent.

† Dipole reference solvent.

TABLE 11

GAS CHROMATOGRAPHIC RESULTS FOR PATS PLASTICIZER AT 373 K (100°C)

Solvent	Code	$V^{\circ} \times 10^3$ (m^3/kg)	ΔG_{ads} (kJ/mole)	ΔG_{add} (kJ/mole)	Λ (kJ/mole)	δ_p (T=25°C) (mJ/m^2) ^{1/2}	Ω_1^{∞}	χ_1^{∞}
Acetaldehyde	L1	3.70	15.33	7.92	7.5	27.68 ^a	11 ^b	2.28
Acetone	K1	1.6	17.2	4.0	3.6	25.72	60	3.89
Acetonitrile	O1	9.3	12.70	10.8	10.3	37.0	30	3.15
Acrylonitrile	O2	4.3	14.3	7.2	6.6	36.14	44	3.62
Allyl alcohol	H11	2.96	15.16	5.64	5.5	14.4	106	4.49
Benzene *	E1	3.1	14.12	0.0	0.0	0.0	47	3.76
Carbon tetrachloride	J5	2.79	12.32	6.65	6.7	0.0	24	3.70
1-Chlorobutane	J6	2.1	14.9	2.0	1.8	15.36	58	3.74
1,2-Dichloroethane	J2	2.2	14.4	4.6	4.3	15.49	58	4.29
Chloroform	J4	1.57	14.9	4.0	4.0	8.69	37	4.0
Cyclohexane *	D2	2.85	14.1	0.0	0.0	0.0	49	3.7
Diethyl amine	N4	15.	9.	8.	8.	8.96	5	1.3
Diethyl ether	M1	0.45	20.	- 1.3	- 1.4	8.64	88	4.25
Ethanol	H2	4.55	14.55	8.2	8.0	16.93	43	3.5
Ethyl acetate	L6	1.35	16.3	2.1	1.8	13.78	85	4.4
Ethyl cyanide	O3	2.65	15.36	6.0	5.5	33.76	117	4.5
Ethyl formate	L9	1.3	16.9	3.5	3.3	16.53	51	3.9
Fluorobenzene	J12	3.28	13.29	0.91	0.75	11.06	41	3.8
Furan †	F1	1.19	17.53	0.25	0.29	6.19	33	3.5
n-Heptane * †	A7	3.76	12.8	0.07	0.14	0.0	53	3.7
n-Hexane * †	A6	2.06	15.1	0.13	0.05	0.0	46	3.5
i-butylamine	N14	11.	10.	7.	7.	11.02	9	2.
i-octane	B4	2.7	13.35	- 3.1	- 3.	0.0	64	3.9
Methanol	H1	11.37	12.83	11.9	11.7	20.45	16	2.5
Methyl acetate	L5	1.6	16.	4.1	3.9	14.79	46	3.8
3-Methyl-2-butanone	K3	2.6	14.3	2.6	2.2	20.70	77	4.3
Methylene chloride	J1	1.67	15.8	5.4	5.2	14.87	24	3.5
Methyl ethyl ketone	K4	1.60	16.42	2.7	2.3	22.41	95	4.4

TABLE 11 (Continued)

Solvent	Code	$V^{\circ} \times 10^3$ (m^3/kg)	ΔG_{ads} (kJ/mole)	ΔG_{add} (kJ/mole)	Λ (kJ/mole)	δ^{p} (mJ/m^2) ^{1/2}	Ω_1^{∞}	X_1^{∞}
n-Pentane *†	A5	1.23	17.4	0.06	0.13	0.00	42	3.3
Propanol	H3	1.72	16.8	3.8	3.65	15.06	180	4.9
2-Propanol	H4	1.4	17.4	3.1	2.9	14.89	130	4.6
Tetrahydrofuran +	F2	1.8	16.0	1.2	1.	14.88	58	3.9
2,2,2 Trifluoroethanol	J18	0.87	17.3	5.7	5.4	18.26	570	6.6

a Value at 25°C.

b Virial coefficient effects not included (less than 10% error).

* Polarizability reference solvent.

† Dipole reference solvent.

TABLE 12
REFERENCE LINE PARAMETERS FOR PATS ANALYSIS

Temp	Reference Line	Solvent Used	Slope (see note a)	Intercept (kJ/mol)
40°C	Dispersion: Aliphatic	<u>n</u> -pentane	1.62 ± 0.06	25.22 ± 0.69
		<u>n</u> -hexane		
		<u>n</u> -heptane		
	Aromatic	benzene	1.6	23.8
	Dipole:	<u>n</u> -pentane <u>n</u> -hexane <u>n</u> -heptane Furan Diethyl Ether	0.530 ± 0.039	0.02 ± 0.08
70°C	Dispersion: Aliphatic	<u>n</u> -pentane	1.54 ± 0.09	29.64 ± 1.03
		<u>n</u> -hexane		
		<u>n</u> -heptane		
	Aromatic	benzene	1.5	26.8
		Cyclic cyclohexane	1.5	27.7
	Dipole:	<u>n</u> -pentane <u>n</u> -hexane <u>n</u> -heptane diethyl ether furan tetrahydrofuran methylcyclohexane	0.572 ± 0.069	3.14 ± 1.61
100°C	Dispersion: Aliphatic	<u>n</u> -pentane	1.14 ± 0.1	28.49 ± 1.20
		<u>n</u> -hexane		
		<u>n</u> -heptane		
	Aromatic	benzene	1.14	26.0
		Cyclic cyclohexane	1.14	26.4
	Dipole:	<u>n</u> -pentane <u>n</u> -hexane <u>n</u> -heptane diethyl ether furan tetrahydrofuran	0.048 ± 0.083	0.59 ± 1.53

^aThe values of the slopes are reported in 10¹⁸ kJ·m³/mol for the dispersion contribution and 10³⁰ kJ/(mol·C·m) for the permanent dipole contribution.

TABLE 13
SPECIFIC INTERACTION PARAMETERS FOR SOLVENTS
INTERACTING WITH PATS PLASTICIZER

Solvent:	Λ (kJ/mol)	δ_P (MJ/m ³) ^{1/2}	Solvent:	Λ (kJ/mol)	δ_P (MJ/m ³) ^{1/2}
<u>T = 313 K (40°C):</u>			<u>T = 373 K (100°C):</u>		
Acetaldehyde	2.6	27.7	Methanol	11.7	20.45
Methylene chloride	2.5	14.87	Acetonitrile	10.3	37.1
			Ethanol	8.0	16.93
			Diethylamine	8.	8.96
			Acetaldehyde	7.5	27.68
			i-butylamine	7.	11.02
			Carbon tetrachloride	6.7	0.0
			Acrylonitrile	6.6	36.14
			Propionitrile	5.5	33.76
			Allyl alcohol	5.5	14.4
			2,2,2-Trifluoroethanol	5.4	18.3
			Methylene chloride	5.2	14.87
			1,2-Dichloroethane	4.3	15.49
			Chloroform	4.0	8.64
			Methyl acetate	3.9	14.79
			Propanol	3.65	15.06
			Acetone	3.6	25.72
			Ethyl formate	3.3	16.53
			2-Propanol	2.9	14.89
			Methyl ethyl ketone	2.3	22.41
			3 Methyl-2-Butanone	2.2	20.70
			Ethyl acetate	1.8	13.78
			1-Chlorobutane	1.8	15.36
<u>T = 343 K (70°C)</u>					
Methanol	13.17	20.45			
i-butyl amine	4.5	11.02			
Diethyl amine	4.3	8.96			
Acetaldehyde	4.2	27.68			
Methylene chloride	4.2	14.87			
Chloroform	3.5	8.64			
Methyl acetate	1.4	14.79			
Ethyl formate	1.0	16.53			

TABLE 14

ACTIVITY EXPRESSIONS FOR BINARY AND TERNARY SYSTEMS

For random coil polymer molecules (Isotropic phase)^a: 1,2 = solvent, 3 = polymer

Binary solution

$$\ln a_1 = \frac{\mu_1 - \mu_1^0}{RT} = \ln \phi_1 + \left(1 - \frac{1}{x_{13}}\right)\phi_3 + x_{13}\phi_3^2$$

Ternary solution

$$\ln a_1 = \ln \phi_1 + (1 - \phi_1) - \left(\frac{1}{x_{12}}\right)\phi_2 - \left(\frac{1}{x_{13}}\right)\phi_3 + \left(\frac{2}{x_{13}}\right) + (\phi_2 x_{12} + \phi_3 x_{13})(\phi_2 + \phi_3) - x_{23}\left(\frac{1}{x_{12}}\right)\phi_2\phi_3$$

For rod-like polymer molecules (Anisotropic phase):

Binary solution

$$\ln a_1 = \frac{\mu_1 - \mu_1^0}{RT} = \ln \phi_1 + \left(\frac{y}{x_{13}} - \frac{1}{x_{13}}\right)\phi_3 + \frac{2}{y} + x_{13}\phi_3^2$$

Ternary solution

$$\ln a_1 = \ln \phi_1 + \phi_3\left(\frac{y}{x_{13}} - \frac{1}{x_{13}}\right) + \phi_2\left(1 - \frac{1}{x_{12}}\right) + \frac{2}{y} + (\phi_2 x_{12} + \phi_3 x_{13})(\phi_2 + \phi_3) - x_{23}\left(\frac{1}{x_{12}}\right)\phi_2\phi_3$$

^aFlory, Ref.

TABLE 15

ILLUSTRATIVE GAS CHROMATOGRAPHY DATA FOR FORMIC ACID/m-CRESOL/TRIPHENYLATED PBO SYSTEM

Run	^a Liquid Solvent Flow rate (cm ³ /min)	Col Temp (°C)	Inlet Press (psig)	f _p	t _{g1} (min)	t _{g2} (min)	t _r (min)	Q _{solv} (Vap) $\left(\frac{\text{cm}^3}{\text{min}}\right)$	^b Q _{HE} (gas) $\left(\frac{\text{cm}^3}{\text{min}}\right)$	Col Flow Rate $\left(\frac{\text{cm}^3}{\text{min}}\right)$	V _{g1} (cm ³ /gm)	V _{g2} (cm ³ /gm)
∞	--	250.8	16.8	0.61	0.47	1.8	0.37	--	8.5	8.5 ^b	2.5	37.2
∞	--	251.1	16.5	0.61	0.47	1.8	0.38	--	--	8.6 ^c	2.8	38.8
1/5	0.046/0.19	250.1	16.7	0.61	0.44	1.8	0.36	1.3	9.4	10.6 ^d	2.7	49.8
2/5	0.065/0.19	250.8	20.6	0.55	0.41	1.4	0.29	1.5	10.5	12.0 ^d	4.2	38.5
3/5	0.095/0.19	248.1	18.1	0.58	0.40	1.6	0.26	1.8	10.4	12.1 ^d	5.4	50.4
5/5	0.19/0.19	252.1	17.5	0.59	0.11	0.4	0.09	2.9	22.0	24.8 ^d	1.4	22.7
5/1	0.19/0.046	251.6	20.7	0.55	0.36	1.2	0.27	2.3	10.5	12.8 ^d	3.8	39.6

a) Volumetric flow rate of solvent liquid (at column pressure and room temperature) determined from the syringe pump's settings for solvent 1 and solvent 2 (formic acid/m-cresol respectively)

b) He flow rate (thru packed column) at soap bubble meter at room temperature

c) He flow rate (thru packed column) using air peak retention time and the column void volume determined from the first infinite dilution experiment above

d) He flow rate (thru packed column) at soap bubble meter at room temperature plus volumetric flow rate of solvent vapor (at 1 atm. room temperature) calculated from solvent liquid volume flow rate (at syringe pump), liquid volume, molecular weight, and ideal gas law

TABLE 16

ILLUSTRATIVE PHASE EQUILIBRIUM RESULTS FOR FORMIC ACID/m-CRESOL/TRIPHENYLATED PBO SYSTEM

Run	Weight Fraction Activity Coefficient Ω_1	Ω_1	Total Solvent Pressure (atm)	Vapor Phase ^a Composition y_1	y_2	Liquid Phase Composition w_1	w_2	Solvent Activities a_1	a_2
∞	7.0	1.92							
∞	6.1	1.84							
1/5	9.6	1.4	0.19	0.39	0.61	0.00030	0.023	0.0029	0.034
2/5	6.3	1.86	0.22	0.48	0.52	0.00060	0.018	0.0038	0.033
3/5	5.0	1.50	0.24	0.58	0.42	0.0011	0.021	0.0053	0.032
5/5	18.0	3.07	0.19	0.73	0.27	0.00027	0.0046	0.0049	0.014
5/1	8.1	2.10	0.32	0.92	0.08	0.0013	0.0034	0.011	0.0071

^aOn a helium-free basis

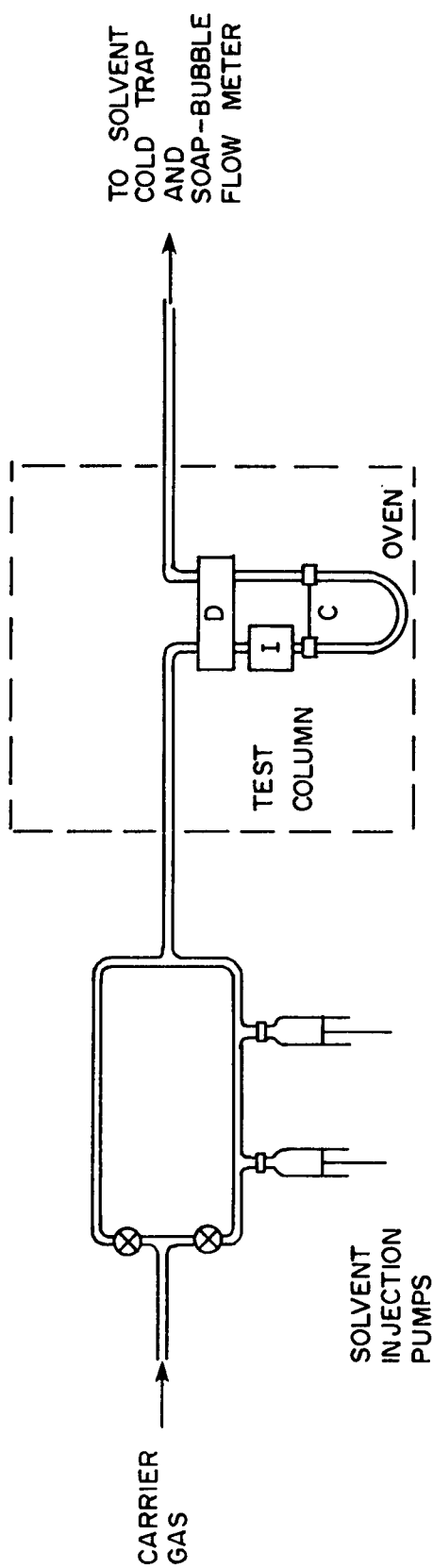
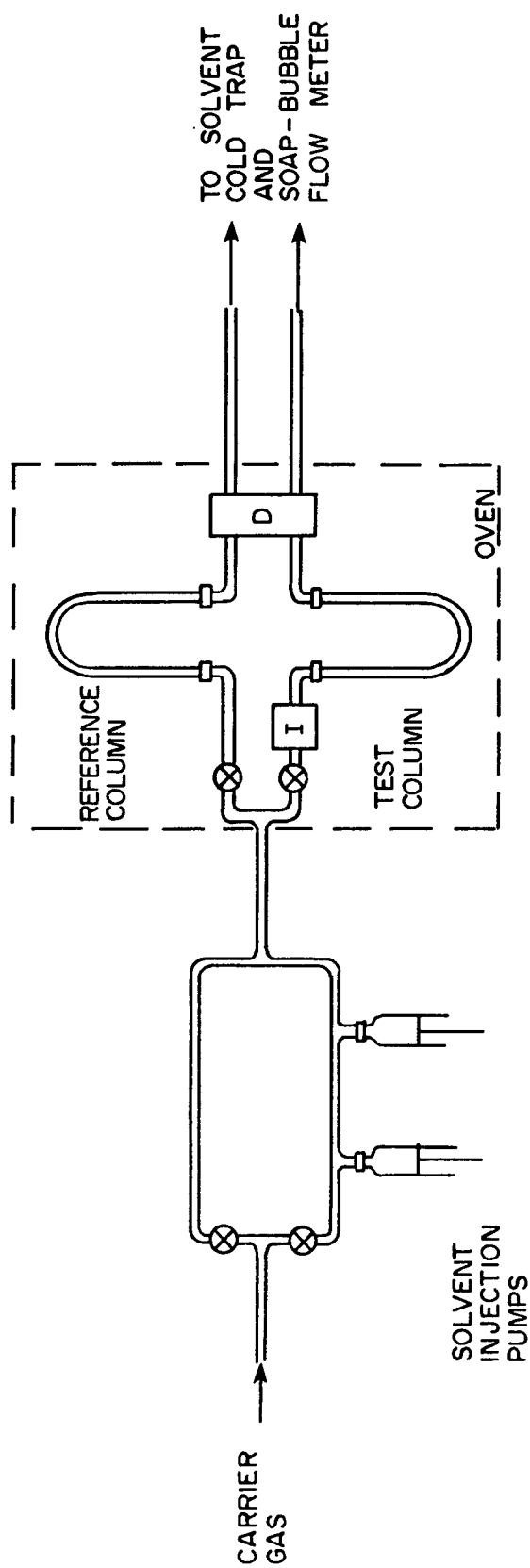


Figure 1. Gas Chromatography Apparatus

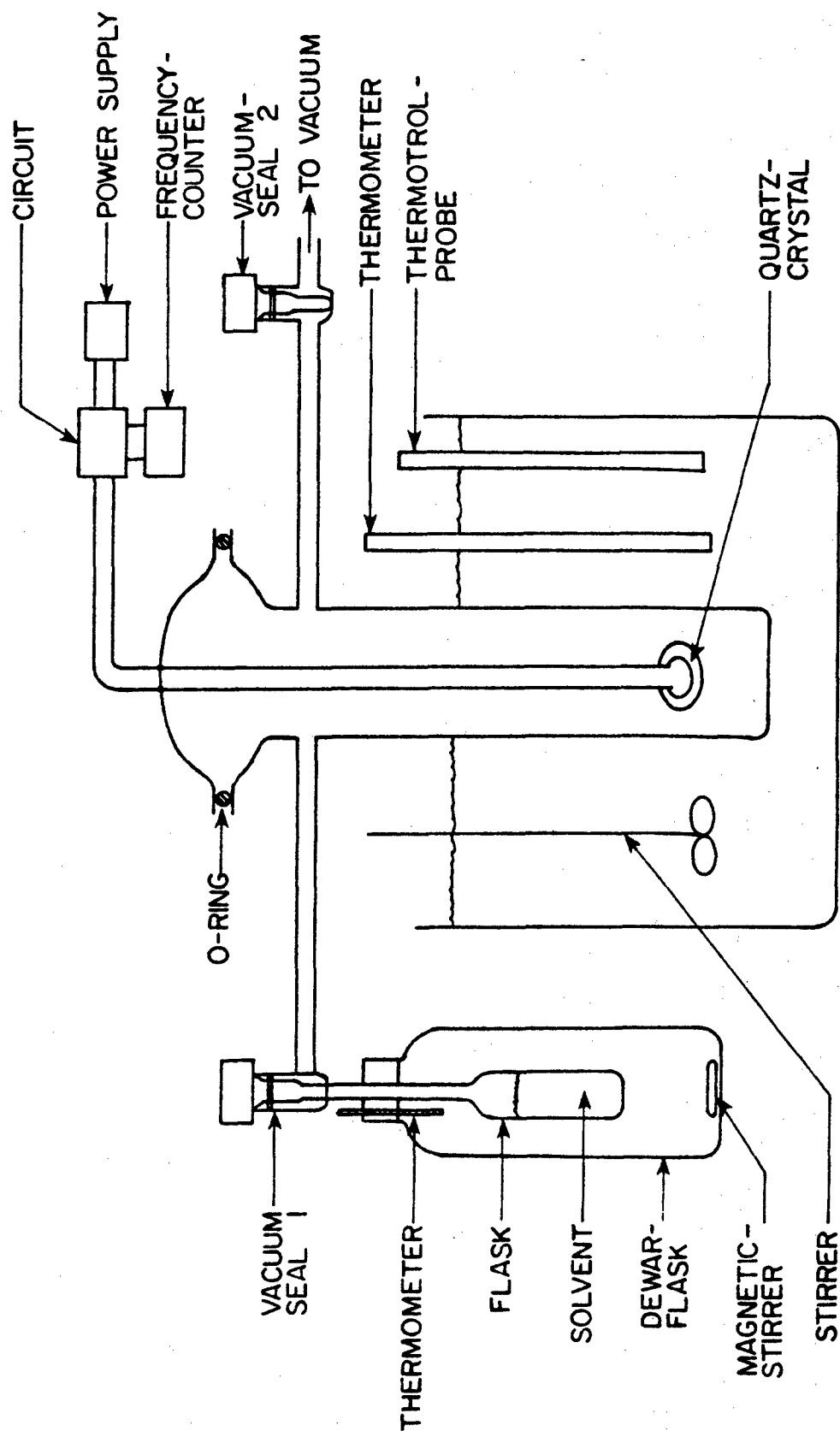


Fig. 2. Schematic diagram of piezoelectric apparatus.

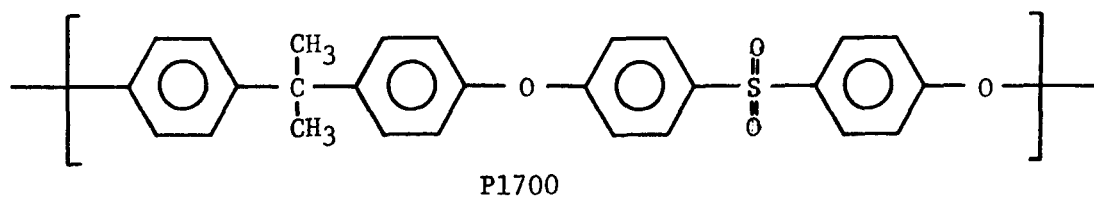
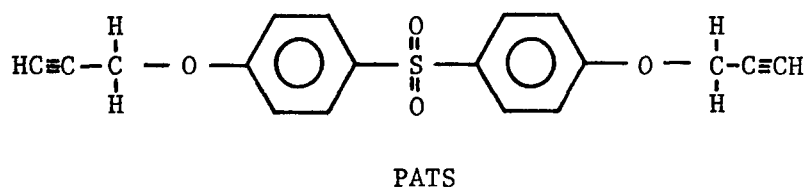
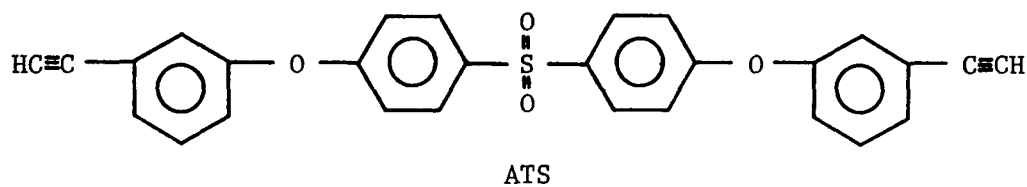
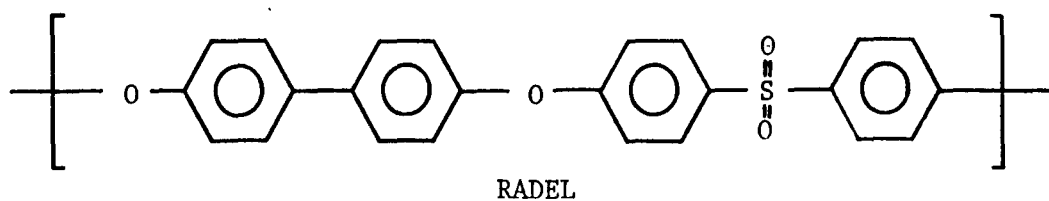
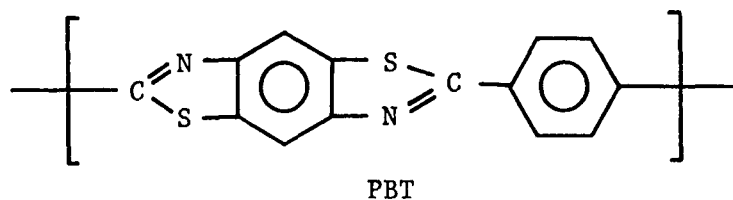


Figure 3. Polymer and Plasticizer Structures

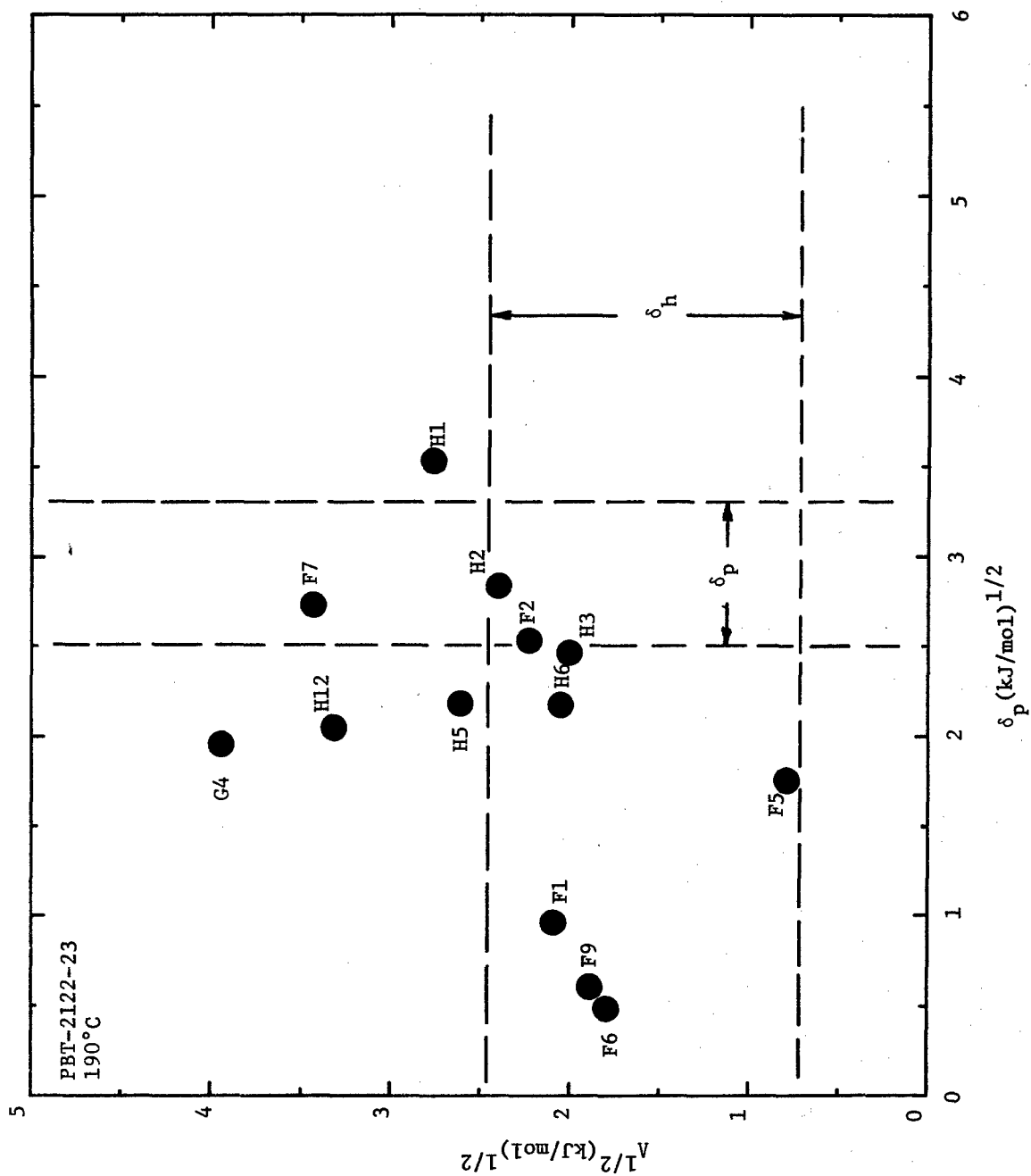


Figure 4a. Solubility Parameter Plot Showing Energy of Specific Interactions for Solvents with PBT 2122-23 at 190°C

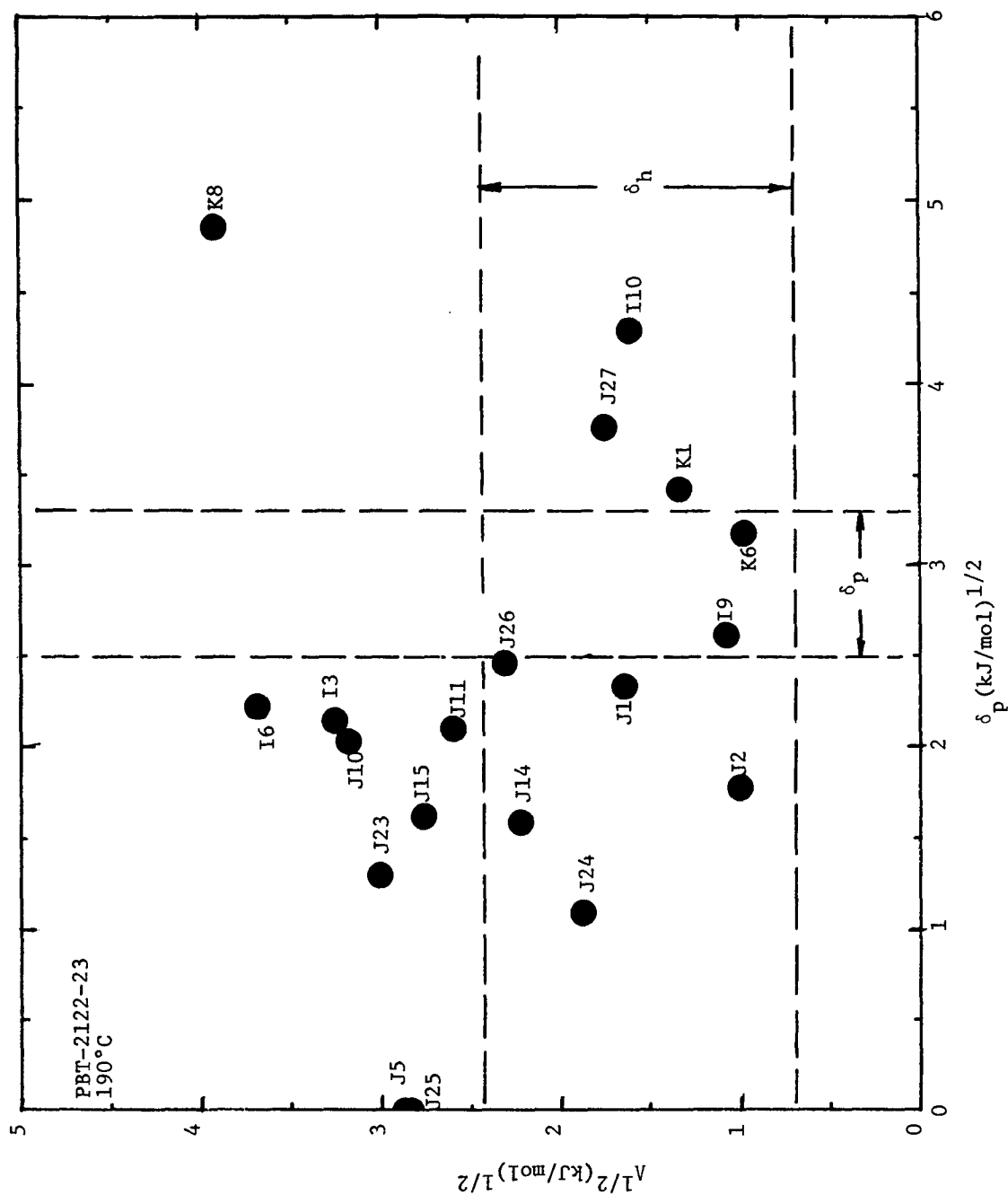


Figure 4b. Solubility Parameter Plot Showing Energy of Specific Interactions for Solvents with PBT 2122-23 at 190°C

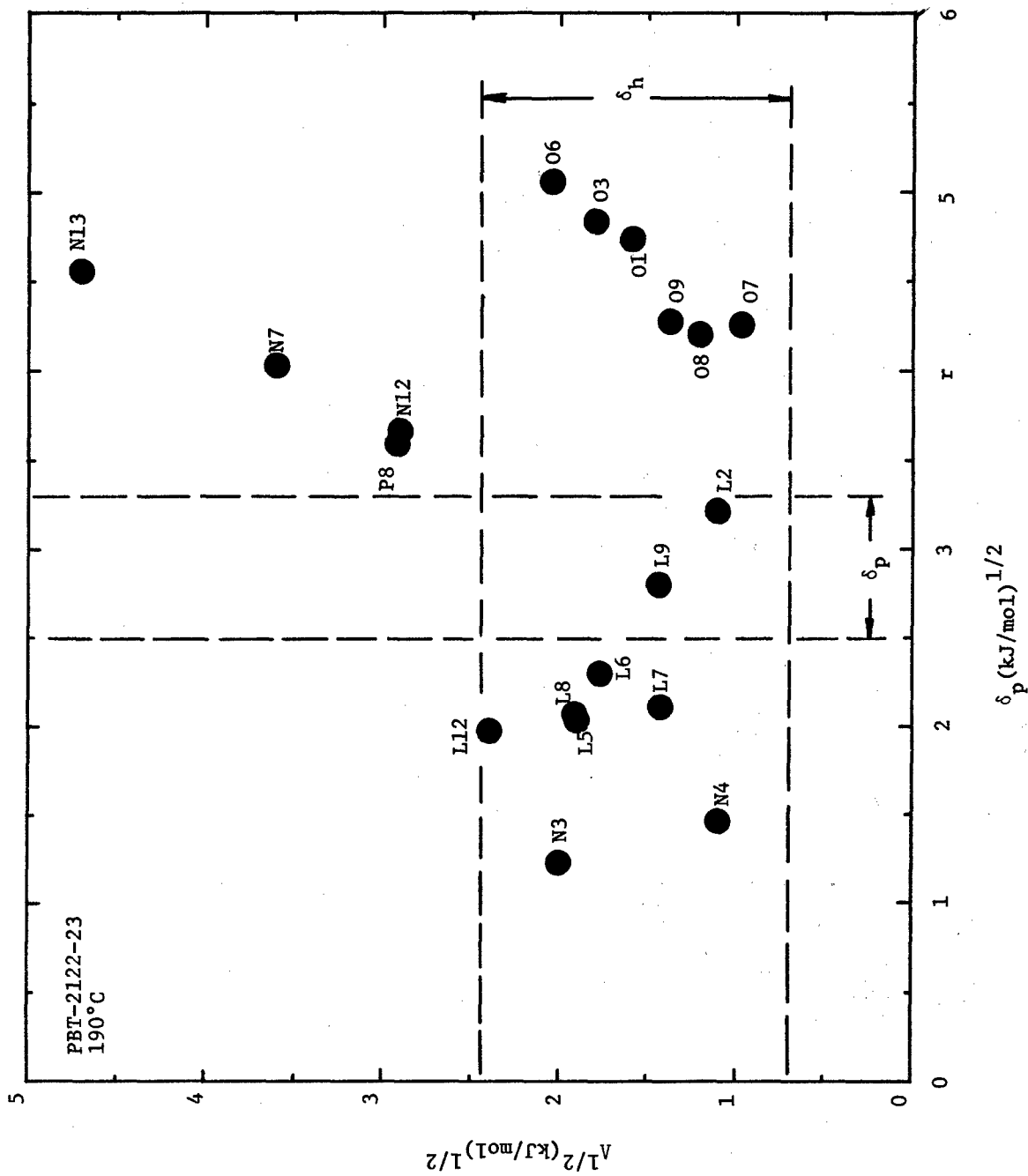


Figure 4c. Solubility Parameter Plot Showing Energy of Specific Interactions for Solvents with PBT 2122-23 at 190°C

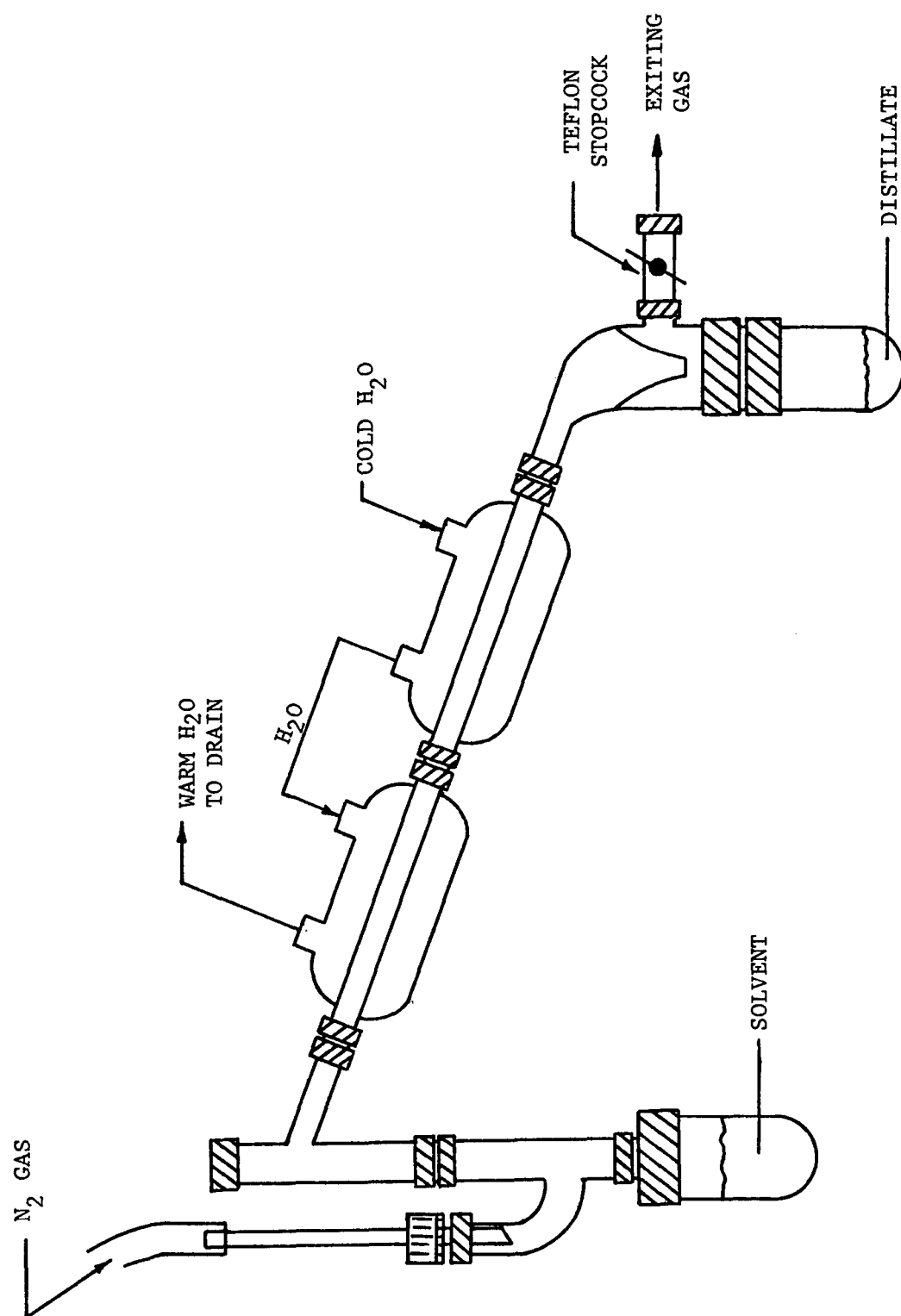


Figure 5. Distillation Apparatus Used for Solvent Purification

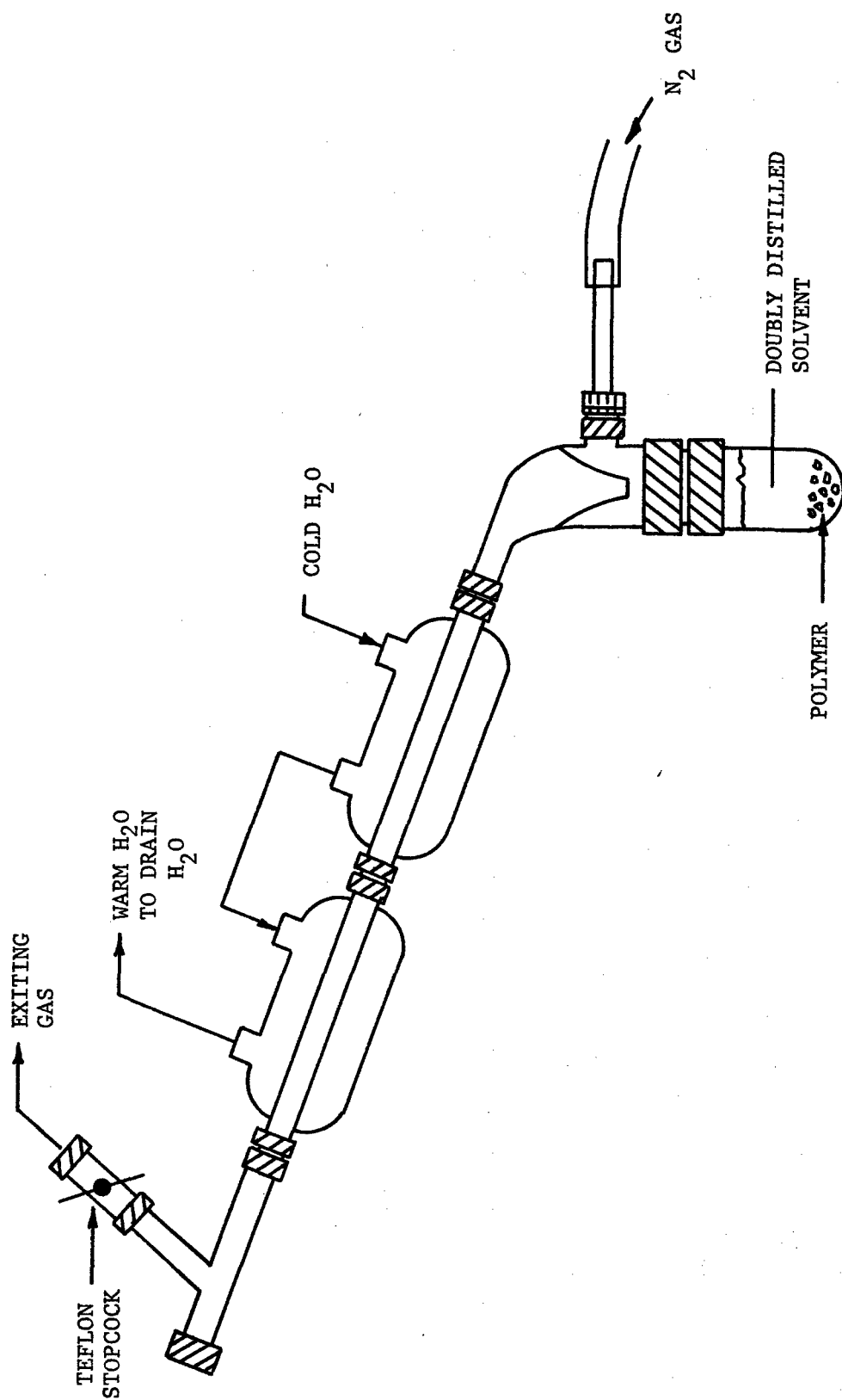


Figure 6. Reflux Apparatus Used for PBT Solubility Tests

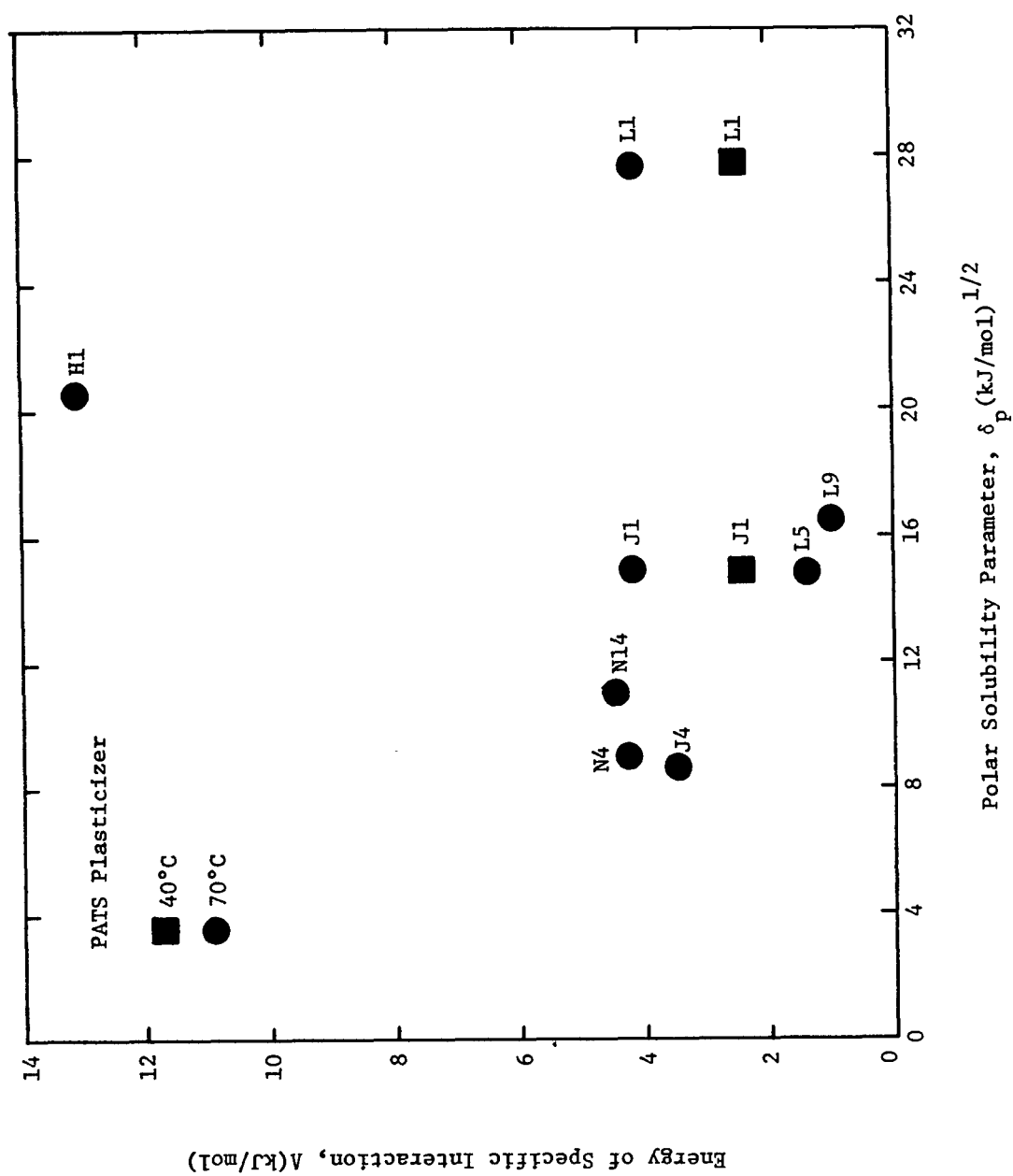


Figure 7. Solubility Parameter Plot Showing Energy of Specific Interaction for Solvents with PATS at 40°C and 70°C

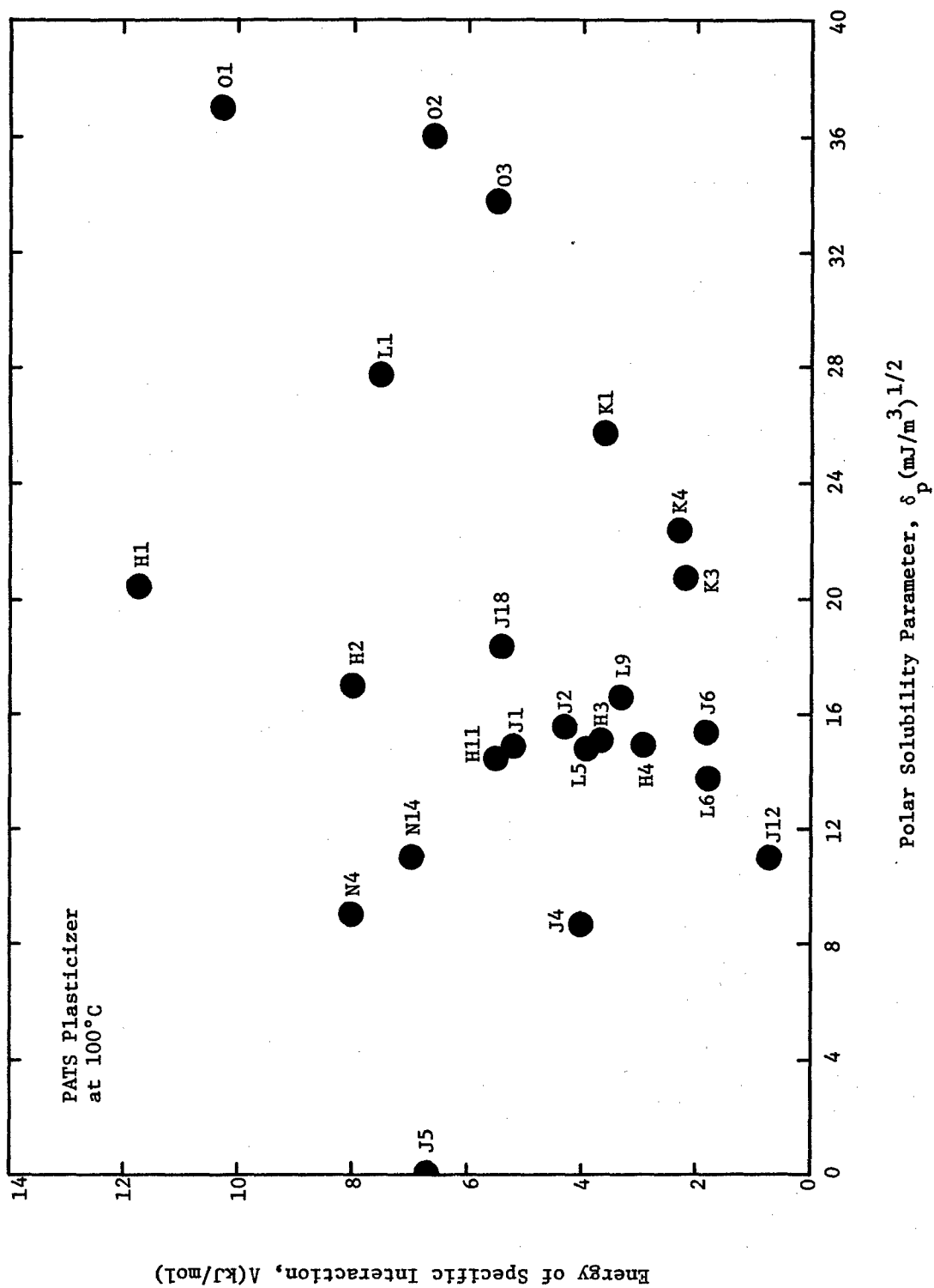


Figure 8. Solubility Parameter Plot Showing Energy of Specific Interaction for Solvents with PATS at 100°C

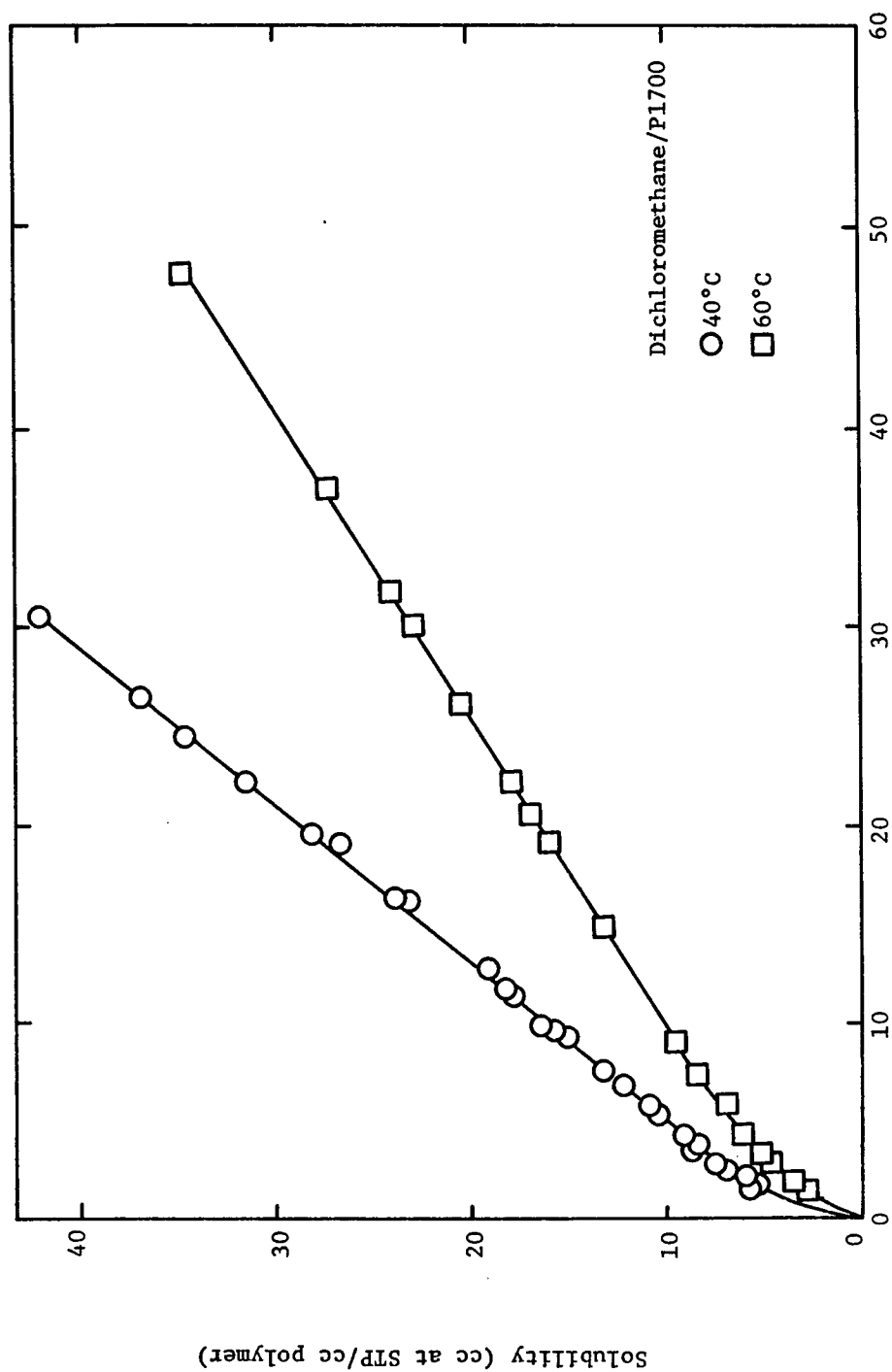


Figure 9. Solubility of Dichloromethane in P1700 Polysulfone as a Function of Pressure at 40°C and 60°C

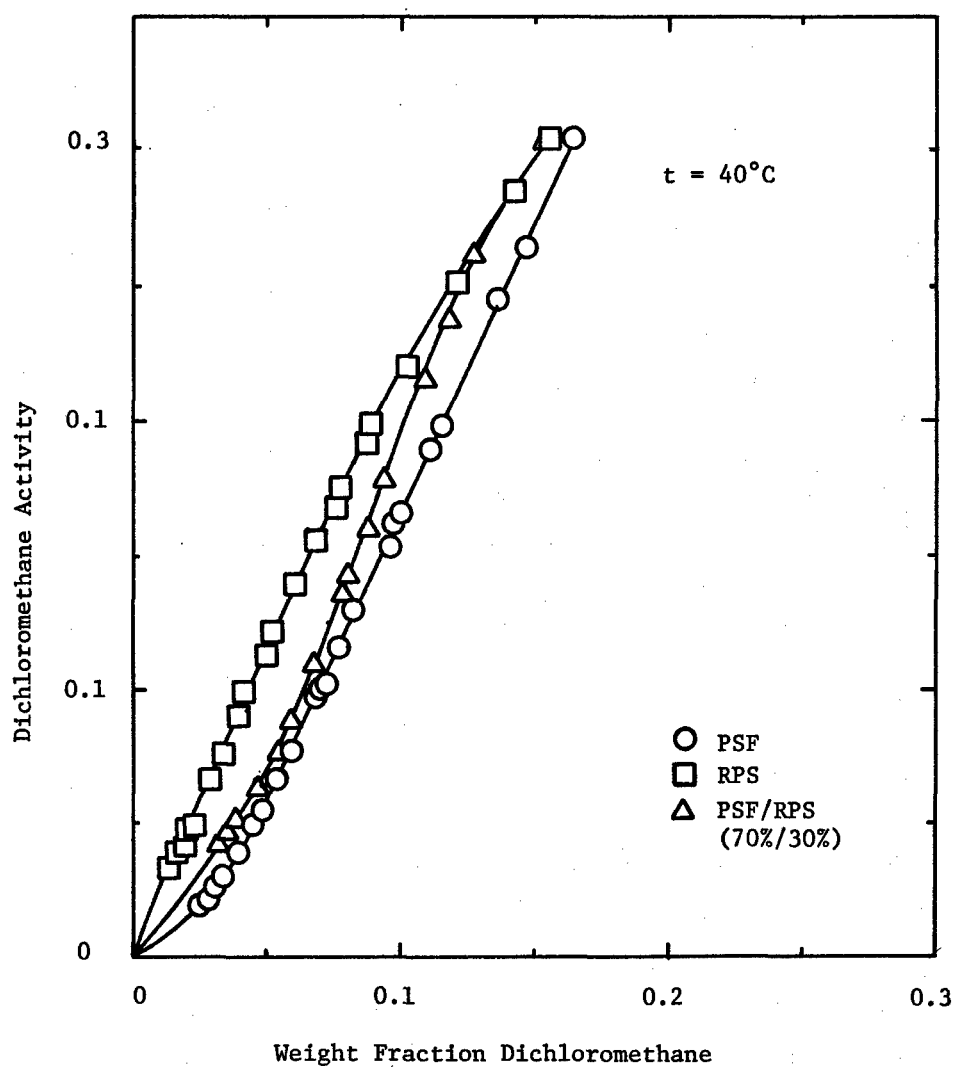


Figure 10. Activity of Dichloromethane in P1700 Polysulfone as a Function of Solvent Weight Fraction at 40°C

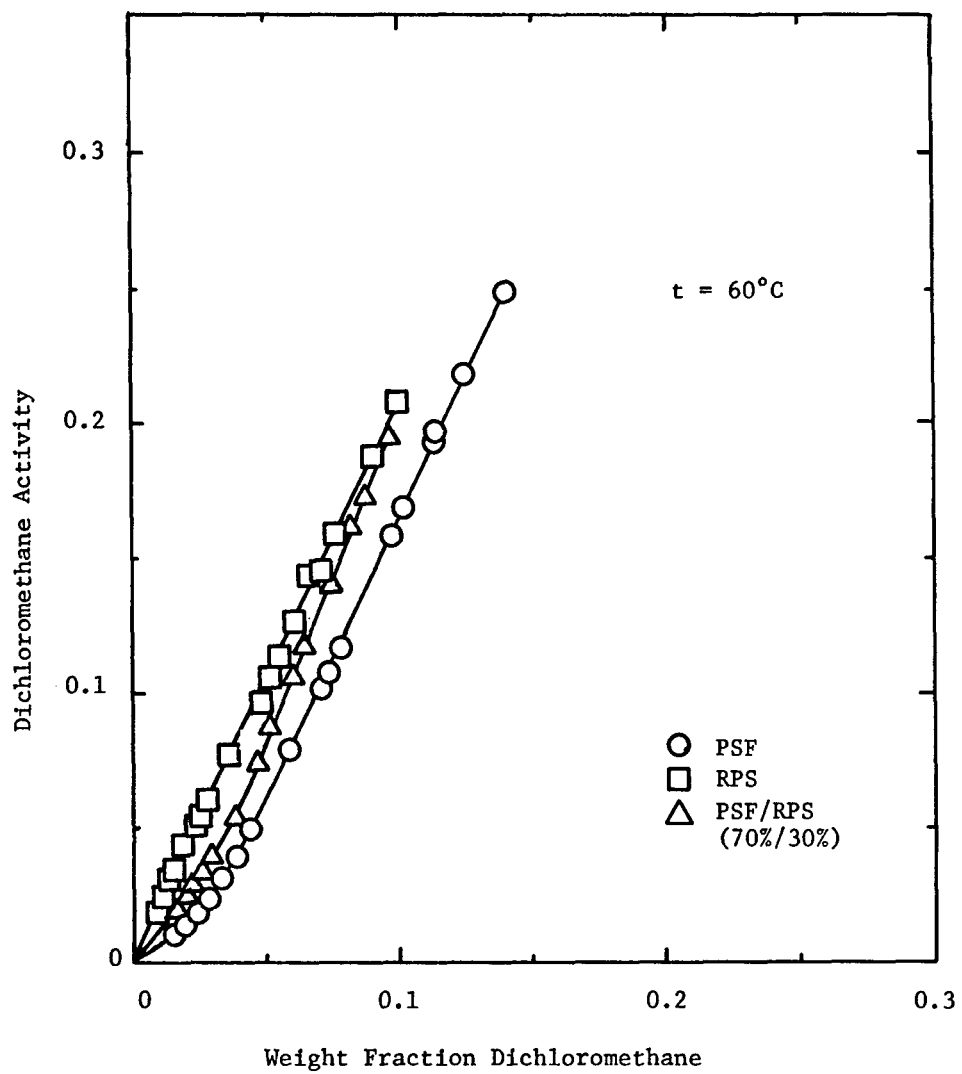


Figure 11. Activity of Dichloromethane in P1700 Polysulfone as a Function of Solvent Weight Fraction at 60°C

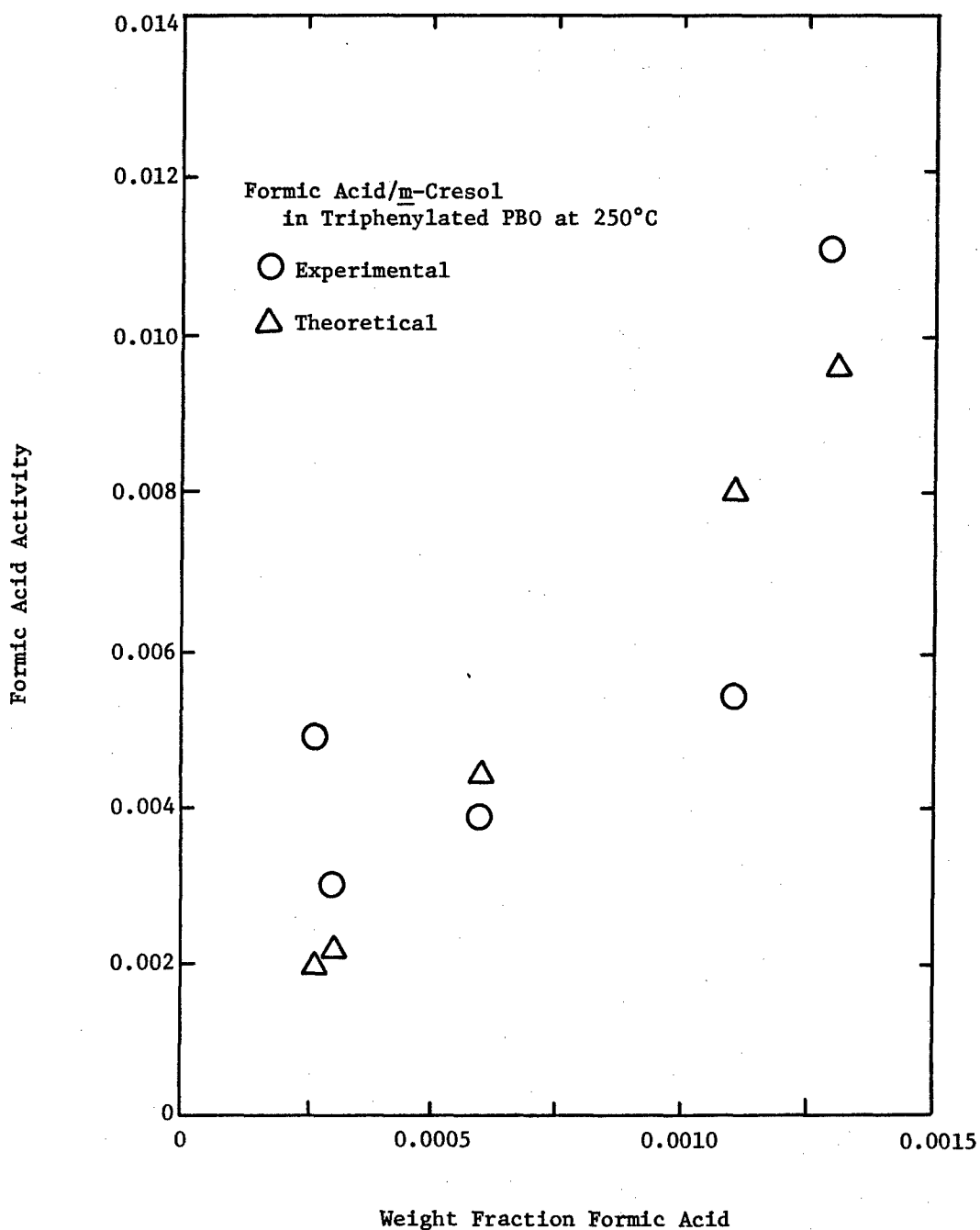


Figure 12. Activity of Formic Acid in Triphenylated PBO as a Function of Solvent Weight Fraction

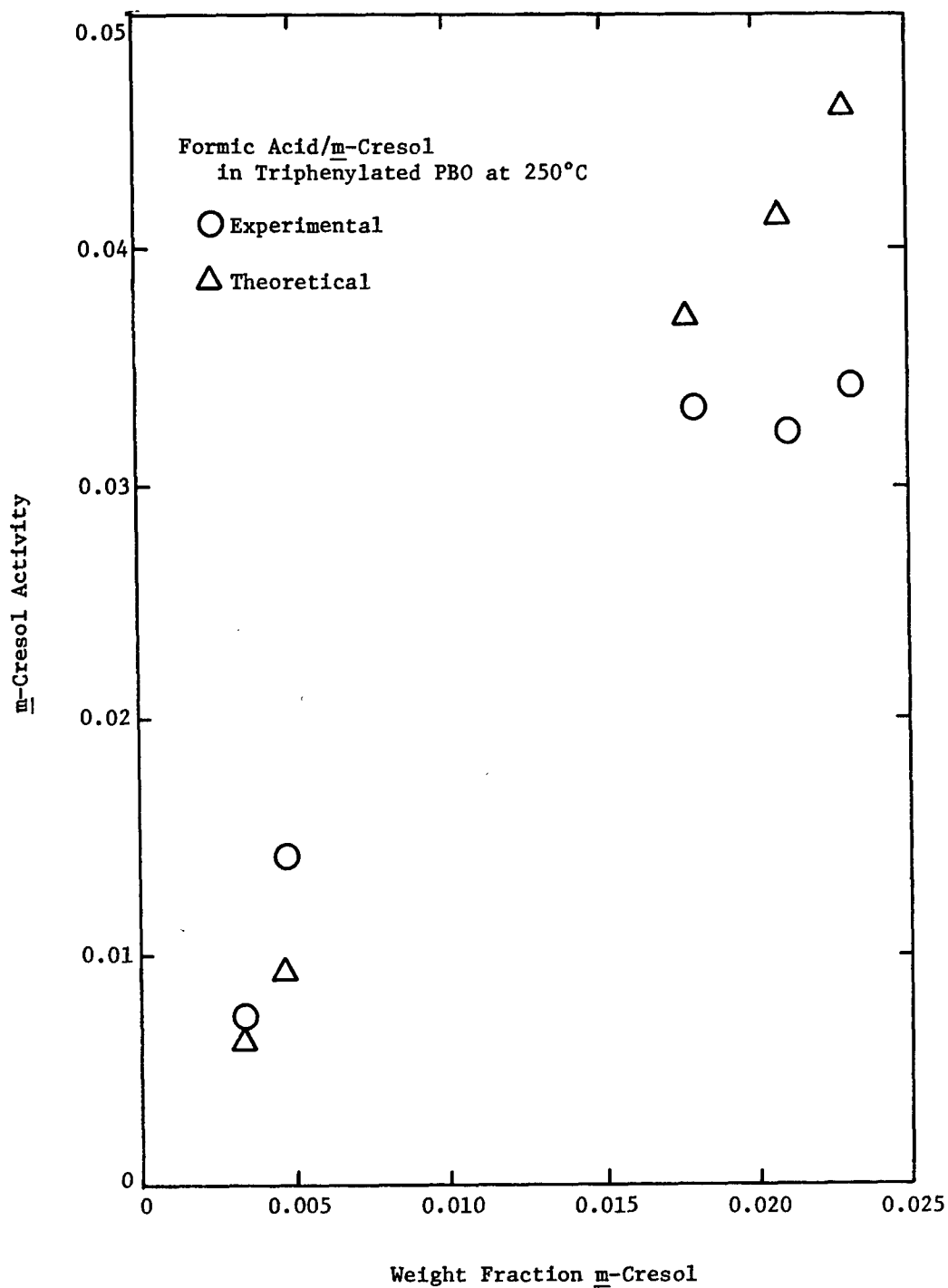


Figure 13. Activity of m-Cresol in Triphenylated PBO as a Function of Solvent Weight Fraction